

# Indo-Japan Workshop on Interface Phenomena for Spintronics (IJW-IPS 2022)

## Abstract Book

March 08-10, 2022

### Organized by

National Institute of Science Education and Research (NISER), Bhubaneswar, India  
&  
Institute for Materials Research (IMR), Tohoku University, Sendai, Japan



## COMMITTEE

### **Patron**

Prof. Sudhakar Panda, Director, NISER, India

### **Convener**

Dr. Subhankar Bedanta, NISER, India

### **Co-conveners**

- Prof. Takeshi Seki, Tohoku Univ., Japan
- Dr. Braj Bhusan Singh, NISER, India
- Prof. Koki Takanashi, Tohoku Univ., Japan

# Indo-Japan Workshop on Interface Phenomena for Spintronics (IJW-IPS 2022)

## Program Day 1 (08.03.2022)

(Program starts at 10.00 AM IST)

### Zoom Link

<https://us06web.zoom.us/j/83943470117?pwd=TFRVQ3B0TWkEcnVnVINHNERoMEJXZz09>

Meeting ID: 839 4347 0117; Passcode: 551236

10.00-10.30 AM	<b><u>Inauguration</u></b> <ul style="list-style-type: none"><li>➤ Welcome address by Dr. Subhankar Bedanta, Convener, IJW-IPS 2022, NISER, India.</li><li>➤ Address by Prof. Sudhakar Panda, Director, NISER, Bhubaneswar.</li><li>➤ Address by Prof. Bedangadas Mohanty, Dean of Faculty Affairs, NISER, Bhubaneswar.</li><li>➤ Address by Prof. Takeshi Seki, Co-convener, IJW-IPS 2022, Tohoku University, Japan.</li><li>➤ Address by Prof. Koki Takanashi, Co-convener, IJW-IPS 2022, Tohoku University, Japan</li><li>➤ Vote of thanks by Dr. Braj Bhusan Singh, Co-convener, IJW-IPS 2022, NISER, India.</li></ul>
<b>Session I</b>	
10.30-11.00 AM	<b>Prof. Anjan Barman</b> , SNBNCBS, India. <i>Ultrafast Spin Dynamics and Spin Waves in 2D Material/Ferromagnet Heterostructures</i>
11.00-11.30 AM	<b>Prof. Takeshi Seki</b> , IMR, Japan. <i>Large antisymmetric interlayer exchange coupling.</i>
11.30-12.00 AM	<b>Prof. Ashwin Tulapurkar</b> , IIT Bombay, India. <i>Inverse of voltage-controlled magnetic anisotropy (VCMA) effect and investigation in graphene/FM structures</i>
12.00-12.30 AM	<b>Prof. Ruma Mandal</b> , Tohoku University, Japan <i>Magnetization Dynamics Study of High PMA Ultrathin Magnetic Heterostructures</i>
12.30-1.30 PM	<b>LUNCH BREAK</b>
<b>Session II</b>	
01.30-02.00 PM	<b>Prof. Ken-ichi Uchida</b> , NIMS, Japan. <i>Future directions in spin caloritronics</i>
02.00-02.30 PM	<b>Dr. Braj Bhusan Singh</b> , NISER, India. <i>Spin to charge conversion in polycrystalline topological insulator</i>
02.30-03.00 PM	<b>Prof. P. S Anil Kumar</b> , IISc, India. <i>Asymmetric magnetic domain wall motion under lateral and normal space inversion asymmetry with interfacial Dzyaloshinskii-Moriya interaction</i>
03.00-03.30 PM	<b>Dr. Surendra Singh</b> , BARC, India. <i>Investigation of emerging phenomena at the interface of heterostructures using polarized neutron reflectivity</i>

## Program Day 2 (09.03.2022)

### Zoom Link

<https://us06web.zoom.us/j/86317654121?pwd=SFhRNXFHZ29Fb1hvNnRZM2xSL3lyUT09>

Meeting ID: 863 1765 4121; Passcode: 263750

Session III	
10.00-10.30 AM	<b>Dr. Subhankar Bedanta</b> , NISER, India. <i>Exciting physics at the interface of organic semiconductor/ferromagnet interfaces</i>
10.30-11.00 AM	<b>Prof. Keita Ito</b> , Tohoku University. <i>Fabricating <math>L1_0</math>-ordered FeNi films by denitriding FeNiN films</i>
11.00-11.30 AM	<b>Dr. Anjana Dogra</b> , NPL, India. <i>2DEG characteristic difference between stoichiometric LaScO<sub>3</sub>/STO and non-stoichiometric Ca<sub>x</sub>Ta<sub>y</sub>O<sub>3+δ</sub>/STO</i>
11.30-12.00 AM	<b>Prof. Kohei Fujiwara</b> , Tohoku University, Japan. <i>Topological Hall effect in multilayers of kagome-lattice ferromagnet Fe<sub>3</sub>Sn and Pt</i>
12.00-12.30 AM	<b>Prof. Bhaskaran Muralidharan</b> , IIT Bombay, India. <i>New directions in 2D quantum materials and interfaces with Rashba interaction</i>
12.30-1.30 PM	<b>LUNCH BREAK</b>
Session IV	
01.30-02.00 PM	<b>Prof. Takahiro Moriyama</b> , Kyoto University, Japan. <i>Spin dynamics and transport in antiferromagnets</i>
02.00-02.30 PM	<b>Dr. Sujit Das</b> , IISc, Bangalore, India. <i>Polar topology: A new era of ferroelectrics</i>
02.30-04.30 PM	<b>POSTER SESSION</b> <a href="https://drive.google.com/file/d/1W6LmiOc0G7tIxS5TFyAEOyPkU4UP0mKG/view?usp=sharing">https://drive.google.com/file/d/1W6LmiOc0G7tIxS5TFyAEOyPkU4UP0mKG/view?usp=sharing</a>

## Program Day 3 (10.03.2022)

### Zoom Link

<https://us06web.zoom.us/j/81941398966?pwd=T29xdC9RSW9zREVZzZWNGRDRVHhKZz09>

Meeting ID: 819 4139 8966; Passcode: 886950

Session V	
10.00-10.30 AM	<b>Prof. Yuya Sakuraba</b> , NIMS, Japan. <i>Development of high performance giant magnetoresistive device by interface control</i>
10.30-11.00 AM	<b>Prof. Pranaba Kishor Muduli</b> , IIT Delhi, India. <i>Interfacial origin of unconventional spin-orbit torques in <math>\text{Py}/\text{IrMn}_3</math></i>
11.00-11.30 AM	<b>Prof. Takahide Kubota</b> , Tohoku University, Japan. <i>Manganese-based Materials for Spintronics Applications</i>
11.30-12.00 AM	<b>Dr. Suvankar Chakraverty</b> , INST, India. <i><math>\text{KTaO}_3</math> – The New Kid on the Spintronics Block</i>
12.00-12.30 AM	<b>Prof. Debakanta Samal</b> , IOP, India. <i>Emergent quantum transport due to quenched magnetic impurity scattering by antiferromagnetic proximity in <math>\text{SrCuO}_2/\text{SrIrO}_3</math></i>
12.30-1.30 PM	<b>LUNCH BREAK</b>
Session VI	
01.30-02.00 PM	<b>Prof. Masaki Mizuguchi</b> , Nagoya University, Japan. <i>Electric field effect of <math>\text{Fe}/\text{MgO}</math> interface in magnetic tunnel junctions</i>
02.00-02.30 PM	<b>Dr. Prasanta Muduli</b> , IIT Madras, India. <i>Nanoscale nonlocal devices to study quantum materials</i>
02.30-03.00 PM	<b>Dr. Takumi Yamazaki</b> , Tohoku University, Japan. <i>Optical thermometry for investigating spin-caloritronic phenomena</i>
03.00-03.30 PM	Concluding session

# Poster Session

09.03.2022 (Wednesday): 02.30 – 4.30 PM (IST)

Poster ID	Author	Address	Abstract Title	FRAME room no. (Poster location) for poster presentation
P01	Dr. Dipraj Saikia	Duliajan College, Assam	Room Temperature Ferromagnetism in half metallic Co doped CdS diluted magnetic semiconductor for spintronics	01 (A)
P02	Mr Jadupati Nag	IIT Bombay, Mumbai	CoFeVSb: A Promising Candidate for Spin Valve and Thermoelectric Applications	01 (I)
P03	Mr Manish	INST Mohali, Mohali	Tuning the electric properties of conducting interface at EuO-KTaO <sub>3</sub> with light as external stimuli	01 (D)
P04	Dr Midhunlal P V	JAIN (Deemed to be University), Karnataka	Probing the fully compensated ferrimagnet Mn <sub>2</sub> V <sub>0.5</sub> Co <sub>0.5</sub> Al: Neutron diffraction and ab initio studies	01 (L)
P05	Dr Zainab Hussain	IIT Bombay, Mumbai	Formation of Nickel Silicide and Appearance of Anomalous behaviour of Magnetic Anisotropy in Nickel thin films	02 (A)
P06	Mr Soumyaranjan Ratha	Akita University, Akita	Enhancement of magnetic properties by Lanthanides and Co doping in Bismuth Ferrite thin films fabricated by pulsed DC reactive sputtering method	02 (I)
P07	Mr Abhishek Panghal	Shiv Nadar University, Uttar Pradesh	Room Temperature Ferromagnetism in Ni Doped MoO <sub>3</sub> Nanoflowers	02 (D)
P08	Ms sonali kakkar	INST Mohali, Punjab	Magnetic studies of nanostructures and effect of spin-orbit interaction	02 (L)
P09	Ms Purbasha Sharangi	NISER, Bhubaneswar	Spinterface-Induced Modification in Magnetic Properties in Co <sub>40</sub> Fe <sub>40</sub> B <sub>20</sub> /Fullerene Bilayers	03 (A)
P10	Mr Rahul Gupta	IIT Bombay, Mumbai	Nonlinear dynamics of two pinned Bloch domain walls inside an optical cavity	03 (I)
P11	Ms Smridhi Chawla	Delhi University, Haryana	Understanding thermally assisted diffusion and phase transition in FePt/Si Thin Films	03 (D)
P12	Mr Abhisek Mishra	NISER, Bhubaneswar	Inverse spin Hall effect in sputter deposited MoS <sub>2</sub> /CoFeB bilayers	03 (L)
P13	Ms Akariti Sharma	PRL, Ahmedabad	Superconductivity in nickelates via increasing c-axis in films	14 (I)

P14	Dr Neha Kapila Sharma	Institute of Physics, Bhubaneswar	Transition Metal Substituted TMDC (MoS <sub>2</sub> /WS <sub>2</sub> ) Heterostructure for Realization of Dilute Magnetic Semiconductors	04 (A)
P15	Mrs P. Kavitha	Chaitanya Deemed to University, Telengana	Synthesis of nanostructured magnesium oxide by sol gel method and its characterization	04 (I)
P16	Ms Swati Verma	Guru Panak Dev University, Punjab	Effect of Zn <sup>2+</sup> -Zr <sup>4+</sup> Substitution on Magnetic Properties M-type Strontium Hexaferrite	04 (D)
P17	Mr Shaktiranjana Mohanty	NISER, Bhubaneswar	Effect of Ir spacer layer on perpendicular synthetic antiferromagnetic coupling in Co/Pt multilayers	04 (L)
P18	Mr Nanhe Kumar Gupta	IIT DELHI	Structural changes on the post annealing of Ta/Co60Fe20B20/Ta heterostructures: Effects on static and dynamics magnetization properties	05 (A)
P19	Mr Bibekananda Paikaray	IIT Hyderabad	Reconfigurable logic operations via gate controlled skyrmion motion in a nanomagnetic device	05 (I)
P20	Mr Vishal Kumar	Guru Nanak Dev University, Amritsar	Effect of Calcination Temperature on the Structural, Surface Morphology and Magnetic Properties of M-type Barium Strontium Hexaferrite	05 (D)
P21	Mr Harsh Vardhan	Amity University, Noida	Thickness dependent structural and magnetic properties investigation of CoFeB films interfaced with 4d (Ru) and 5d (Ta) heavy metals	05 (L)
P22	Ms Yasmeen Jafri	Amity University, Noida	Magnetic properties investigation of ferromagnetic films on ion irradiated Si	06 (A)
P23	Ms Esita Pandey	NISER, Bhubaneswar	Tailoring Dzyaloshinskii-Moriya interaction and domain wall dynamics in Pd/Co/C60/Pd	06 (I)
P24	Mr Brindaban Ojha	NISER, Bhubaneswar	Driving skyrmions with low threshold current density in Pt/CoFeB thin film	06 (D)
P25	Dr Anupama Swain	NISER, Bhubaneswar	180° Magnetization Reversal in Fe/BaTiO <sub>3</sub> (110) Multiferroics	06 (L)
P26	Mr Mohammed Azharudheen. N	NISER, Bhubaneswar	Spin to charge conversion in IrO <sub>x</sub> /Ni80Fe20 bilayers	07 (A)
P27	Ms Swayang Priya Mahanta	NISER, Bhubaneswar	Spinterface modulated magnetic properties of CoFeB/Alq <sub>3</sub> system	07 (I)
P28	Mr Pradeep Kumar	IIT, Roorkee	Spin Valve effect in FL-MoS <sub>2</sub> and ferromagnetic shape memory alloy based magnetic tunnel junction	07 (D)
P29	Ms Sukhmanbir Kaur	Guru Nanak Dev University, Punjab	Effect of Cr doping on the Structural, Surface Morphology, Magnetic and Antimicrobial Properties of Cobalt ferrite	07 (L)

P30	Dr Manjari Shukla	School of Materials Science & Technology, Varanasi	Role of chemical pressure in spin-disordered Ho <sub>2</sub> GexTi <sub>2-x</sub> O <sub>7</sub> system	08 (A)
P31	Ms Anshu Gupta	INST Mohali, Punjab	Signatures of Rashba Effect in Angle Resolved Magnetoresistance	08 (I)
P32	Dr B Ravi Kumar	IISc, Bangalore	Tilted anisotropy induced deterministic magnetization switching in perpendicularly magnetized Ta/Pt/CoFeB/Au multilayer	08 (D)
P33	Mr Shubham Kumar	Amity University, Noida	Rapid thermal annealing on FePtCu based systems for enhanced transformation kinetics and improved structural properties	08 (L)
P34	Ms Sadhana Singh	UGC-DAE CSR, Indore	Stabilization of Magnetic Helix in Exchange-Coupled trilayer	09 (A)
P35	Ms Suchetana Mukhopadhyay	SNBNCBS, Kolkata	Femtosecond laser-driven ultrafast demagnetization in ferromagnetic thin films: a comparative study using two theoretical models	09 (I)
P36	Mr Pratap Kumar Pal	SNBNCBS, Kolkata	Variation of Magnon–Magnon Coupling Strength with Microwave Power and Bias-Field Angle in Ni <sub>80</sub> Fe <sub>20</sub> Nanocross Array	09 (D)
P37	Mr K Chandrakanta	NIT, Rourkela	Magnetic field-induced magnetodielectric coupling and dielectric relaxation response in KBiFe <sub>2</sub> O <sub>5</sub>	09 (L)
P38	Mrs Priyanka Garg	IISc, Bangalore	Probing magnetic anisotropy and spin-reorientation transition in 3D antiferromagnet, Ho <sub>0.5</sub> Dy <sub>0.5</sub> FeO <sub>3</sub>  Pt using spin Hall magnetoresistance	10 (A)
P39	Dr Aditya A. Wagh	IISc, Bangalore	Highly tunable spin Hall magnetoresistance in magnetoelectric Z-type hexaferrite, Sr <sub>3</sub> Co <sub>2</sub> Fe <sub>24</sub> O <sub>41</sub>  Pt hybrids	10 (I)
P40	Ms Venuka Bhasin	Guru Nanak Dev University, Punjab	Effect of Cr doping on the Structural, Surface Morphology, Magnetic and Antimicrobial Properties of Nickel ferrite	10 (D)
P41	Mr Koustuv Roy	NISER, Bhubaneswar	Spin pumping and inverse spin Hall effect study in CoFeB/ IrMn bilayers	10 (L)
P42	Mr Vireshwar Mishra	IIT, Delhi	On the Room Temperature Weak Localization and Anomalous Temperature Dependence of Phase Coherence Length in L21 ordered Heusler Alloy CoFeMnSi Thin Films	11 (A)
P43	Dr S. Shanmukharao Samatham	CBIT, Hyderabad	Correlating magnetic and synchrotron x-ray diffraction studies of chiral magnet MnSi	11 (I)
P44	Ms Soma Dutta	SNBNCBS, India	Dominant mechanism behind Ultrafast demagnetization correlating with Gilbert damping in $\beta$ -Ta/CoFeB bilayers	11 (D)
P45	Ms Anamika Kumari	INST Mohali, Punjab	A scheme to determine the carrier density distribution, potential profile, and subband quantization of a conducting interface LaVO <sub>3</sub> /SrTiO <sub>3</sub>	11 (L)
P46	Mr Abhishek Ranna	IISER Mohali	Controlling Interfacial Magnetism of Transition Metal Oxides in Proximity of Ferroelectrics	12 (A)



P47	Mr Pushpendra Gupta	NISER, Bhubaneswar	Frequency dependent inverse spin Hall effect in $\text{La}_{0.67}\text{Sr}_{0.33}\text{MnO}_3/\text{Pt}$ bilayer system	12 (I)
P48	Mr Surinder Singh	Guru Nanak Dev University, Amritsar	Structural and Magnetic Investigation of Sol-gel Derived $\text{LaFeO}_3$ doped $\text{Na}_{0.5}\text{Bi}_{0.5}\text{TiO}_3$ Ceramics	12 (D)
P49	Mr Amit Kumar	Hiroshima University, Hiroshima	Electron-Phonon interaction on the Surface of the Three-Dimensional Topological Insulators	12 (L)
P50	Ms Sreya Pal	SNBNCBS, Kolkata	Reconfigurable Magnonics Driven by Spin Texture in Diatomic Nanodot Array	13 (A)
P51	Mr Bharathiganesh Devanarayanan	Physical Research Laboratory, Ahmedabad	Itinerant Magnetism in $\text{CaMn}_2\text{Al}_{10}$ : Self-Consistent Renormalisation (SCR) Theory study	13 (I)
P52	Ms Susree Sucharita Mohapatra	NISER, Bhubaneswar	Study of skyrmion and antiskyrmion Hall Effect in a synthetic ferrimagnet	13 (D)
P53	Ms Gaurav Kanu	NISER, Bhubaneswar	Domain wall and Skyrmion dynamics on synthetic antiferromagnet for variable tensile stress - a micromagnetic study	13 (L)
P54	Mr Shashi Ranjan Kumar	Devi Ahilya University, Indore	Effects of Swift heavy ion-irradiation on Magnetic properties of Co-codoped $\text{TiO}_2$	14 (A)

## Frame room links

### Virtual interaction Room

<https://framevr.io/virtual-interaction-room>

### Room for poster session

Room-01: <https://framevr.io/room-01>

Room-02: <https://framevr.io/room-02>

Room-03: <https://framevr.io/room-03>

Room-04: <https://framevr.io/room-04>

Room-05: <https://framevr.io/room-05>

Room-06: <https://framevr.io/room-06>

Room-07: <https://framevr.io/room-07>

Room-08: <https://framevr.io/room-08>

Room-09: <https://framevr.io/room-09>

Room-10: <https://framevr.io/room-10>

Room-11: <https://framevr.io/room-11>

Room-12: <https://framevr.io/room-12>

Room-13: <https://framevr.io/room-13>

Room-14: <https://framevr.io/room-14>

Room\_15: <https://framevr.io/room-15>

# Ultrafast Spin Dynamics and Spin Waves in 2D Material/Ferromagnet Heterostructures

Anjan Barman<sup>1\*</sup>

<sup>1</sup>S. N. Bose National Centre for Basic Sciences, Block JD, Sector 3, Salt Lake, Kolkata, 700106, India

\*abarman@bose.res.in (representative author)

The 2D material/ferromagnet interface promises a plethora of new science and technology. They will form important building block for new-generation spintronics due to their unique spin transport, spin-orbit coupling and interface hybridization, which may provide new opportunities for the spin-based device fabrication [1]. For the ultra-high speed spintronics applications, it is essential to have a deep insight about the magnetization dynamics occurring over nanosecond to femtosecond timescale. The optimization of these devices demands understanding and possible control of ultrafast demagnetization, Gilbert damping as well as spin-wave propagation.

We will discuss the ultrafast spin dynamics occurring over femtosecond to nanosecond timescale measured by an all-optical time-resolved magneto-optical Kerr effect technique [2] in single layer graphene (SLG)/CoFeB thin film heterostructures with varying CoFeB thickness. We will compare the results with reference CoFeB thin films without SLG underlayer. The modulation of Gilbert damping with CoFeB layer thickness is extensively modelled to extract the spin-mixing conductance for SLG/CoFeB interface and isolate the contribution of two-magnon scattering from spin pumping. In SLG/CoFeB, we will establish an inverse relationship between the ultrafast demagnetization time and the Gilbert damping parameter dominated by the interfacial spin accumulation and pure spin currents transport via spin pumping mechanism [3].

The interfacial Dzyaloshinskii Moriya interaction (iDMI) is crucial for stabilizing chiral spin textures, which are important for future spintronic devices. Here, we will present direct evidence of iDMI in graphene(MoS<sub>2</sub>)/ferromagnet heterostructures from the asymmetry in spin-wave dispersion using Brillouin light scattering (BLS) technique. Linear scaling of iDMI with the inverse of ferromagnetic thicknesses confirms purely interfacial origin of iDMI. We will study the roles of defect induced extrinsic spin-orbit coupling and Rashba spin-orbit coupling in determining the iDMI by extensive experiment and analyses [4-5].

[1] D. Pesin and A. H. MacDonald, Nat. Mater. **11**, 409 (2012).

[2] S. N. Panda et al. Sci. Adv. **5**, eaav7200 (2019).

[3] S. N. Panda, Nanoscale **13**, 13709 (2021).

[4] A. K. Chaurasiya et al. Phys. Rev. B **99**, 035402 (2019).

[5] A. Kumar et al., Appl. Phys. Lett. **116**, 232405 (2020).

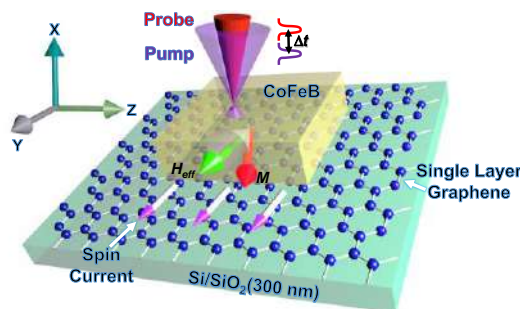


Fig. 1. Schematic of spin current driven ultrafast spin dynamics in graphene/CoFeB heterostructure.

# Large antisymmetric interlayer exchange coupling

T. Seki, H. Masuda, and K. Takanashi

Institute for Materials Research, Tohoku University, Sendai 980-8577, Japan

Email: takeshi.seki@tohoku.ac.jp

**Abstract:** The antisymmetric interlayer exchange coupling (AIEC) was recently discovered, playing pivotal roles in magnetization switching of a synthetic antiferromagnet (SAF) through inducing magnetization canting. In this take, large AIEC is reported for perpendicularly magnetized Pt/Co/Ir/Co/Pt with wedge-shaped layers. The effective field of the AIEC is related with symmetric interlayer exchange coupling, providing guides to enhance the AIEC. We develop an extended Stoner-Wohlfarth model for a SAF, revealing key factors in its magnetization switching. Combining the theoretical knowledge and the experimental results, *perpendicular* magnetization switching is achieved solely by *in-plane* magnetic field.

## 1. INTRODUCTION

Metallic superlattices consisting of Co/Cu/Co and Co/Ir/Co are representatives to show the symmetric interlayer exchange coupling (IEC) and had extensively been studied from 1980 to 1990 [1]. Recently, the long-range antisymmetric exchange interaction (antisymmetric IEC) between ferromagnetic layers via a nonmagnetic interlayer was observed in a metallic superlattice when the in-plane spatial symmetry inversion was broken in the film structure [2-5]. However, the mechanism of antisymmetric IEC has not been understood well, and the potential of antisymmetric IEC has been unclear. Thus, the systematic experiments exploiting well-controlled in-plane structural asymmetry are indispensable. In this talk, we show the systematic investigation of the antisymmetric IEC for the wedge-shaped Pt/Co/Ir/Co/Pt to clarify the nature of the antisymmetric IEC.

## 2. EXPERIMENTAL RESULTS

The 9 nm square-size double-wedged Ta (1 nm)/Pt (2 nm)/Co ( $t_{\text{Co}}$ )/Ir ( $t_{\text{Ir}}$ )/Co (0.5 nm)/Pt (2 nm)/Ta (1 nm) film was deposited on a SiO<sub>x</sub> substrate using DC magnetron sputtering equipped with a linear shutter. The  $t_{\text{Co}}$  and  $t_{\text{Ir}}$  were continuously varied from 0.6 to 1.6 nm and from 0 to 1.5 nm, respectively, to induce the in-plane spatial inversion symmetry breaking. The wedge direction of the Ir layer was orthogonal to that of the bottom Co layer. The double-wedged thin film was patterned into the Hall bar-shaped electronic devices, and the magnetic properties were investigated using the anomalous Hall effect (AHE). The IEC of the Co/Ir/Co system was confirmed from the periodic change of the saturation field ( $\mu_0 H_s$ ) against  $t_{\text{Ir}}$ . The AHE under the application of an in-plane magnetic field ( $H_{\text{ip}}$ ) of 50 mT was also measured. The hysteresis loops of the AHE were largely shifted, indicating the existence of the antisymmetric IEC. The largest difference in the switching field shift ( $\Delta\mu_0 H_{\text{sw,max}}$ ) between the opposite  $H_{\text{ip}}$  directions was 14.8 mT for the device with  $t_{\text{Co}} \sim 0.80$  nm and  $t_{\text{Ir}} \sim 0.27$  nm, which was an order of magnitude larger than the values reported previously (0.7~1.7 mT [3,5]). Similar to the  $t_{\text{Ir}}$  dependence of  $\mu_0 H_s$ , the  $\Delta\mu_0 H_{\text{sw}}$  was monotonically decreased from  $t_{\text{Ir}} \sim 0.27$  nm to  $t_{\text{Ir}} \sim 0.87$  nm and increased over  $t_{\text{Ir}} \sim 0.87$  nm, suggesting the correlation between the symmetric

IEC and the antisymmetric IEC. Furthermore, we theoretically proposed the tunability of the effective field due to the antisymmetric IEC by the ratio of the antisymmetric IEC energy ( $D_{\text{AIEC}}$ ) and the antiferromagnetic coupling strength from the numerical calculation and the extended Stoner-Wohlfarth model. The extended Stoner-Wohlfarth model also suggested that the perpendicular magnetization is switched by solely applying  $H_{\text{ip}}$  in the presence of the antisymmetric IEC. We experimentally demonstrated the  $H_{\text{ip}}$ -induced perpendicular magnetization switching for the double-wedged Pt/Co/Ir/Co/Pt under  $\mu_0 H_{\text{ip}} = 80$  mT. Perpendicular magnetization was switched when  $H_{\text{ip}}$  was applied only in the direction where  $\Delta\mu_0 H_{\text{sw,max}}$  was observed, which corresponds to the direction perpendicular to  $D_{\text{AIEC}}$ . Our demonstration paves a new way toward the manipulation of three-dimensional chiral magnetic structures.

## REFERENCES

- [1] M. D. Stiles, *J. Magn. Magn. Mater.* **200**, 322-337 (1999).
- [2] E. Y. Vedmedenko *et al.*, *Phys. Rev. Lett.* **122**, 257202 (2019).
- [3] D.-S. Han *et al.*, *Nat. Mater.* **18**, 703 (2019).
- [4] A. Fernández-Pacheco *et al.*, *Nat. Mater.* **18**, 679 (2019).
- [5] K. Wang *et al.*, *Commun. Phys.* **4**, 10 (2021).

## **Inverse of voltage-controlled magnetic anisotropy (VCMA) effect and investigation in graphene/FM structures**

Ashwin Tulapurkar

*Solid State Devices Group, Department of Electrical Engineering, Indian Institute of Technology Bombay, Mumbai 400076, India.*

Control of magnetization direction is important for writing magnetic random access memories. Control of magnetization by electric field (or equivalently by voltage) is being extensively explored as a possible candidate for writing. This is based on the control of magnetic anisotropy by voltage i.e. VCMA effect. The various effects used in spintronics also have inverse effects, which could find potential applications as well. In this talk, I will describe our experimental findings of reciprocal of the VCMA effect [1]. By this effect, we can generate charge current from oscillating magnetization, which can be used for probing magnetization dynamics.

To demonstrate this effect, we fabricated stack consisting of bottom layer/FM/MgO/top layer. Pillars of 80 um X 3 um with top and bottom contacts were formed (port 1). A co-planar waveguide (CPW) insulated from the pillar was formed on the top (port 2). The scattering parameters (S parameters) of this two-port device were measured for different orientations of the external magnetic field. The VCMA effect gives rise to transmission from port 1 to port 2, whereas the transmission from port 2 to 1 arises from the inverse VCMA effect. The role of VCMA and its inverse were confirmed by the angular dependence of the S-parameters. A circuit model will be discussed to explain the observed results.

I will further discuss our recent results on graphene/FM system obtained using STFM/R technique. Possible VCMA effects obtained by doping the graphene by metalloporphyrins will be discussed.

[1] Sci. Adv. 6, eabc2618 (2020)

# Magnetization Dynamics Study of High PMA Ultrathin Magnetic Heterostructures

Ruma Mandal<sup>1,2</sup> and Yukiko K Takahashi<sup>2</sup>

<sup>1</sup>WPI-Advanced Institute for Materials Research, Tohoku University, Sendai, Japan

<sup>2</sup>Research Center for Magnetic and Spintronic Materials, National Institute for Materials Science, Tsukuba, Japan.

Email: mandal.ruma.c8@tohoku.ac.jp

Ultra-thin ferromagnetic films with the perpendicular magnetic anisotropy (PMA) have been received a lot of attention for the spintronics application. Especially, spin transfer torque magnetoresistive random access memories (STT-MRAMs), consisting of arrays of magnetic tunneling junctions (MTJs), need the ultra-thin PMA film in order to increase the capacity. A recent critical issue of high-speed<sup>1-3</sup> and energy-efficient spintronic devices is coexistence of low magnetic Gilbert damping constant ( $\alpha$ ) and large PMA. Several kinds of ultra-thin ferromagnetic films were reported to have PMA, such as Fe<sup>1</sup>, Co<sub>2</sub>FeAl (CFA)<sup>2</sup>, FeCo<sup>3</sup> and CoFeB<sup>4</sup>. To continue such developmental process investigation of  $\alpha$  as well as high PMA in the ultra-thin regime is extremely important. Here in this presentation we will discuss about three different high PMA ferromagnetic heterostructures (CoFeAl, FeCo and Fe/MAO) with their damping analysis by time-resolved magneto-Kerr effect and discuss the origin of  $\alpha$  based on the microstructure observation and the first principal calculation.

CFA Heusler alloys are one of the attractive ferromagnetic electrode materials due to the high spin polarization, high Curie temperature of 1000 K and low  $\alpha$  below 0.001. Recently, Wen *et al* demonstrated high TMR ratio of 132% in the perpendicular MTJ<sup>5</sup>. However, we have experimentally observed an increase in  $\alpha$  of thin CFA/MgO hetero-structured films as shown in Fig. 1. From the microstructure analyses, we have found the significant diffusion of Al atoms near the interface of CFA and MgO layers. The first-principles calculations have indicated that the

increase in  $\alpha$  arises from the increase in DOS near the E<sub>F</sub> induced by the out-diffusion of Al atoms from the CFA layer to the MgO layer.

Tetragonally distorted FeCo alloys are one of the candidates for the ferromagnetic materials for STT-MRAM. Large PMA of 0.57 MJ/m<sup>3</sup> was found for the ultra-thin FeCo sandwiched by Rh layers. To further investigate the potential of this material for the ferromagnetic layer in STT-MRAM, we have estimated  $\alpha$ . We have found that 1.0 nm thick sample shows unusually high  $\alpha$  value of 0.04(Fig. 2). The detail microstructure observation shows the significant diffusion of Rh and the first principal calculation shows the inter-diffused Rh causes the increase in  $\alpha$ . Judging from the large PMA and  $\alpha$ , 1.0-nm-thick FeCo film is suitable for the reference layer in STT-MRAM.

Fe (0.7 nm)/MgAl<sub>2</sub>O<sub>4</sub>(3 nm) heterostructure was chosen to study the spin-resolved contributions of  $\alpha$  and PMA by varying the *ex situ* annealing temperature, which acts as a catalyst to vary the PMA energy densities according to the oxidation degree. Here, the optimized procedure for interface engineering is implemented to achieve an extremely low magnetic Gilbert damping constant (0.013) (Fig. 3) and a strong interfacial PMA energy (0.8MJm<sup>-3</sup>) for epitaxial thin films. By employing different interfacial atomic configurations in a first-principles calculation, this study explains the origin of the PMA energy and  $\alpha$ . These detailed findings facilitate towards promising future spintronic applications.

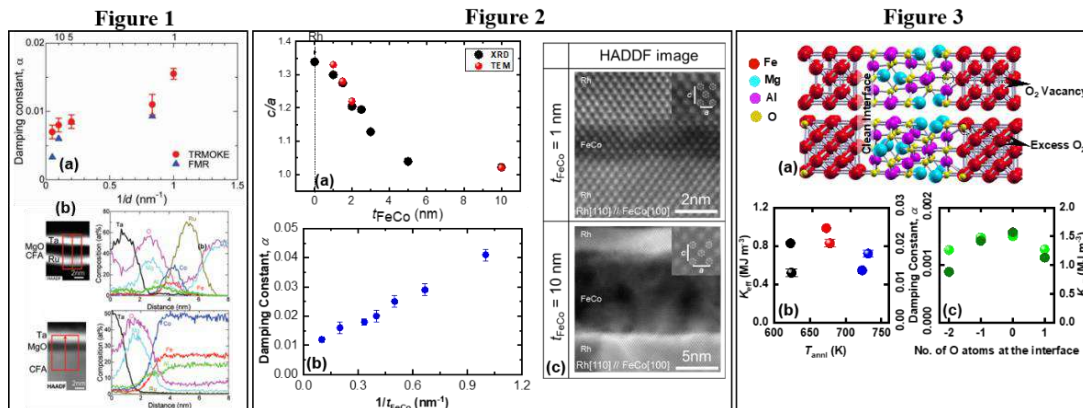


Figure 1: (a) Damping constant (b) elemental mapping with compositional profile of CFA film.

Figure 2: (a) c/a ratio, (b)  $\alpha$  as a function of film thickness (c) microstructural investigation of FeCo film.

Figure 3: (a) Schematic of Fe/MAO interface (b-c) calculated and experimental  $K_{\text{eff}}$  and  $\alpha$  of Fe/MAO interface

## References:

- [1] J.W. Koo et al. APL103, 192401 (2013).[2]Z.C. Wen et al. APL 98, 242507 (2011). [3] T. Burkert et al. PRL93, 027203 (2004). [4] S. Ikeda et al. Nat. Mater9, 721 (2010).[5] Z.C. Wen et al., Adv. Mater26, 6483 (2014).

Topic:

## Future directions in spin caloritronics

Ken-ichi Uchida<sup>1-3</sup>

<sup>1</sup>National Institute for Materials Science, Tsukuba, 305-0047, Japan

<sup>2</sup>Institute for Materials Research, Tohoku University, Sendai 980-8577, Japan

<sup>3</sup>Center for Spintronics Research Network, Tohoku University, Sendai 980-8577, Japan

Email: UCHIDA.Kenichi@nims.go.jp

**Abstract:** In the field of spin caloritronics, the interconversion between spin, charge, and heat currents has been actively investigated from the viewpoints of fundamental physics and thermal energy engineering. In this talk, we summarize basic behaviors, spin-charge-heat current conversion symmetries, and functionalities of spin-caloritronic phenomena and provides directions on future studies in this field.

### 1. INTRODUCTION

In spin caloritronics, novel phenomena, principles, and functionalities based on the interplay between spin, charge, and heat currents have been discovered and investigated [1,2]. This field is still in development, and there are remaining challenges with regard to fundamental physics and materials science. In this talk, we discuss the prospect of spin caloritronics based on recent research activities.

### 2. FUNDAMENTAL PHYSICS VIEWPOINT

Although conventional spin caloritronics focuses on linear-response transport phenomena, investigations on nonlinear spin caloritronics have been recently initiated [3,4]. Fundamental thermoelectric effects consist of not only the Seebeck and Peltier effects but also the Thomson effect, which is a representative nonlinear thermoelectric conversion phenomenon proportional to a temperature gradient and charge current applied to a conductor. As the first step in nonlinear spin caloritronics, the direct observation of the magneto-Thomson effect was reported [3], where a strong magnetic field dependence of the Thomson coefficient appeared in Bi<sub>88</sub>Sb<sub>12</sub>. In the nonlinear regime, several spin-caloritronic phenomena, such as electron-driven spin-dependent Thomson and magnon-driven spin Thomson effects, remain to be observed. Exploring these phenomena will further invigorate the fundamental studies on spin caloritronics.

Moreover, the expansion of the physics of spin caloritronics to other fields and materials is important. One of such research directions is polarization caloritronics using ferroelectrics [5,6]; Bauer et al. theoretically predicted unconventional thermoelectric effects based on the dielectric polarization transport. The experimental verification of such phenomena requires the interdisciplinary fusion of spin caloritronics, ferroelectrics, and nanoscale science. In [7], a new field called opto-spin-caloritronics has been proposed, where 2D van der Waals ferromagnets play an essential role to optically control and enhance thermo-spin conversion properties. Combined with sophisticated interface engineering in magnetic heterostructures, 2D and low-dimensional materials may be key materials in next-generation spin caloritronics.

### 3. MATERIALS SCIENCE VIEWPOINT

To realize the application of spin caloritronics, it is necessary to significantly improve the thermo-spin/thermoelectric conversion performance. Thus, it is essential to develop materials with high spin-charge-heat interconversion properties. The recent fusion of spin caloritronics and topological materials science is a part of this effort.

In addition to monolithic materials, hybrid or composite materials can be used to enhance the thermo-spin and magneto-thermoelectric conversion performances. For example, the hybrid thermoelectric generation based on the spin Seebeck and anomalous Nernst effects is enabled in ferromagnetic metal/ferromagnetic insulator junction systems and ferromagnetic/nonmagnetic bulk nanocomposites. Furthermore, Zhou et al. proposed and demonstrated unconventional transverse thermoelectric generation appearing in thermoelectric semiconductor/magnetic metal hybrid materials [8]. As this effect originates from the artificial hybridization of the Seebeck effect in the thermoelectric semiconductor and anomalous Hall effect in the magnetic metal, it is called the Seebeck-driven transverse thermoelectric generation. Zhou et al. showed that an n-type Si/Co<sub>2</sub>MnGa (p-type Si/Co<sub>2</sub>MnGa) hybrid material exhibits a transverse thermopower of 82.3  $\mu\text{VK}^{-1}$  ( $-41.0 \mu\text{VK}^{-1}$ ) at room temperature, which is much larger than the anomalous Nernst coefficient. These experiments confirmed the usefulness of hybrid or composite materials, which may be a breakthrough approach for the application of spin caloritronics.

### REFERENCES

- [1] K. Uchida, Proc. Jpn. Acad., Ser. B **97**, 69 (2021).
- [2] K. Uchida and R. Iguchi, J. Phys. Soc. Jpn. **90**, 122001 (2021).
- [3] K. Uchida et al., Phys. Rev. Lett. **125**, 106601 (2020).
- [4] R. Modak et al., Appl. Phys. Rev. **9**, 011414 (2022).
- [5] G. E. W. Bauer, R. Iguchi, and K. Uchida, Phys. Rev. Lett. **126**, 187603 (2021).
- [6] P. Tang et al., Phys. Rev. Lett. **128**, 047601 (2022).
- [7] M.-H. Phan et al., Appl. Phys. Lett. **119**, 250501 (2021).
- [8] W. Zhou et al., Nature Mater. **20**, 463 (2021).

# Spin to charge conversion in polycrystalline topological insulator

Braj Bhusan Singh<sup>\*1</sup>, Sukanta Kumar Jena<sup>1</sup>, Manisha Samanta<sup>2</sup>, Kanishka Biswas<sup>2</sup>, and Subhankar Bedanta<sup>1</sup>

<sup>1</sup>Laboratory for Nanomagnetism and Magnetic Materials (LNMM), School of Physical Sciences, National Institute of Science Education and Research (NISER), HBNI, Jatni-752050, India

<sup>2</sup>Nehru Centre for Advanced Scientific Research, Jakkur, Bangalore, 560064, India

\*Email: [brajbhusan@niser.ac.in](mailto:brajbhusan@niser.ac.in)

The generation and efficient transport of pure spin current is a prerequisite for the development of next-generation spintronics devices [1,2]. Production of spin current in ferromagnetic (FM)/nonmagnetic (NM) heterostructures through pumping of spin waves from a FM layer by ferromagnetic resonance spectroscopy is a widely used method [3]. Efficient conversion from charge to spin current depends on the strength of spin orbit coupling (SOC) of the NM layer. Topological insulator materials have drawn attention due to spin momentum locking of surface states which give high SOC [4]. However, it is a big question whether the polycrystalline or amorphous nature of topological insulators will preserve their surface states or not. Measurement of spin to charge conversion in such polycrystalline topological insulators will help to understand the underlying physics. Here, we fabricated polycrystalline  $\text{Bi}_2\text{Se}_3$  using electron beam evaporation and observed the inverse spin Hall effect through spin pumping by the CoFeB layer. Magnetotransport studies and structural characterization have shown the excellent quality of  $\text{Bi}_2\text{Se}_3$ . A typical frequency-dependent inverse spin Hall voltage ( $V$ ) is shown in figure 1 [5].

## References

- [1] Y. Tserkovnyak, A. Brataas, G. E. W. Bauer, and B. I. Halperin, *Nonlocal Magnetization Dynamics in Ferromagnetic Heterostructures*, Rev. Mod. Phys. **77**, 1375 (2005).
- [2] B. B. Singh and S. Bedanta, *Large Spin Hall Angle and Spin-Mixing Conductance in the Highly Resistive Antiferromagnet  $\text{Mn}_2\text{Au}$* , Phys. Rev. Applied **13**, 044020 (2020).
- [3] K. Chen and S. Zhang, *Spin Pumping in the Presence of Spin-Orbit Coupling*, Phys. Rev. Lett. **114**, 126602 (2015).
- [4] A. R. Mellnik, J. S. Lee, A. Richardella, J. L. Grab, P. J. Mintun, M. H. Fischer, A. Vaezi, A. Manchon, E.-A. Kim, N. Samarth, and D. C. Ralph, *Spin-Transfer Torque Generated by a Topological Insulator*, Nature **511**, 449 (2014).
- [5] B. B. Singh, S. K. Jena, M. Samanta, K. Biswas, and S. Bedanta, *High Spin to Charge Conversion Efficiency in Electron Beam-Evaporated Topological Insulator  $\text{Bi}_2\text{Se}_3$* , ACS Appl. Mater. Interfaces **12**, 53409 (2020).

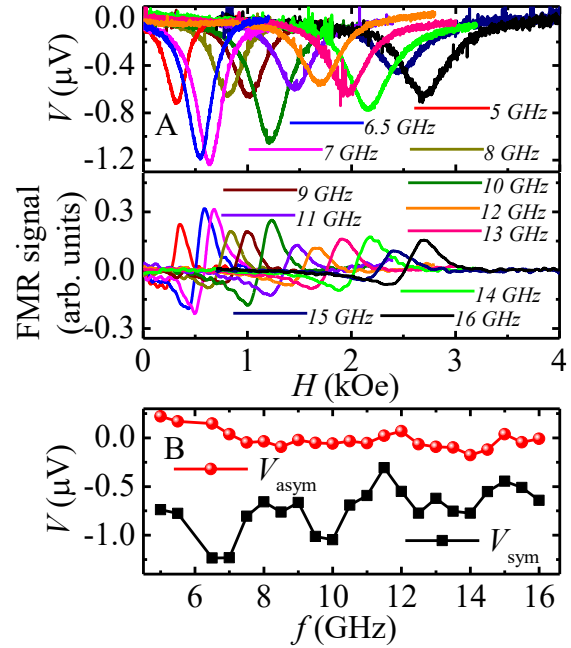


Figure 1(A) Frequency dependent  $V$  versus  $H$  (Top panel) and FMR signal (Bottom panel) for sample  $\text{Bi}_2\text{Se}_3/\text{CoFeB}/\text{TaO}_x$ . (B) The symmetric and antisymmetric components  $V_{\text{sym}}$  and  $V_{\text{asym}}$  versus frequency. for sample  $\text{Bi}_2\text{Se}_3/\text{CoFeB}/\text{TaO}_x$

**Asymmetric magnetic domain wall motion under lateral and normal space inversion  
asymmetry with interfacial Dzyaloshinskii-Moriya interaction**

P. S. Anil Kumar, IISc Bangalore



## **Investigation of emerging phenomena at the interface of heterostructures using polarized neutron reflectivity**

Surendra Singh

Solid State Physics Division, Bhabha Atomic Research Centre Mumbai 400085

### Abstract:

The magnetic interaction at interfaces between different ferromagnetic materials can be modified by exploiting interface morphology, which subsequently can be utilized to engineer materials with magnetic properties that are significantly different from the bulk. The rare-earth/transition-metal (RE/TM) ferromagnetic (FM) multilayers are a classic example, where a strong antiferromagnetic (AFM) exchange coupling at interfaces can lead to novel magnetic states and phase transitions between them. The compensated RE-TM heterostructures and alloy films are intensively investigated because of their possible promising applications in the field of all-optical switching, and magnetic storage devices with high speed and density. Here, I will describe two systems (Fe/Ge [1] and Gd/Co [2-4] heterostructures), which are promising systems to be used for possible application in the field of spintronics as interface structure, morphology and magnetism in these systems play important role for possible applications. I will discuss these aspects of interface characterization using polarized neutron reflectivity in this talk.

[1] S. Singh et al., Applied Surface Science, 570, 151193 (2021).

[2] S. Singh et al., Physical Review B 100, 140405 (R) (2019).

[3] M A Basha et al., Journal of Applied Physics, 128, 103901 (2020).

[4] M A Basha et al., Journal of Magnetism and Magnetic Materials, 516, 167331 (2020).

# Exciting physics at the interface of organic semiconductor/ferromagnet interfaces

Subhankar Bedanta<sup>a</sup>

<sup>a</sup>Laboratory for Nanomagnetism and Magnetic Materials, School of Physical Sciences, National Institute of Science Education and Research (NISER), An OCC of Homi Bhabha National Institute (HBNI), Jatni 752050, Odisha, India

\*Email: sbedanta@niser.ac.in

**Abstract:** Spin dependent hybridization phenomena that occur at the ferromagnet (FM)/organic semiconductor (OSC) interface is very promising for fabricating highly efficient spintronic device. The effect of such hybridized interface (known as 'spinterface') on tailoring fundamental magnetic properties of various FM/OSC and non-magnet (NM)/OSC system is studied in details. Magnetization reversal mechanism found to be strongly modified by the introduction of a fullerene (C<sub>60</sub>) layer on top of a FM or NM layer. In addition the induction of magnetic moment from the FM to the C<sub>60</sub> layer has also been observed by polarized neutron reflectivity (PNR) studies. Although made up of light element carbon (C), fullerene molecule shows an enhanced spin-orbit-coupling due to their curved structure. Owing to the enhanced SOC of C<sub>60</sub> a pronounced spin-pumping and inverse spin Hall effect (ISHE) has also been observed in a CoFeB/C<sub>60</sub> system. In addition the emergence of Dzyaloshinskii-Moriya interaction (DMI) from a Co/C<sub>60</sub> interface makes fullerene very promising carbon allotrope for spintronic device applications.

## 1. INTRODUCTION

Interface induced phenomenon in FM/OSC is an emerging topic towards organic spintronics [1, 2]. Buckminsterfullerene (C<sub>60</sub>) is a potential candidate for organic spintronics due to many desirable properties viz. low spin orbit coupling, long spin diffusion lengths and large spin relaxation times at room temperature etc. [3]. It has been observed that C<sub>60</sub> acquire ferromagnetism when deposited on top of FM [3-6]. A broadening and shifting of the molecular density of states (DOS) has been observed due to the interfacial hybridization occur at FM/OSC interface. We primarily aim to tailor magnetic properties of several FM/OSC or NM/OSC systems, by utilizing the interfacial hybridization phenomena.

## 2. EXPERIMENTAL DETAILS

Metallic and OSC layers have been prepared by magnetron sputtering and thermal evaporation techniques, respectively. Magnetization reversal and domain imaging performed by magneto optic Kerr effect (MOKE) based microscopy. Layer selective and element specific magnetic moments has been quantified using PNR and X-ray magnetic circular dichroism (XMCD) techniques, respectively. ISHE measurements have been performed using ferromagnetic resonance (FMR) spectroscopy. Interfacial DMI has been quantified by the asymmetric domain expansion method using MOKE microscope.

## 3. RESULTS AND DISCUSSIONS

We have prepared single layers of Fe, Co and CoFeB, and compared the magnetic properties with the bilayers of Fe/C<sub>60</sub>, Co/C<sub>60</sub> and CoFeB/C<sub>60</sub>. The films were prepared on both MgO (001) and Si (100) substrates to study the effect of crystallinity. MOKE based microscopy measurements shows a pronounced effect of the magnetic C<sub>60</sub> layer on the hysteresis loop and the domain images of the FM (Fe, Co or CoFeB) layers [4-7]. Finite magnetic moment is found to induce in the

C<sub>60</sub> layer in case of in-plane anisotropic Fe/C<sub>60</sub> and Co/C<sub>60</sub>, as studied by PNR technique [4-6]. However, for Cu/C<sub>60</sub> system, a charge transfer takes place from Cu to C<sub>60</sub> leading to a modified DOS and introduction of ferromagnetism in Cu [8]. Modification of perpendicular magnetic anisotropy (PMA) by the insertion of organic layer has also been investigated both experimentally and theoretically. In this context a model Pt/Co/C<sub>60</sub> system has been fabricated which shows an increase in PMA and decreases in the domain size by introducing a C<sub>60</sub> layer on top of Pt/Co [9]. Further, we have also observed an enhancement in domain wall velocity and emergence of interfacial DMI in a Pd/Co/C<sub>60</sub> system owing to the curvature enhanced SOC of C<sub>60</sub> [10]. Such enhanced SOC effect of C<sub>60</sub> has also give rise to few other phenomena, spin pumping and ISHE at the CoFeB/C<sub>60</sub> interface [11].

## 4. ACKNOWLEDGEMENT

I like to sincerely acknowledge my co-workers Dr. Srijani Mallik, Ms. Purbasha Sharangi, Dr. Sagarika Nayak, Ms. Esita Pandey, Dr. Braj Bhusan Singh., and my collaborators Prof. Thomas Brueckel, Dr. Stefan Mattauch, Dr. Biswarup Satpati for their continuous support. I also thank various funding agencies (DAE, DST-SERB, DST-Nanomission, NFFA etc.) for their generous funding to support our work.

## 4. REFERENCES

- [1] S. Sanvito, Nat. Phys. **6** (2010), 562–564.
- [2] W. Naber *et al.*, J. Phys. D: Appl. Phys. **40** (2007), R205.
- [3] T. Moorsom, *et al.*, Phys. Rev. B **90** (2014), 125311.
- [4] S. Mallik *et al.*, Scientific Reports **8** (2018), 5515.
- [5] S. Mallik *et al.*, Nanotechnology **30** (2019), 435705.
- [6] S. Mallik, *et al.*, Appl. Phys. Lett. **115** (2019), 242405.
- [7] P. Sharangi *et al.*, J. Phys. Chem. C, **125**, 25350 (2021)
- [8] P. Sharangi *et al.*, Phys. Chem. Chem. Phys., **23** (2021), 6490–6495.
- [9] P. Sharangi *et al.*, [arXiv: 2012.12777](https://arxiv.org/abs/2012.12777) (under review).
- [10] E. Pandey *et al.*, manuscript under preparation.
- [11] P. Sharangi *et al.*, [arXiv: 2106.06829](https://arxiv.org/abs/2106.06829) (manuscript under review)

## Fabricating L1<sub>0</sub>-ordered FeNi films by denitridding FeNiN films

**Keita Ito<sup>1,2</sup>, Takumi Ichimura<sup>1</sup>, Masahiro Hayashida<sup>1</sup>, Takahiro Nishio<sup>3</sup>, Hiroaki Kura<sup>3</sup>,  
Hideto Yanagihara<sup>4</sup>, Koki Takanashi<sup>1,2,5</sup>**

<sup>1</sup>Institute for Materials Research, Tohoku University, Sendai, Japan

<sup>2</sup>Center for Spintronics Research Network, Tohoku University, Sendai, Japan

<sup>3</sup>Advanced Research and Innovation Center, DENSO CORPORATION, Aichi, Japan

<sup>4</sup>Department of Applied Physics, University of Tsukuba, Ibaraki, Japan

<sup>5</sup>Center for Science and Innovation in Spintronics, Tohoku University, Sendai, Japan

Email: keita.ito.e3@tohoku.ac.jp

**Abstract:** An L1<sub>0</sub>-ordered FeNi alloy has been focused on as a high saturation magnetization and large uniaxial magnetic anisotropy material for a new permanent magnet material. In this presentation, we would like to introduce recent progress on the synthesis of L1<sub>0</sub>-FeNi films using a topotactic denitridding method to FeNiN films and show the possibility of applying L1<sub>0</sub>-FeNi to permanent magnets.

### 1. INTRODUCTION

An L1<sub>0</sub>-ordered FeNi alloy has been focused as a rare-earth free high uniaxial magnetic anisotropy energy ( $K_u$ ) ferromagnetic material [1]. The synthesis of polycrystalline L1<sub>0</sub>-FeNi powder by denitridding FeNiN powder was reported, and a degree of order ( $S_{\text{FeNi}}$ ) of 0.71 was achieved [2]. FeNiN(100) films were grown by co-deposition molecular beam epitaxy (MBE) on SrTiO<sub>3</sub>(001) substrates, and L1<sub>0</sub>-FeNi(100) films were fabricated by denitridding the FeNiN(100) films [3]. Although its  $S_{\text{FeNi}}$  was large (0.87),  $K_u$  was smaller than the value expected from the relationship between  $S_{\text{FeNi}}$  and  $K_u$  in L1<sub>0</sub>-FeNi(001) films fabricated by the alternating deposition of Fe and Ni [4]. It was considered that the net  $K_u$  value was suppressed due to the formation of two nanometer-sized variants with in-plane  $c$ -axis intersecting at 90° [3]. Therefore, the exact  $K_u$  value, which is not suppressed by the existence of variants, can be evaluated by fabricating variant-free L1<sub>0</sub>-FeNi films. The purpose of this work is fabrication of variant-free L1<sub>0</sub>-FeNi(110) films by denitridding epitaxially grown FeNiN(110) films and evaluation of exact  $K_u$  value.

### 2. EXPERIMENT

FeNiN films (20 nm) were epitaxially grown on LaAlO<sub>3</sub>(110) substrates by co-deposition of Fe, Ni, and radio-frequency N<sub>2</sub> plasma by MBE changing substrate temperatures ( $T_s$ ) from 150 to 350 °C. L1<sub>0</sub>-FeNi films were fabricated by denitridding the FeNiN films at 200 °C for 2 h under the H<sub>2</sub> gas with a flow rate of 2.0 L/min. The structures of the samples were characterized by X-ray diffraction (XRD) measurements. For evaluation of  $S_{\text{FeNi}}$ , anomalous XRD measurements were conducted. The  $K_u$  values of the L1<sub>0</sub>-FeNi films were calculated from in-plane magnetization curves of the samples measured at room temperature.

### 3. RESULTS

A variant-free FeNiN(110) film was obtained at  $T_s = 350$  °C. After denitridding,  $S_{\text{FeNi}} = 0.22$  and  $K_u = 0.31$  MJ/m<sup>3</sup> were achieved. In order to improve the degree of order of FeNiN ( $S_{\text{FeNiN}}$ ) and  $S_{\text{FeNi}}$ , a FeNiN(110)

film was annealed at 325 °C for 20 h under NH<sub>3</sub> gas with a flow rate of 5.0 L/min. As a result,  $S_{\text{FeNiN}}$  improved from 0.82 to 0.92, and  $S_{\text{FeNi}} = 0.45$  and  $K_u = 0.55$  MJ/m<sup>3</sup> were obtained. At around  $S_{\text{FeNi}} = 0.5$ , the variant-free (110)-oriented film fabricated by denitridding shows a larger  $K_u$  than those of the (100)-oriented films with variants, and shows a similar value with that of the (001)-oriented films grown by the alternating deposition method [3]. Therefore, it is expected that larger  $S_{\text{FeNi}}$  and  $K_u$  will be realized by further optimization of the growth and denitridding conditions of the FeNiN(110) films.

### ACKNOWLEDGEMENT

This work was supported by the Future Pioneering Program “Development of magnetic material technology for high-efficiency motors” (JPNP14015) commissioned by the New Energy and Industrial Technology Development Organization (NEDO), Japan. The anomalous XRD was conducted at the BL46XU of SPring-8 (2021B1924), Japan. We thank Dr. T. Koganezawa, JASRI, for his support in the anomalous XRD

### REFERENCES

- [1]. K. Takanashi *et al.*, J. Phys. D: Appl. Phys. **50**, 4830032 (2017).
- [2]. S. Goto *et al.*, Sci. Rep. **7**, 13216 (2017).
- [3]. K. Ito *et al.*, Appl. Phys. Lett. **116**, 242404 (2020).
- [4]. T. Kojima *et al.*, Jpn. J. Appl. Phys. **51**, 010204 (2012).

## 2DEG characteristic difference between stoichiometric LaScO<sub>3</sub>/STO and non-stoichiometric Ca<sub>x</sub>Ta<sub>y</sub>O<sub>3+δ</sub>/STO

Anjana Dogra<sup>1,2</sup>, Sumit Kumar<sup>1,2</sup>, Biswarup Satpati<sup>3</sup>, D S Rana<sup>4</sup>, A. K. Shukla<sup>1,2</sup>, Sunil Ojha<sup>5</sup>,  
Sonu Chhillar<sup>6</sup>, C.S.Yadav<sup>6</sup>, Bhasker Gahtori<sup>1,2</sup>, J. J. Pulikkotil<sup>1,2</sup>,

<sup>1</sup>CSIR-National Physical Laboratory, Dr. K. S. Krishnan Road, New Delhi 110012, India

<sup>2</sup>Academy of Scientific and Innovative Research, CSIR-NPL Campus, New Delhi 110012, India

<sup>3</sup>Surface Physics & Material Science Division, Saha Institute of Nuclear Physics, Kolkata 700 064, India

<sup>4</sup>Indian Institute of Science Education and Research Bhopal, Bhopal 462066, India.

<sup>5</sup>Inter University Accelerator Centre, Aruna Asaf Ali Marg, New Delhi, 110067 India.

<sup>6</sup>School of Basic Sciences, Indian Institute of Technology Mandi, Kamand, Mandi-175075, India

### ABSTRACT

Two different oxide interfaces has been explored to demonstrate quasi-2 dimensional electron gas (q-2DEG) i.e. LaScO<sub>3</sub>/SrTiO<sub>3</sub> (LSO/STO) and Ca<sub>x</sub>Ta<sub>y</sub>O<sub>3+δ</sub>/STO (CTO/STO). With the similar pulsed laser deposition conditions LSO/STO comes out to be stoichiometric whereas CTO/STO is non-stoichiometric. Both the systems are highly crystalline with abrupt heterointerface and exhibit layer by layer growth. The experiment shows that a q-2DEG type charge transport in LaScO<sub>3</sub> that occurs beyond 3unit cell (uc) alike LAO/STO, exhibits the mixed Ti<sup>4+</sup> and Ti<sup>3+</sup> valence states suggesting an intrinsic electronic reconstruction at the interface, leading to metallic nature. However in the case of CTO/STO q-2DEG becomes effective only after 8uc of the film-thickness and the non-stoichiometry of epitaxial thin films, obtained from Rutherford backscattering measurements, makes the origin mechanism quite complex with active role of lattice structure and disorder. For both the concentrations the measured room temperature carrier concentration ( $n_s$ ) of the order of  $10^{13}$  cm<sup>-2</sup> at the interface and carrier mobility ( $\mu_H$ ) of 4-7 cm<sup>2</sup>V<sup>-1</sup>s<sup>-1</sup>. However we also show that conductivity is not abruptly changing with thickness of CTO/STO interface after critical thickness and mobility is also not a function of film thickness, the nature that yet not observed in earlier systems or our LSO/STO system. The study offers a new perovskite interface for unraveling the q-2DEG phenomena towards a clear mechanism and futuristic applications.

## Topological Hall effect in multilayers of kagome-lattice ferromagnet Fe<sub>3</sub>Sn and Pt

K. Fujiwara<sup>1</sup> and A. Tsukazaki<sup>1,2,3</sup>

<sup>1</sup>IMR, Tohoku Univ., <sup>2</sup>CSRN, Tohoku Univ., <sup>3</sup>CSIS, Tohoku Univ.

Email: kohei.fujiwara@tohoku.ac.jp

**Abstract:** A triangular-based kagome lattice composed of magnetic elements provides an attractive arena for exploring nontrivial magnetic phases, spin textures, and topological electronic states. By fabricating multilayers of kagome-lattice ferromagnet Fe<sub>3</sub>Sn and Pt, we show that the inherent coplanar spin state with in-plane magnetic anisotropy in the Fe<sub>3</sub>Sn kagome plane can be changed to a non-coplanar one through the interfacial Dzyaloshinskii-Moriya interaction. On the basis of the observation of topological Hall effect, which evidences finite scalar spin chirality, we discuss the possible formation of skyrmion crystal phase.

### 1. INTRODUCTION

Magnetic materials with a triangular-based lattice have garnered attention for their exotic magnetic properties arising from the geometrical frustration. Recently, from the perspective of topological physics, renewed interest has arisen, particularly on kagome-lattice ferromagnets. For example, Co<sub>3</sub>Sn<sub>2</sub>S<sub>2</sub> and Fe<sub>3</sub>Sn<sub>2</sub> exhibit large intrinsic anomalous Hall effect and anomalous Nernst effect owing to the topological band feature that is cooperatively produced by the linearly dispersed band, spin-orbit coupling, and ferromagnetic order. Utilizing these superior functionalities is now envisaged in spintronics.

The triangular-based kagome lattice may also be suited to delicate control of spin interactions and resulting spin textures. One interesting target is a vortex-like swirling spin texture called the magnetic skyrmion, which is proposed to be used as a new information carrier in magnetic memory devices [1]. In non-centrosymmetric bulk crystals [2], the formation of the magnetic skyrmion is discussed based on the detection of topological Hall effect (THE) that reflects finite scalar spin chirality. In this study, by fabricating an interface of kagome-lattice ferromagnet Fe<sub>3</sub>Sn (Fig. 1(a)) with in-plane magnetic anisotropy and Pt, we have modulated the spin interactions through the interfacial Dzyaloshinskii-Moriya interaction (DMI) and observed THE [3].

### 2. RESULTS AND DISCUSSION

The  $t$ -nm-thick Fe<sub>3</sub>Sn films were deposited on 10-nm-thick Pt(111) / Al<sub>2</sub>O<sub>3</sub>(0001) by radio-frequency magnetron sputtering (Fig. 1(b)). The D<sub>0</sub>1<sub>9</sub>-type kagome-lattice Fe<sub>3</sub>Sn phase and its  $c$ -axis oriented growth were identified by transmission electron microscopy analysis. Figures 1(c) and (d) show the results of Hall effect measurement for  $t = 0.80$  nm with the bulk-like in-plane anisotropy and  $t = 0.40$  nm with perpendicular-like anisotropy, respectively, as confirmed by magnetization measurement. While the Hall resistance  $R_{yx}$  of  $t = 0.80$  nm is governed by the ordinary Hall component proportional to the applied magnetic field and the anomalous Hall component proportional to the magnetization,  $R_{yx}$  of  $t = 0.40$  nm shows hump-like anomalies (indicated by the black arrows in (d)) that are explained neither by ordinary

Hall effect nor by anomalous Hall effect. From control experiments using different multilayer structures, we reveal that the  $R_{yx}$  humps originate from THE due to a non-coplanar spin state with finite spin chirality induced by the interfacial DMI. The calculation of the effective size of the magnetic skyrmion and numerical simulation that takes into account the contribution corresponding to the interfacial DMI are also presented. Our results shed light on a new attractive potential of kagome-lattice ferromagnets—spin chirality engineering towards skyrmion-based spintronic devices.

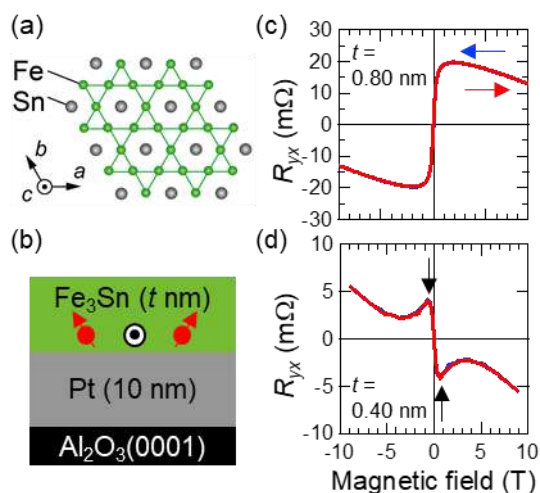


Fig. 1. (a) Fe<sub>3</sub>Sn kagome layer in D<sub>0</sub>1<sub>9</sub>-type Fe<sub>3</sub>Sn. (b) Schematic image of Fe<sub>3</sub>Sn( $t$  nm) on Pt / Al<sub>2</sub>O<sub>3</sub>(0001) substrate and non-coplanar spin state induced by the interfacial DMI ( $\mathbf{D}$ : DMI vector). (c) and (d) Hall resistance  $R_{yx}$  versus magnetic field curves measured for  $t = 0.80$  nm and 0.40 nm at 400 K, respectively. The blue and red arrows indicate the field-sweep directions.

### ACKNOWLEDGEMENT

The authors thank the collaborators, Y. Kato and Y. Motome of Univ. Tokyo, and K. Nomura, T. Seki, and K. Takanashi of IMR, Tohoku. Univ.

### REFERENCES

- [1] A. Fert *et al*, *Nat. Rev. Mater.* **2**, 17031 (2017).
- [2] N. Kanazawa *et al*, *Adv. Mater.* **29**, 1603227 (2017).
- [3] K. Fujiwara *et al*, *Commun. Mater.* **2**, 113 (2021).

# New directions in 2D quantum materials and interfaces with Rashba interaction

Bhaskaran Muralidharan

Department of Electrical Engineering, Indian Institute of Technology Bombay, India

**ABSTRACT:** Using advanced quantum transport modeling on 2D-Xene materials and structures, we propose two novel device functionalities: 1) an all-electrical valley filter using kink states at the interface of quantum spin Hall and the quantum valley Hall state [1] and 2) a quantum topological field effect transistor [2], that can beat the Boltzmann tyranny via engineering the anti-ferromagnetic order.

First, we propose a realizable device design for an all-electrical robust valley filter [1] that utilizes spin protected topological interface states hosted on monolayer 2D-Xene materials with large intrinsic spin-orbit coupling. In contrast with conventional quantum spin-Hall edge states localized around the X-points, the interface states appearing at the domain wall between topologically distinct phases are either from the K or K' points, making them suitable prospects for serving as valley-polarized channels. Our numerical simulations confirm the role of spin-orbit coupling in achieving an improved valley filter performance with a perfect quantum of conductance attributed to the topologically protected interface states. Our analysis further elaborates clearly the right choice of material, device geometry and other factors that need to be considered while designing an optimized valleytronic filter device.

The topological quantum field-effect transition in buckled 2D-Xenes can potentially be engineered to enable sub-thermionic transistor operation coupled with dissipationless ON-state conduction. Detailing the complex band translation physics related to the quantum spin Hall effect phase transition, it is shown that a gating strategy to beat the thermionic limit can be engineered at the cost of sacrificing the dissipationless ON-state conduction. It is then demonstrated that an out-of-plane antiferromagnetic exchange introduced in the material via proximity coupling can incite transitions between the quantum spin-valley Hall and the spin quantum anomalous Hall phase, which can ultimately ensure the topological robustness of the ON state while surpassing the thermionic limit. Our work thus underlines the operational criteria for building topological transistors using quantum materials that can overcome the Boltzmann's tyranny while preserving the topological robustness.

References:

[1] K. Jana and B. Muralidharan, ArXiv:2107.13318, NPJ 2D Materials and Applications (in press) (2022).

[2] S. Banerjee et.al., ArXiv: 2202.12044 (2022).

**BIO OF THE SPEAKER:** Dr. Bhaskaran Muralidharan obtained his B.Tech in Engineering Physics from the Indian Institute of technology (IIT) Bombay in 2001, his M. S. and Ph. D in Electrical Engineering from Purdue University, West Lafayette, USA in 2003 and 2008 respectively. His doctoral work was under the supervision of Prof. Supriyo Datta. Between 2008-2012, he was a post-doctoral associate at the Massachusetts Institute of Technology (MIT) and at the Institute for theoretical Physics at the University of Regensburg, Germany. Since 2012, he has been a faculty in the Department of Electrical Engineering at IIT Bombay, where he is currently a full Professor. He was also the recipient of the APS-IUSSTF professorship award in 2014, the Shastri Indo Canada fellowship 2019 and the SERB-STAR award in 2020. He is also an Associate Editor in the IEEE Transactions on Nanotechnology, on the Editorial board of Scientific Reports and an Editor in Materials for Quantum Technology (IOP).

# Spin dynamics and transport in antiferromagnets

Takahiro Moriyama  
Institute for Chemical Research, Kyoto University, Japan  
Email: mtaka@scl.kyoto-u.ac.jp

**Abstract:** In this presentation, we will discuss our recent results on spin dynamics and spin transport in antiferromagnets.

In antiferromagnetic spintronics where manipulation of the antiferromagnetic spins is a central technological challenge [1], it is important to understand the spin transport and dynamics properties in antiferromagnets. We have recently explored a spin transport in insulating antiferromagnets as well as the control of THz antiferromagnetic dynamics.

We revealed a high-speed spin transport in antiferromagnetic oxides [2] and also showed a long-distance spin transport in crystalline NiO with a particular crystalline orientation [3].

The frequency-domain THz spectroscopies of antiferromagnet led to detail quantitative analysis of the antiferromagnetic damping [4], observation of the THz spin pumping effect in NiO/Pt and NiO/Pd and determination of the spin mixing conductance [5], and control of the antiferromagnetic resonance properties by various cation substitutions of antiferromagnetic oxides [6, 7].

In the presentation, we will discuss above topics in detail.

## REFERENCES

- [1] V. Baltz, T. Moriyama et al., *Rev. Mod. Phys.* **90**, 015005 (2018).
- [2] Y. Sasaki, T. Moriyama, et al., *Appl. Phys. Lett.* **117**, 192403 (2020) [Editor's pick].
- [3] T. Ikebuchi, T. Moriyama et al., *Appl. Phys. Exp.* **14**, 123001 (2021).
- [4] T. Moriyama et al., *Phys. Rev. Mater.* **3**, 051402 (2019).
- [5] T. Moriyama et al., *Phys. Rev. B* **101**, 060402 (2020).
- [6] T. Moriyama et al., *Phys. Rev. Mater.* **4**, 074402 (2020).
- [7] K. Hayashi, T. Moriyama et al., *Appl. Phys. Lett.* **119**, 032408 (2021).

# Polar topology: A new era of ferroelectrics

Sujit Das

Material Research Centre, Indian Institute of Science, Bangalore, 560012, India

## ABSTRACT

Complex topological configurations are a fertile arena to explore novel emergent phenomena and exotic phases in condensed-matter physics. The recent discovery of polarization vortices and the associated complex-phase coexistence and response under applied fields in ferroelectric oxide superlattices, has opened up new vistas to explore topology, emergent phenomena, and approaches for manipulating such features with electric fields<sup>1,2</sup>. Here, by varying epitaxial constraints we report the discovery of room-temperature polar skyrmions in a lead-titanate layer confined by strontium-titanate layers<sup>3</sup>. Phase-field modeling and second-principles calculations reveal that the polar skyrmions have a skyrmion number of +1, and resonant soft X-ray diffraction experiments show circular dichroism confirming chirality. Such nanometer-scale polar skyrmions are the electric analogs of magnetic skyrmions, and could advance ferroelectrics towards new levels of functionality such as negative permittivity, topological phase transition.<sup>4,6</sup> Such functionality has promise for high-frequency electronic applications.<sup>6</sup>

## References

- [1] Yadav, A.K., Nelson, C.T. *et al.*, Observation of polar vortices in oxide superlattices. *Nature* **530**, 198-201 (2016).
- [2] Damodaran, A., Clarkson, J., Hong, Z., Liu, H. *et al.*, Phase coexistence and electric-field control of toroidal order in oxide superlattices. *Nat. Mater.* **16**, 1003 (2017).
- [3] Das, S *et al.*, Observation of room temperature polar skyrmions. *Nature* **568**, 368-372 (2019).
- [4] Li, Q., ....., Das, S. *et al.*, Collective excitations of polar vortices. *Nature* **592**, 376-380 (2021)
- [5] Yadav, A. K., ....., Das, S. *et al.*, Spatially Resolved Steady State Negative Capacitance. *Nature* **565**, 468-471 (2019).
- [6] Das, S. *et al.*, Local negative permittivity and topological phase-transition in polar skyrmions. *Nature Materials* **20**, 194 (2021)



Topic:

## Development of high performance giant magnetoresistive device by interface control

Yuya Sakuraba

Research Center for Magnetic and Spintronic Materials, National Institute for Materials Science (NIMS)

Senri 1-2-1 Tsukuba Japan 305-0047

Email: SAKURABA.Yuya@nims.go.jp

**Abstract:** Recent studies on giant magnetoresistive effect through various heterointerface structures will be introduced. Our study clearly confirmed that even a monolayer structure at the interface strongly affects the spin-dependent transport properties and thus important for developing high performance applications.

### 1. INTRODUCTION

Giant magnetoresistive (GMR) effect is the most traditional spintronic phenomenon and has been utilized for various applications. In particular, the current-perpendicular-to-plane (CPP) GMR is expected to be used for next generation read head for higher capacity HDD. There are also many applications of magnetic sensors using the current-in-plane (CIP) GMR devices. It is well known that the magnitude of magnetoresistance effect is the most important parameters for applications and strongly depends on the not only ferromagnetic material (FM) but the non-magnetic (NM) spacer material and its interface with the FM. Our recent studies have investigated the effect of CIP and CPP spin-dependent transport through the various interfaces such as the half-metallic Heusler/NM interface with the accurately termination-controlled structure [1], half-metallic Heusler/non-half-metallic FM interface [2] and the perfectly lattice matched fully-bcc structure with metastable bcc Cu spacer [3].

### 2. GMR THROUGH VARIOUS INTERFACE

#### 2.1. CPP-GMR with half-metallic Heusler alloy

Large MR ratio at room temperature has been observed in the CPP-GMR with highly spin-polarization in half-metallic Heusler alloys. In our recent studies, we inserted ultrathin Ni layer at the half-metallic  $\text{Co}_2\text{FeGa}_{0.5}\text{Ge}_{0.5}$  (CFGG) and Ag interface and investigate its effect on the interfacial spin-dependent transport [1]. As a result of the MR measurement, we found clear enhancement of MR ratio by inserting just 0.2 nm-thick Ni at the interface (Fig. 1). The state-of-the-art TEM technique enabled us to visualize the interfacial termination; the inserted Ni replaces with the second termination layer from the Ag spacer. (Fig. 1) First principles calculation based on the interfacial structure modelled by TEM images clearly found that the interfacial transmittance of the majority-spin electron can be enlarged by the substitution of one Co layer with Ni, which indicates the even monolayer at the interface critically affects the interfacial spin-dependent transport and MR properties.

Previous many studies on the CPP-GMR have investigated the various combination of FM/NM. However, we recently investigated the effect on interfacial transmittance at the two FM materials, namely half-metallic  $\text{Co}_2\text{Fe}_{0.4}\text{Mn}_{0.6}\text{Si}$  (CFMS) and

CoFe interface. Because of strong exchange coupling between two FM layers, it is not easy to evaluate the effect of spin-dependent interfacial band matching at FM/FM interfaces. Therefore, we have fabricated the devices with CoFe/CFMS/Ag/CFMS/CoFe structure with different thickness CFMS and CoFe layers. We have successfully elucidated the strong positive contribution of the CFMS/CoFe interface scattering on the MR ratio, which was also supported by the first principles calculation of the transmittance. [2]

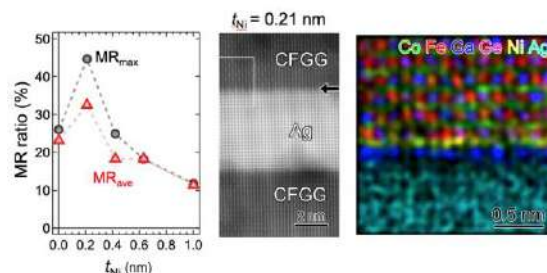


Fig. 1. Inserted Ni thickness layer dependence of MR ratio in CFGG/Ni/Ag/Ni/CFGG CPP-GMR device. The microstructure analysis for the film with  $t_{\text{Ni}} = 0.2$  nm.

#### 2.1. CIP-GMR with the metastable bcc Cu

The interfacial lattice and electronic band matching is also important for CIP-transport. We recently found that very simple CoFe/Cu/CoFe epitaxial film grown on the MgO (001) substrates shows the highest MR ratio of 42% ever reported. Our microstructure analysis found the formation of bcc-Cu in between bcc CoFe gives the suitable electronic band matching to obtain giant CIP-GMR effect. [3] To utilize such large MR effect for practical applications, we developed the structure with CoFe/Rh/CoFe/Cu/CoFe asymmetrically stacked structure and obtained a high linearity of MR response through the biquadratic coupling through Rh layer. [4] Obtained linear sensitivity of 0.047%/mT is comparable to the value observed in the TMR devices with much more complicated stacking structure.

### REFERENCES

- [1]. B. Bükler et al., Phys. Rev. B 103, L140405 (2021)
- [2]. Y. Fujita, et al., Phys. Rev. B 104, L140403 (2021)
- [3]. K. Fathoni et al., APL Materials 7, 111106 (2019)
- [4]. D. Taparia et al., J. Phys. D 54, 255004 (2021).

# **Interfacial origin of unconventional spin-orbit torques in Py/IrMn<sub>3</sub>**

**P. K. Muduli**

**<sup>1</sup>Department of Physics, Indian Institute of Technology Delhi, Hauz Khas, New Delhi-110016, India**

**\*Email: muduli@physics.iitd.ac.in**

The metallic ferromagnet/anti-ferromagnet induces exchange bias, which can be utilized for the field-free operation of memory devices [1]. NiFe/IrMn system, in particular, has been widely studied for the presence of exchange bias. IrMn can also be used for generating spin-orbit torques (SOTs), replacing the role of heavy metal in ferromagnet/heavy metal systems-a conventional system for the generation of SOT [2]. Recently, a giant facet-dependent SOT has also been observed in this system [3]. Here, with the help of angle-resolved spin-torque ferromagnetic resonance measurements, we demonstrate the presence of large unconventional out-of-plane anti-damping torques along with conventional SOTs in polycrystalline IrMn<sub>3</sub> thin films interfaced with NiFe. The NiFe/IrMn<sub>3</sub> system shows a large out-of-plane spin Hall efficiency ( $> 0.12$ ) and in-plane spin Hall efficiency ( $>0.08$ ). However, using a Cu spacer between NiFe/ IrMn<sub>3</sub> interface, all the unconventional components can be obliterated. We also observe a large in-plane spin Hall efficiency ( $>0.16$ ) for the sample with Cu spacer. These results signify the direct correspondence of interfacial effects rather than bulk induced effects and pave a path for efficient spintronic devices with interfacial engineering.

[1] Y.-W. Oh, et al., Nat. Nano. 11, 878 (2016).

[2] W. Zhang, et al., Phys. Rev. Lett. 113, 196602 (2014).

[3] J. Zhou, et al., Phys. Rev. B 101, 184403 (2020).

Topic:

## Manganese-based Materials for Spintronics Applications

Takahide Kubota

Department of Advanced Spintronics Medical Engineering, Graduate School of Engineering,  
Tohoku University, Sendai 980-0845, Japan  
Email: takahide.kubota@tohoku.ac.jp

**Abstract:** In this presentation the author discusses fundamental magnetic properties and perspective for spintronic application of manganese-based materials showing perpendicular magnetic anisotropy and low saturation magnetization.

### 1. INTRODUCTION

Manganese (Mn) is an interesting transition metal element showing various magnetic phases, such as noncollinear-antiferromagnetism (for  $\alpha$ -phase), spin liquid (for  $\beta$ -phase), collinear-antiferromagnetism (for  $\gamma$ - and  $\gamma'$ -phases) [1,2]. Because of the half-filled 3d-valence electron number, relatively large spin magnetic moment can be achieved for Mn atoms when those electrons are localized. In the spintronics research field, Heusler alloys is a functional material class showing, *e.g.*, half-metallic electronic structure which is important for maximizing signals in electronic devices using spin transport phenomena [3]. Among the Heusler alloys, cobalt (Co) based compositions, such as  $\text{Co}_2\text{MnSi}$ , are representative materials for those half-metallic properties demonstrated both in theories and experiments [4-7]. Although the half-metallic Co-Heusler alloys triggered the material study, other properties are also essential for memory device applications, such as magnetoresistive random access memories (MRAMs). For MRAM applications, a reduction of writing current using spin-transfer-torque (STT) is a crucial issue, for which a perpendicularly magnetized material showing high uniaxial anisotropy ( $K_u$ ) with low saturation magnetization ( $M_s$ ) is required. However,  $K_u$  and  $M_s$  are small and large for the Co-based Heusler alloys.

### 2. MANGANESE-BASED MATERIALS

#### 2.1. $\text{Mn}_2$ -Heusler alloys

Some  $\text{Mn}_2$ -Heusler alloys, such as  $\text{Mn}_2\text{VAI}$ ,  $\text{Mn}_2\text{CoGa}$ , also exhibit half-metallic electronic structures with low  $M_s$  because of the ferrimagnetism, however those  $K_u$  are low because of the cubic symmetry of the crystal structures [6,8]. In a recent study, the authors investigated the lattice strain ( $c/a$  ratio where  $c$  and  $a$  are out-of-plane and in-plane lattice constants, respectively) dependence of  $K_u$  in  $\text{Mn}_2\text{CoGa}$  films [9]. The  $c/a$  ratios were successfully controlled by changing underlayer materials and the layer thickness of the  $\text{Mn}_2\text{CoGa}$  layer. The values of  $K_u$  exhibited a positive correlation with  $c/a$ , which reaches about  $1.5 \times 10^5 \text{ J/m}^3$  at room temperature with a  $c/a$  ratio of 1.04. Results of first principles calculations supported the experimental  $c/a$  dependence of  $K_u$ . The first principles calculation also demonstrated relatively high spin polarization of  $\text{Mn}_2\text{CoGa}$  with the strained lattice [9].

#### 2.2. tetragonal Mn-Intermetallic compounds

As another materials class showing low  $M_s$  and high  $K_u$ , Mn-intermetallic compounds showing  $\text{Cu}_2\text{Sb}$ -type crystal structure, *e.g.*  $\text{MnAlGe}$ , is focused here. The Mn atoms exhibits relatively small magnetic moment in the  $\text{Cu}_2\text{Sb}$ -type structure because of those itinerant electronic structure [10]. In addition, recent studies demonstrated that the film samples exhibited relatively large  $K_u$  [11]. The detail will be discussed in the presentation

### ACKNOWLEDGEMENT

The author would like to thank Prof. Koki Takanashi, Prof. Takeshi Seki, Prof. Keita Ito, and the laboratory members for all their supports and discussion. The author also would like to thank Prof. Subhankar Bedanta for fruitful collaboration, and Prof. Yohei Kota for theoretical calculations. The core of experiments was done in Takanashi's laboratory of Institute for Materials Research, Tohoku Univ. This work was partly supported by KAKENHI (JP20K05296), Murata Science Foundation (H30-027), and a cooperative research program (No. 20G0414) of the CRDAM-IMR, Tohoku Univ.

### REFERENCES

- [1]. J. M. D. Coey, Magnetism and Magnetic Materials, Cambridge University Press, Cambridge, 2009.
- [2]. R. Umetsu, *Materia Jpn.* **59**, 125 (2020).
- [3]. C. Felser and A. Hirohata, Ed., Heusler Alloys, Springer International Publishing, Switzerland, 2016.
- [4]. J. Kubler *et al.*, *Phys. Rev. B* **28**, 1745 (1983).
- [5]. S. Ishida *et al.*, *J. Phys. Soc. Jpn.* **64**, 2152 (1995).
- [6]. I. Galanakis *et al.*, *Phys. Rev. B* **66**, 174429 (2002).
- [7]. Y. Sakuraba *et al.*, *Jpn. J. Appl. Phys.* **44**, L1100 (2003).
- [8]. V. Allijani *et al.*, *Appl. Phys. Lett.* **99**, 222510 (2011).
- [9]. T. Kubota *et al.*, *Phys. Rev. Mater.* *in press*; arXiv: 2108.11547.
- [10]. K. Motizuki *et al.*, Electronic Structure and Magnetism of 3d-Transition Metal Pnictides, Springer, Berlin Heidelberg, 2009
- [11]. T. Kubota *et al.*, *Appl. Phys. Lett.* **118**, 262404 (2021).

# KTaO<sub>3</sub> – The New Kid on the Spintronics Block

*Suvankar Chakraverty*

Quantum Materials and Devices Unit, Institute of Nano Science and Technology, Sector-81, Punjab, 140306,  
India.

## **Abstract**

Long after the heady days of high-temperature superconductivity, the oxides came back into the limelight in 2004 with the discovery of the two-dimensional electron gas in SrTiO<sub>3</sub> and several heterostructures based on it. Not only do these materials exhibit interesting physics, they have opened up new vistas in oxide electronics and spintronics. However, much of the attention has recently shifted to KTaO<sub>3</sub>, a material with all the ‘good’ properties of SrTiO<sub>3</sub> (simple cubic structure, high mobility, etc.) but with the additional advantage of a much larger spin-orbit coupling. In this state-of-the-art review of the fascinating world of KTaO<sub>3</sub>, we attempt to cover the remarkable progress made, particularly in the last five years. We also indicate certain unsolved issues, while suggesting future research directions as well as potential applications. The range of physical phenomena associated with the two-dimensional electron gas trapped at the interfaces of KTaO<sub>3</sub>-based heterostructures include spin polarization, superconductivity, quantum oscillations in the magnetoresistance, spin-polarized electron transport, persistent photocurrent, Rashba effect, topological Hall effect, and inverse Edelstein Effect. We aim to discuss, on a single platform, the various fabrication techniques, the exciting physical properties and future application possibilities of this family of materials.

# Emergent quantum transport due to quenched magnetic impurity scattering by antiferromagnetic proximity in SrCuO<sub>2</sub>/SrIrO<sub>3</sub>

Subhadip Jana,<sup>1,2</sup> T. Senapati,<sup>3,2</sup> S.N. Sarangi,<sup>1</sup> K. Senapati,<sup>3,2</sup> and D. Samal<sup>1,2</sup>

<sup>1</sup>*Institute of Physics, Bhubaneswar, 751005, India*

<sup>2</sup>*Homi Bhabha National Institute, AnushaktiNagar, Mumbai, 400094, India*

<sup>3</sup>*School of Physical Sciences, National Institute of Science Education and Research, Bhubaneswar, 752050, India*

**Abstract:** The interplay among different types of microscopic electron scattering process in a conducting system greatly influences the observed macroscopic physical properties. Gaining control over these scatterings in complex materials is a critical step to advance the understanding that can have technological implications. We find the evidence for quenched magnetic impurity scattering in a spin orbit coupled semimetal SrIrO<sub>3</sub> proximitized with an antiferromagnetic SrCuO<sub>2</sub> layer from quantum interference originated magnetoconductance study. Further, we remarkably observe chiral anomaly induced topological Dirac semimetallic transport behaviour in SrCuO<sub>2</sub>/SrIrO<sub>3</sub> bilayer as a consequence of quenched magnetic impurity scattering. Compared to the results on bare SrIrO<sub>3</sub> film, antiferromagnetic proximity effect in SrCuO<sub>2</sub>/SrIrO<sub>3</sub> is found to be an effective way to quench magnetic impurity scattering and preserve quantum phenomena in SrIrO<sub>3</sub>.

Topic:

## Electric field effect of Fe/MgO interface in magnetic tunnel junctions

Masaki Mizuguchi

Nagoya University, Furo-cho, Chikusa, Nagoya, Japan

Email: mizuguchi.masaki@material.nagoya-u.ac.jp

**Abstract:** X-ray fluorescence holography of thin films with a magnetic tunnel junction structure under an electrical field was measured to investigate the change of atomic structures. Clear holography patterns were observed for a stack of Ru (5 nm) / Cr (10 nm) / MgO (3 nm) / Fe (0.7 nm) / Cr (40 nm) / MgO(001)-substrate, and the patterns were substantially different depending on the applied voltage. This reveals that an atomic local structure of Fe changes by electric field.

### 1. INTRODUCTION

An electric field effect on spintronic devices such as magnetic tunnel junction (MTJ) is attracting attention because it enables us to control various functions of the devices[1, 2]. However, the origin of the effect based on the change of atomic structures has not been elucidated[3]. X-ray fluorescence holography (XFH) is a powerful tool for resolving the local structure, enabling the three-dimensional atomic environment to be visualized around a selected element within a radius of nanometers orders[4]. Thus, this method would be utilized for the investigation of the electric-field effect on atomic structures in spintronic devices. In this study, XFH of thin films with an MTJ structure under an electrical field was measured to investigate the change of atomic structures.

### 2. EXPERIMENTALS

An MTJ device with a stack of Ru (5 nm) / Cr (10 nm) / MgO (3 nm) / Fe (0.7 nm) / Cr (40 nm) / MgO(001)-substrate was fabricated by sputtering in ultrahigh vacuum. A device portion was microfabricated to  $30 \times 30 \mu\text{m}^2$  and electrodes to apply voltage were equipped. XFH data were measured at incident X-ray energies of 7.5–11.0 keV in 0.5 keV steps at BL39XU of the SPring-8 synchrotron radiation facility. Fe  $K\alpha$  fluorescent X-rays from the samples were analyzed and focused on an avalanche photodiode detector by using a toroidally bent graphite crystal. The azimuthal angle of the sample and the incident angle were varied during the measurements.

### 3. FIGURES AND IMAGES

Figure 1 shows resonant X-ray fluorescence holography patterns of an MTJ device with a stack of Ru (5 nm) / Cr (10 nm) / MgO (3 nm) / Fe (0.7 nm) / Cr (40 nm) / MgO(001)-substrate with 0 V and -1 V. Clear holography patterns were observed, and the patterns were substantially different depending on the applied voltage. This reveals that an atomic local structure of Fe changes by electric field. In the presentation, more precise analysis of the holography patterns will be discussed.

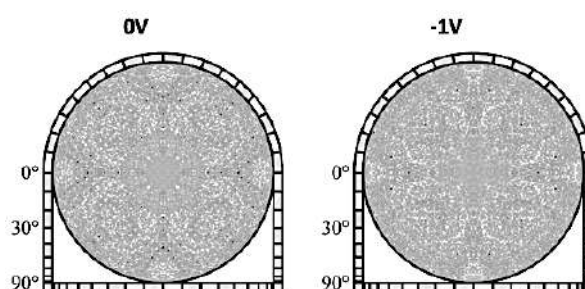


Fig.1. Resonant X-ray fluorescence holography patterns of an MTJ device with a stack of Ru (5 nm) / Cr (10 nm) / MgO (3 nm) / Fe (0.7 nm) / Cr (40 nm) / MgO(001)-substrate with 0 V and -1 V.

### ACKNOWLEDGEMENT

This study was performed under the collaboration with Dr. Himanshu Sharma, Dr. Naohisa Happo, Dr. Kouichi Hayashi, Dr. Koji Kimura, Dr. Artoni Ang, Dr. Qingyi Xiang, Dr. Hiroaki Sukegawa, and Dr. Seiji Mitani. This study was partly supported by a Grant-in-Aid for Scientific Research on Innovative Areas (Grant Number:

17H05208) from Japan Society for the Promotion of Science.

### REFERENCES

- [1] T. Maruyama, M. Mizuguchi *et al.*, *Nat. Nanotech.*, **4**, 158 (2009).
- [2] T. Nozaki *et al.*, *Phys. Rev. Appl.*, **5**, 044006 (2016).
- [3] V. B. Naik, *et al.*, *Appl. Phys. Lett.*, **105**, 052403 (2014).
- [4] K. Hayashi, *et al.*, *J. Phys. D*, **24**, 093201 (2012).

# Nanoscale nonlocal devices to study quantum materials

Dr Prasanta Kumar Muduli  
Indian Institute of Technology Madras, India

## Abstract:

In this talk, I will discuss a nanoscale quantum device called a “nonlocal spin-valve device.” I will demonstrate various ways the nonlocal spin-valve device can be used to explore different quantum phenomena. I will introduce a recent experimental technique called the “spin absorption method” to study different spin-to-charge conversion processes like the spin Hall effect and Rashba–Edelstein effect. First, I will show direct and inverse Rashba–Edelstein effect measurements at the  $\text{Bi}_2\text{O}_3/\text{Cu}$  interface using the spin absorption method [1]. Next, I will present another example work where spin Hall angle and spin-diffusion length of Weyl semimetal  $\text{Mn}_3\text{Sn}$  were measured using the spin absorption method [2]. In the end, I will present the recent breakthrough discovery of the magnetic spin Hall effect in a single crystal  $\text{Mn}_3\text{Sn}$  nanodevice [3].

[1] Hironari Isshiki, Prasanta Muduli, Junyeon Kim, Kouta Kondou, and YoshiChika Otani, *Phys. Rev. B* 102, 184411 (2020).

[2] P. K. Muduli, T. Higo, T. Nishikawa, Danru Qu, H. Isshiki, K. Kondou, S. Nakatsuji, and YoshiChika Otani, *Phys. Rev. B* 99, 184425 (2019).

[3] M. Kimata, H. Chen, K. Kondou, S. Sugimoto, P. K. Muduli, M. Ikhlas, Y. Omori, T. Tomita, A. H. MacDonald, Satoru Nakatsuji, YoshiChika Otani, *Nature* 565, 627(2019).

Topic:

## Optical thermometry for investigating spin-caloritronic phenomena

Takumi Yamazaki<sup>1,2</sup>

<sup>1</sup> Institute for Materials Research, Tohoku University, Sendai, Japan

<sup>2</sup> Center for Spintronics Research Network, Tohoku University, Sendai, Japan

Email: takumi.yamazaki.d5@tohoku.ac.jp

**Abstract:** Spin-caloritronic phenomena have gained much attention from the viewpoints of not only fundamental physics but also thermoelectric applications. We investigate the spin caloritronic phenomena using the optical thermometry called lock-in thermoreflectance (LITR). The LITR can access the transient response of the spin-caloritronic phenomena, and thus reveals the different frequency response of the temperature amplitude induced by the spin Peltier effect and anomalous Ettingshausen effect. I will also report that the LITR is applied to the junction system using a ferromagnetic metal and antiferromagnetic insulator.

### 1. INTRODUCTION

Spin caloritronics is the research field of studying the interconversion between spin, charge, and heat currents [1,2]. Some of the spin-caloritronic phenomena that output heat currents have gained much attention for applying thermal management technologies. The spin Peltier effect (SPE) [3,4] and the anomalous Ettingshausen effect (AEE) [5] are the representative example of such phenomena; the former generates a heat current from a spin current at the junction comprised of a magnetic material, whereas the latter is one of the magneto-thermoelectric effects in a ferromagnetic metal. These phenomena have been investigated by employing the thermal measurement techniques with high sensitivity. Although early study of the SPE was conducted by the contact-type thermometry, such measurements are often disturbed by the heat loss to the temperature detectors. To solve this problem, the non-contact type temperature measurements, such as the lock-in thermography [4] and the optical thermometry called lock-in thermoreflectance (LITR) [6] has been introduced the spin caloritronics. In this presentation, I will talk about the usability of LITR method for investigating the spin-caloritronic phenomena that output heat currents.

### 2. EXPERIMENTAL PROCEDURES

The LITR is a combination of a lock-in detection and an optical thermometry using the temperature dependence of reflectivity. The sample used in this study consists of a metal film on a substrate, where the spin-caloritronic phenomena including the SPE and AEE appear. When an ac charge current and an external magnetic field are applied to the sample, the temperature modulation induced by the SPE and/or AEE occurs. This temperature modulation is detected by monitoring the intensity change of the reflected light from the sample surface covered with the Au transducer. Since the Joule heating contribution has the higher-harmonic component, it can be separated from the spin-caloritronic phenomena by using the lock-in detection.

### 3. RESULTS AND DISCUSSION

Since the LITR captures the MHz-level thermal response, it can reveal the different frequency response of the SPE and AEE. The lock-in frequency dependence of the SPE-induced temperature amplitude in  $Y_3Fe_5O_{12}/Pt$  junction gradually decreases, whereas that of the AEE-induced temperature amplitude in Ni film shows almost constant. The difference is attributed to the different length scale of the heat current; while the transient response of the AEE is determined by the thickness of Ni layer, that of the SPE is determined by the length scale of the SPE-induced heat current in the  $Y_3Fe_5O_{12}$  layer [6].

I will also report our on-going result of the LITR measurement for the Pt/antiferromagnetic insulator NiO/ferromagnetic metal junction system. We measured the NiO thickness dependence of the temperature amplitude due to the spin-caloritronic phenomena in the trilayer system. Our optical LITR method can successfully estimate the spin transmission length of NiO, which is consistent with the previous reports using the electrical measurement [7,8].

### ACKNOWLEDGEMENT

The author would like to thank K. Uchida, H. Nagano, R. Iguchi, K. Takanashi, T. Seki, and T. Kubota for collaboration of this work. This work was supported by JST CREST (Grant No. JPMJCR17I1), JSPS KAKENHI (Grants No. 19H02585, 18K14116, 18H05246, 18J23465, and 21K20392).

### REFERENCES

- [1] G. E. W. Bauer *et al.*, *Nat. Mater.* **11**, 391 (2012).
- [2] K. Uchida, *Proc. Jpn. Acad., Ser. B* **97**, 69 (2021).
- [3] J. Flipse *et al.*, *Phys. Rev. Lett.* **113**, 027601 (2014).
- [4] S. Daimon *et al.*, *Nat. Commun.* **7**, 13754 (2016).
- [5] T. Seki *et al.*, *Appl. Phys. Lett.* **112**, 152403 (2018).
- [6] T. Yamazaki *et al.*, *Phys. Rev. B* **101**, 020415(R) (2020).
- [7] Y. Wang *et al.*, *Science* **366**, 1125 (2019).
- [8] T. Ikebuchi *et al.*, *Appl. Phys. Express* **14**, 123001(2021).



P01

## **Room Temperature Ferromagnetism in half metallic Co doped CdS diluted magnetic semiconductor for spintronics**

D. Saikia<sup>a</sup>, S. Parnamee<sup>b</sup>, and J. P. Borah<sup>b</sup>

<sup>a</sup>*Duliajan College, Duliajan, 706602, Dibrugarh, Assam*

<sup>b</sup>*National Institute of Technology Nagaland, Chumukedema, Dimapur-797103, Nagaland, India*

<sup>a</sup>*Email:dipraj.saikia7@gmail.com*

**Abstract:**

In recent years, diluted magnetic semiconductors (DMS) have attracted growing attention in research due to their potential applications in spintronic devices. Here, in this work, we have synthesized Co doped CdS nanoparticles for different concentrations of dopant by using simple co-precipitation method. The as-synthesized sample are characterized by X ray diffraction (XRD), UV-Vis spectroscopy, Photoluminescence spectroscopy, Vibrational sample magnetometer (VSM) and Transmission electron microscopy (HRTEM). UV-visible spectroscopy depict the enhancement of optical band gap of Co doped CdS nanoparticles compared to the bulk CdS as a result of the quantum confinement effect. Magnetic study confirms the existence of room temperature ferromagnetic ordering in the nanoparticles, as a result of p-d exchange interactions between the localized d spins of Co ions and p-states of S. Theoretical calculations demonstrate the half metallic nature of Co doped CdS system with strong p-d hybridization between the d states of Ni and the S-p states which results the room temperature ferromagnetism. Thus from our study, it can be predicted that Co doped CdS nanoparticles are remarkable DMS candidates for the applications in spintronics.

**Keywords:** DMS, Spintronics, Ferromagnetism

**References:**

1. D Saikia , J.P.Borah, *Physica B* , 565, 25-32 (2019)
2. B. Poornaprakash, P.T. Poojitha, U. Chalapathi, S.-H. Park, *Mater. Lett.* 181, 227 (2016)
3. S.V. Nistor, M. Stefan, L.C. Nistor, D. Ghica, I.D. Vlaicu, *J. Alloys Compd.* 662, 193 (2016)

**P02**

**CoFeVSb: A Promising Candidate for Spin Valve and Thermoelectric Applications**

*by Jadupati Nag et al.*

*Department of Physics, Indian Institute of Technology Bombay, Mumbai 400076, India*

Abstract: We report a combined theoretical and experimental study of a novel quaternary Heusler system CoFeVSb from the viewpoint of room temperature spintronics and thermoelectric applications. It crystallizes in cubic structure with a small DO3-type disorder. The presence of the disorder is confirmed by room temperature synchrotron X-ray diffraction (XRD) and extended X-ray absorption fine structure (EXAFS) measurements. Magnetization data reveal a high ordering temperature ( $> 950\text{K}$ ) with a saturation magnetization of  $2.2 \mu_{\text{B}}/\text{f.u.}$  Resistivity measurements reflect semimetallic nature. Double hysteresis loop along with asymmetry in the magnetoresistance (MR) data reveals room temperature spin-valve feature, which remains stable even at  $300\text{ K}$ . Hall measurements show anomalous behavior with significant contribution from intrinsic Berry phase. This compound also large room-temperature power factor ( $\sim 0.62 \text{ mWatt}/\text{m}/\text{K}^2$ ) and ultra-low lattice thermal conductivity ( $\sim 0.4 \text{ W}/\text{m}/\text{K}$ ), making it a promising candidate for thermoelectric application. Abinitio calculations suggest weak half-metallic behavior and reduced magnetization (in agreement with the experiment) in presence of DO3 disorder. We have also found an energetically competing ferromagnetic (FM)/antiferromagnetic (AFM) interface structure within an otherwise FM matrix: one of the prerequisites for spin-valve behavior. The coexistence of so many promising features in a single system is rare, and hence CoFeVSb gives a fertile platform to explore numerous applications in the future.

P03

## **Tuning the electric properties of conducting interface at EuO-KTaO<sub>3</sub> with light as external stimuli**

*Manish Dumen, Ajit Singh, Chandan Bera and Suvankar Chakraverty\**,

Quantum Materials and Devices Unit, Institute of Nano Science and Technology, Sector- 81,  
Mohali (Punjab), India.

[manishdumen123@gmail.com](mailto:manishdumen123@gmail.com)

8699772332

### **ABSTRACT:**

KTaO<sub>3</sub> based conducting interfaces have gained tremendous interest due to the fact that spin orbit coupling strength is one order of magnitude higher than STO, which makes it a promising candidate for spintronics as well as optoelectronic devices. Here, we have reported the effect of light as external perturbation to tune the electronic properties of conducting interface at EuO-KTaO<sub>3</sub> with different carrier density. Even at a very low power (0.5mW) of laser light, we get a large change in conductivity. Power dependent study is done for light of varying wavelength at low and room temperature for three samples having different carrier density. The larger magnitude of the Persistent Photocurrent (PPC) after the removal of light can play an important role in the fabrication of future memory and photovoltaic devices.

## Probing the fully compensated ferrimagnet $\text{Mn}_2\text{V}_{0.5}\text{Co}_{0.5}\text{Al}$ : Neutron diffraction and *ab initio* studies

P V Midhunlal<sup>1,2</sup>, C Venkatesh<sup>3</sup>, J Arout Chelvane<sup>4</sup>, P D Babu<sup>5</sup> and N Harish Kumar<sup>2</sup>

1. Department of Physics, Faculty of Engineering & Technology, Jain (Deemed to-be-University), Bangalore-562 112, India.
2. Department of Physics, Indian Institute of Technology Madras, Chennai-600036, India.
3. Saha Institute of nuclear physics, Bidhannagar, Kolkata, West Bengal-700064.
4. Defense Metallurgical Research Laboratory, Kanchanbagh (PO), Hyderabad-500058, India.
5. UGC-DAE Consortium for Scientific Research, Mumbai Center, R-5 shed, BARC, Trombay, Mumbai-400085, India.

Email: midhunlalpv3@gmail.com

**Abstract:** Neutron diffraction and *ab initio* studies have been performed on the fully compensated ferrimagnet  $\text{Mn}_2\text{V}_{0.5}\text{Co}_{0.5}\text{Al}$ . The crystal structure and the magnetic configuration of  $\text{Mn}_2\text{V}_{0.5}\text{Co}_{0.5}\text{Al}$  alloy which exhibit fully compensated ferrimagnetic property are identified through combined neutron diffraction and *ab initio* studies. Investigation showed that the  $L2_1$  and  $X_a$  structure of the  $\text{Mn}_2\text{V}_{0.5}\text{Co}_{0.5}\text{Al}$  alloy are well distinguishable from the neutron diffraction pattern which could not be identified from the X-ray diffraction studies. From the *ab initio* calculations, it was evident that the disordered  $L2_1$  structure with the antiparallel coupling between the parallelly aligned moments of  $(\text{Mn}_{(A)}-\text{Mn}_{(C)})$  and  $(\text{V}-\text{Co})$  atom pairs enables the magnetic moment compensation in  $\text{Mn}_2\text{V}_{0.5}\text{Co}_{0.5}\text{Al}$ .

### 1. INTRODUCTION

High  $T_C$  zero moment half-metals can be utilized in devices such as spin-polarized scanning tunnelling microscope (SP-STM) and spin transfer torque (STT) based MTJ as they do not produce any stray field [1]. Half-metallic fully compensated ferrimagnets are a new class of materials which exhibits 100 % spin polarization at Fermi level and zero macroscopic moment due to the complete cancellation of the atomic moments arising from the different magnetic sub-lattices. Due to the zero magnetic moment, these materials are also named as half-metallic antiferromagnets (HMAF). In our recent publication, we have investigated the structural and magnetic properties of  $\text{Mn}_2\text{V}_{1-x}\text{Co}_x\text{Ga}$  ( $x=0, 0.25, 0.5, 0.75, 1$ ) alloys through neutron diffraction and *ab initio* studies [2]. The exact crystal structure and the reason for the magnetic moment compensation was explained in detail. Here we present the structural and magnetic properties of the interesting isostructural  $\text{Mn}_2\text{V}_{0.5}\text{Co}_{0.5}\text{Al}$  through neutron diffraction and *ab initio* studies.

### 2. RESULTS & DISCUSSION

Figure 1 shows the nuclear refinement of the neutron diffraction pattern of  $\text{Mn}_2\text{V}_{0.5}\text{Co}_{0.5}\text{Al}$  for  $2\theta > 40$ . The Rietveld refinement showed that as in the case of previously reported  $\text{Mn}_2\text{V}_{0.5}\text{Co}_{0.5}\text{Ga}$ , two structural models are compatible with the experimental ND pattern. The models are  $L2_1 + (\text{Mn}_{(C)}-\text{Co}$  disorder) and  $X_a + (\text{Mn}_{(B)}-\text{Co}$  disorder). The refined lattice parameter is 5.862 Å. The *ab initio* studies confirmed that the  $L2_1 + (\text{Mn}_{(C)}-\text{Co}$  disorder) structure is having minimum energy. Figure 2 shows the density of states diagram for  $\text{Mn}_2\text{V}_{0.5}\text{Co}_{0.5}\text{Al}$  which shows the gap in one of the spin band.

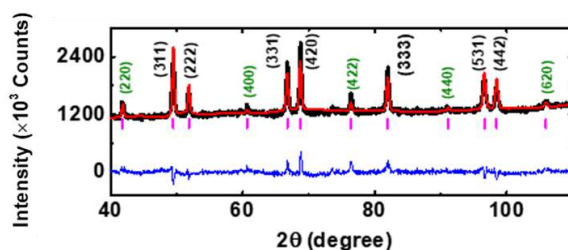


Figure 1: nuclear refinement of the neutron diffraction pattern of  $\text{Mn}_2\text{V}_{0.5}\text{Co}_{0.5}\text{Al}$  for  $2\theta > 40$ .

This indicates that the alloy sample under consideration is half-metallic.

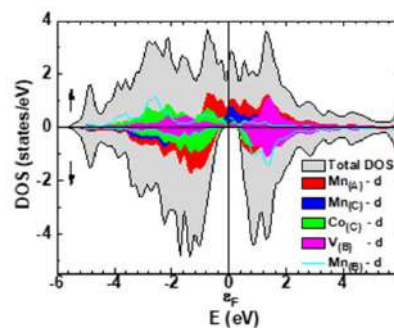


Figure 2: density of states diagram for  $\text{Mn}_2\text{V}_{0.5}\text{Co}_{0.5}\text{Al}$

### REFERENCES

- [1] Galanakis, I., and Şaşıoğlu, E. (2011). High  $T_C$  half-metallic fully-compensated ferrimagnetic Heusler compounds. *Appl. Phys. Lett.* **99**, 1–4
- [2] P V Midhunlal, C Venkatesh, J Arout Chelvane, P D Babu and N Harish Kumar, (2022), "Neutron diffraction and *ab initio* studies on the fully compensated ferrimagnetic characteristics of  $\text{Mn}_2\text{V}_{1-x}\text{Co}_x\text{Ga}$  ( $x=0,0.25,0.5,0.75,1$ ) Heusler alloys". *J. Phys.: Condens. Matter* **34**, 125801

## Formation of Nickel Silicide and Appearance of Anomalous behaviour of Magnetic Anisotropy in Nickel thin films

Zainab Hussain<sup>1</sup>, V.Raghavendra Reddy<sup>2</sup> and Subhabrata Dhar<sup>1</sup>

<sup>1</sup>Department of Physics, Indian Institute of Technology, Bombay, Mumbai, Maharashtra, India

<sup>2</sup>UGC-DAE Consortium for Scientific Research, University Campus, Khandwa Road, Indore 452001, India.

Email: zaineb92@gmail.com

**Abstract** In the present work, we have study the formation of nickel silicide at the interface of nickel and silicon (Si), when the nickel (~18nm) is deposited on Si substrate (Si/Ni). Further, we have determined formation of different phases of nickel silicide with temperature annealing by using X-ray reflective (XRR). Besides this, we have investigated the magnetic properties, i.e. magnetic anisotropy and magnetic domain microstructure of as-deposited nickel thin film. For the sake of comparison of interface effect and magnetic properties, we have deposited another Ni film with a buffer layer of Pt between the nickel and Si substrate (Ni/Pt/Si), and examine its magnetic and structural properties. It is found that Si /Pt /Ni is textured along (111) direction, and it has no magnetic anisotropy. However, for Ni/Si, we observed anomalous magnetic anisotropy behaviour (referred to as the collapse of hard axes), i.e., anomalous behaviour of magnetic reversal process at hard axes of magnetization due to magnetic dispersion.

### 1. INTRODUCTION

Metal-semiconductor interfaces are of great interest due to their technological importance in semiconductor and spintronic devices [1]. Therefore, it is crucial to study the interface of metal-semiconductor as it benefits in understanding material properties. Furthermore, metal silicide has become the main contact material in advanced electronics devices due to its low resistivity and silicon consumption [1]. Nickel monosilicide (NiSi) manifest to be suitable for high performance as it features the lowest resistivity. In this direction, extensive work has been done; for example, it is shown that nickel silicide forms at the interface of nickel and silicon [2]. Further, it is demonstrated that it follows different phase sequence formation Ni-Ni<sub>2</sub>Si-NiSi while annealing. However, the impact of the interface on the magnetic properties is not much explored in this direction.

Therefore, in this work, we have utilized Kerr microscopy to probe magnetic properties and various structural characterization tools, i.e., X-ray reflectivity, X-ray diffraction, and atomic force microscopy to demonstrate the formation of nickel silicide at the Ni and Si interface, when nickel (~15nm) is deposited at silicon substrate (Si/Ni). For the sake of comparison, we have deposited another film (Si/Pt/Ni), where we deposited an under layer of Pt (~20nm) between the Ni and silicon. Besides this, we have shown the effect of texturing due to Pt under layer on the magnetic anisotropy. On the other hand, from Kerr microscopy investigation, for Si/Ni, we observed anomalous magnetic anisotropy behaviour (referred to as the collapse of hard axes), i.e., anomalous behaviour of magnetic reversal process at hard axes of magnetization due to magnetic dispersion.

### 2. FIGURES AND IMAGES

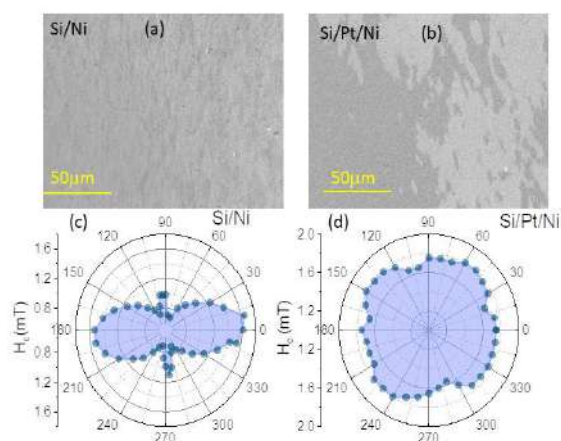


Fig.1. (a-b) shows the Kerr images for both the films captured along the remanence condition. Wide domains appeared for Si/Pt/Ni, whereas, fine ripple kind of domain appears in Si/Ni. (c-d) Shows the in-plane azimuthal angular behavior of coercivity indicating the anomalous uni-axial anisotropy, whereas, for Si/Pt/Ni, it is magnetically isotropic.

### REFERENCES

1. Zhang, S. L. & Zhang, Z. In *Metallic Films for Electronic, Optical and Magnetic Applications*: Woodhead Publishing, 2014, pp. 244–301
2. Van Stiphout, K, J. Phys. D: Appl.Phys. 52, 145301 (2019).
3. Parratt, L. G., Physical Review. 95, 359 (1954)
4. O. Idigoras, A. K. Suszka, P. Vavassori, P. Landeros, J. M. Porro, and A. Berger Phys. Rev. B, 84, 132403 (2011).

## Enhancement of magnetic properties by Lanthanides and Co doping in Bismuth Ferrite thin films fabricated by pulsed DC reactive sputtering method

Soumyaranjan Ratha<sup>1</sup>, Daichi Yamamoto<sup>1</sup>, Kotaro Takeda<sup>1</sup>, Munusamy Kuppan<sup>2</sup>,  
Genta Egawa<sup>3</sup>, and Satoru Yoshimura<sup>3</sup>

<sup>1</sup> Department of Materials Science, Graduate School of Engineering Science, Akita University,  
Akita 010-8502, Japan

<sup>2</sup> Centre for Regional Revitalization in Research and Education, Akita University, Akita 010-8502, Japan

<sup>3</sup> Research Centre of Advanced Materials for Breakthrough Technology, Graduate School of  
Engineering Science, Akita University, Akita 010-8502, Japan

syoshi@gipc.akita-u.ac.jp

**Abstract:** (Bi,*L*)(Fe,Co)O<sub>3</sub> (*L*=La, Nd, Sm, Gd, Dy) multiferroic thin films were fabricated using pulsed DC reactive sputtering technique to obtain high saturation magnetization ( $M_s$ ), perpendicular magnetic anisotropy ( $H_{c\perp}/H_{c\parallel}$ ) and large magnetic Kerr effect ( $\Theta_k$ ). These magnetic properties are very important for realization of high performance magnetic devices driven by electric field. Especially, (Bi,Nd)(Fe<sub>0.75</sub>Co<sub>0.25</sub>)O<sub>3</sub> thin film had a very high  $M_s$  of 140 emu/cm<sup>3</sup> with large  $H_{c\perp}/H_{c\parallel}$  (perpendicular magnetic anisotropy) of 2.6, and (Bi,La)(Fe<sub>0.72</sub>Co<sub>0.28</sub>)O<sub>3</sub> thin film had a very high  $\Theta_k$  of 0.67°. These magnetic properties were excellent compared with the previously reported (Bi,*A*)FeO<sub>3</sub> (*A*=Ca, Sr, Ba) and Bi(Fe,*M*)O<sub>3</sub> (*M*=Co, Mn) thin films.

### 1. INTRODUCTION

The applications of multiferroic thin films are effective in magnetic devices to decrease the power consumption because it is possible to realize the magnetization switching by electric field. Bismuth Ferrite (BFO) is a better candidate for this application as it shows multiferroic properties at room temperature. The G-type antiferromagnetic property of pure BFO needs to be changed to ferrimagnetic property for application point of view by substituting some atoms with it. The (Bi,Ba)FeO<sub>3</sub>, we substituted Ba in A-site of BFO with an appropriate percentage, shows relatively high  $M_s$  of 90 emu/cm<sup>3</sup> [1], but the ratio  $H_{c\perp}/H_{c\parallel}$  of 0.8 &  $\Theta_k$  of 0.03° were not enough for application. In our previous study, we found remarkable improvement in magnetic properties like  $M_s$  of 80 emu/cm<sup>3</sup>, relatively high  $H_{c\perp}/H_{c\parallel}$  of 1.6 [2] and very high  $\Theta_k$  of 0.67° in (Bi,La)(Fe,Co)O<sub>3</sub> by doping La as A-site substituent. In this study, we are going to investigate the improvement of magnetic properties of BFO based thin films by substituting other Lanthanoids in A-site and Co in B-site in (Bi<sub>0.6-0.4</sub>La<sub>0.4-0.6</sub>)(Fe<sub>1-x</sub>Co<sub>x</sub>)O<sub>3</sub> ( $x = 0-0.3$ ) (*L*=La, Nd, Sm, Gd, Dy).

### 2. EXPERIMENTAL

Multilayers of Ta (5 nm) / Pt (100 nm) / (Bi<sub>0.6-0.4</sub>La<sub>0.4-0.6</sub>)(Fe<sub>1-x</sub>Co<sub>x</sub>)O<sub>3</sub> ( $x = 0-0.3$ ) (*L*=La, Nd, Sm, Gd, Dy) (200 nm) were deposited onto a thermally oxidized Si wafer using a UHV sputtering system. After dry-etching of substrate surface, the Ta seedlayer, Pt underlayer and (Bi,*L*)(Fe,Co)O<sub>3</sub> layer were deposited at room temperature, 400 °C, and 695 °C respectively. The VHF (40.68 MHz) plasma irradiation during the RF sputtering deposition of Pt film and pulsed DC reactive sputtering deposition of (Bi,*L*)(Fe,Co)O<sub>3</sub> films were performed with an electric power of 5 W. The frequency pulsed DC was 100 kHz. The concentrations of substituent were confirmed by dispersive X-ray spectroscopy. The hysteresis curve (*M-H*) and  $\Theta_k$  were measured by vibrating sample magnetometer and MOKE measurement equipment respectively.

### 3. RESULTS AND DISCUSSION

Table 1 shows the magnetic properties of (Bi<sub>0.6-0.4</sub>La<sub>0.4-0.6</sub>)(Fe<sub>1-x</sub>Co<sub>x</sub>)O<sub>3</sub> ( $x = 0-0.3$ ) and (Bi<sub>0.6-0.4</sub>La<sub>0.4-0.6</sub>)(Fe<sub>0.8-0.7</sub>Co<sub>0.2-0.3</sub>)O<sub>3</sub> (*L*=La, Nd, Sm, Gd, Dy) thin films. The magnetic properties of (Bi,Ba)FeO<sub>3</sub> are also shown as a reference. The Co substitution in B-site has a great role in improving every magnetic property by increasing the concentration up to 30%. Also enhanced  $M_s$  and  $H_{c\perp}/H_{c\parallel}$  are observed by substituting Neodymium instead of Lanthanum in A-site. Therefore, suitable Lanthanoid substitution in A-site is also key factor to obtain good magnetic properties. The magnetic properties like  $M_s$ ,  $H_{c\perp}/H_{c\parallel}$  and  $\Theta_k$  are increased drastically compared with the previously observed value in (Bi,Ba)FeO<sub>3</sub>. A highest  $M_s$  of 140 emu/cm<sup>3</sup> and large perpendicular magnetic anisotropy are found in (Bi,Nd)(Fe,Co)O<sub>3</sub>, which is suitable for magnetic recording devices, and maximum  $\Theta_k$  of 0.67° is found in (Bi,La)(Fe,Co)O<sub>3</sub>, which is suitable for optical devices.

### 3. TABLE

**Table 1.** Magnetic properties ( $M_s$ ,  $H_{c\perp}$ ,  $H_{c\perp}/H_{c\parallel}$ ,  $\Theta_k$ ) of various BiFeO<sub>3</sub> based thin films

Substitution element	Ba	La				Nd	Sm	Gd	Dy
Co <sup>2+</sup> / Fe <sup>3+</sup> +Co <sup>2+</sup>	0	0	0.05	0.12	0.16	0.28	0.25	0.24	0.27
$M_s$ (emu/cm <sup>3</sup> )	90	15	23	48	69	80	140	110	65
$H_{c\perp}$ (kOe)	2.0	0	0.4	3.1	3.1	2.6	2.1	1.9	2.2
$H_{c\perp}/H_{c\parallel}$	0.8	0	0.2	0.9	1.2	1.6	2.6	2.1	2.8
$\Theta_k$ (°@750nm)	0.03	0		0.08	0.12	0.67	0.34	0.21	0.19

### REFERENCES

- [1]. S. Yoshimura et al., *JJAP-STAP*, **57**, 0902B7 (2018).
- [2]. M. Kuppan et al., *SCIENTIFIC REPORTS*, **11**, 11118 (2021).



## Room Temperature Ferromagnetism in Ni Doped MoO<sub>3</sub> Nanoflowers

Abhishek Panghal, Dharendra Sahoo, Deepak Deepak, Susanta Sinha Roy  
and Bhaskar Kaviraj\*

Department of Physics, Shiv Nadar University, Gautam Buddha Nagar, Uttar Pradesh 201314, India.

\*Corresponding author: [bhaskar.kaviraj@snu.edu.in](mailto:bhaskar.kaviraj@snu.edu.in)

**Abstract:** We report the room temperature ferromagnetism in MoO<sub>3</sub> nanoparticles grown by hydrothermal technique. X-ray diffraction, scanning electron microscopy, and Raman spectroscopy techniques were used to ascertain the crystal structure, morphology, and structural fingerprint. The saturation magnetization of these samples was extracted using vibrating sample magnetometry (VSM). It has been observed that saturated magnetic moment increases as we increase the Nickel concentration.

### 1. INTRODUCTION

In the last three decades, dilute magnetic semiconductors (DMS) have drawn much research interest because of their synergetic magnetic and semiconducting properties, which makes them a promising candidate for spintronic applications. There have been numerous theoretical and experimental studies in two-dimensional (2D) non-magnetic semiconducting systems which behave as DMS by creation and engineering of defects using metallic doping [1-3], vacancies [4] and enhancing edge-rich sites [5]. In this work, we report a single-step, facile, and cost-effective hydrothermal method to synthesize curved Ni-doped MoO<sub>3</sub> nanoflowers without the usage of any capping agent or surfactant stabilizer.

### 2. RESULT AND DISCUSSION

The crystal structures, morphology, and structural fingerprint of as-synthesized nanostructures are analyzed by X-ray diffraction, scanning electron microscopy (SEM), and Raman spectroscopy. To investigate the ferromagnetism of Ni-doped MoO<sub>3</sub> nanocrystals, we performed vibrating sample magnetometer (VSM) measurements at room temperatures (300K). The magnetic measurements depict that as-synthesized Ni-doped MoO<sub>3</sub> nanoflowers manifest ferromagnetic behavior at ambient conditions. The saturated magnetic moment of the MoO<sub>3</sub>, 5% Ni doped MoO<sub>3</sub>, and 10% Ni doped MoO<sub>3</sub> were found to be 0.0796 emu g<sup>-1</sup>, 0.142 emu g<sup>-1</sup>, 0.1644 emu g<sup>-1</sup> respectively.

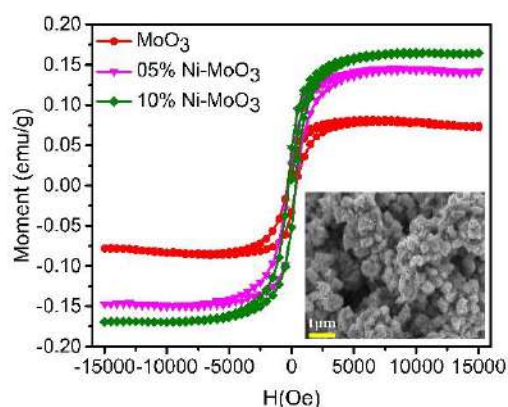


Fig. 1. Magnetic hysteresis loop at room temperature for different concentration of Ni doped MoO<sub>3</sub>. Inset shows the SEM image of the 5% Ni doped MoO<sub>3</sub> nanoflowers.

The result demonstrates that magnetic moment increases with the increase in Ni dopant concentrations. Observed room temperature ferromagnetism may be ascribed to the presence of defects or vacancies on the surface of nanoflowers.

### 3. CONCLUSION

We reported a ferromagnetism in Ni doped MoO<sub>3</sub> at room temperature. The magnetic saturation increases with increase in the Ni doping in MoO<sub>3</sub> which makes it a promising candidate for the spintronic application.

### ACKNOWLEDGEMENT

AP acknowledges Shiv Nadar University for financial support through fellowship during this project.

### REFERENCES

- [1] J. Wang, F. Sun, S. Yang, Y. Li, C. Zhao, M. Xu, Y. Zhang, and H. Zeng, *Appl. Phys. Lett.* **109**, 1 (2016).
- [2] Z.C. Xiang, Z. Zhang, X.J. Xu, Q. Zhang, Q.B. Wang, and C. Yuan, *Phys. Chem. Chem. Phys.* **17**, 15822 (2015).
- [3] L.M. Martinez, J.A. Delgado, C.L. Saiz, A. Cosio, Y. Wu, D. Villagrán, K. Gandha, C. Karthik, I.C. Nlebedim, and S.R. Singamaneni, *J. Appl. Phys.* **124**, (2018).
- [4] B. Xia, T. Wang, W. Xiao, R. Zhang, P. Liu, J. Ding, D. Gao, and D. Xue, *Sci. Rep.* **7**, 1 (2017).
- [5] D. Sahoo, J. Shakya, N. Ali, W.J. Yoo, and B. Kaviraj, *Langmuir* **38**, 1578 (2022).

**Magnetic studies of nanostructures and effect of spin-orbit interaction****Sonali Kakkar<sup>1</sup>, and Chandan Bera<sup>1</sup>**

<sup>1</sup>*Institute of Nano Science and Technology, Sector-81,  
Knowledge City, Sahibzada Ajit Singh Nagar, Punjab, 140306, India.*

2D layered materials and oxide heterointerfaces, in the wake of their paradigm-breaking technical advancement in spintronics, offer a hunting ground for the realization of various features and are attracting broad research efforts worldwide. We study the magnetic properties of layered materials and perovskite oxide heterointerfaces using first-principles calculations with density functional theory (DFT). Layered transition metal ternary chalcogenide CoAsS shows intrinsic magnetism in monolayer form. Direct d-d exchange interactions lead to ferromagnetic (FM) ordering at higher Hubbard U parameter, whereas indirect superexchange interactions lead to antiferromagnetic stability for lower U parameter. In the FM phase of the CoAsS monolayer, a non-trivial Chern number leads to a topological state. Polar-polar perovskite oxide heterostructure LaVO<sub>3</sub>/KTaO<sub>3</sub> is found to exhibit an n-type conducting interface with orbital-dependent Rashba spin splitting and orientation-dependent spin structure. At the EuO/TaO<sub>2</sub> interface of a EuO/KTO superlattice, the spin-polarized two-dimensional electron gas (2DEG) is found in the d<sub>xy</sub> orbitals of interfacial Ta on the KTO side, with magnetic easy axis perpendicular to the interfacial plane. As a result, our work opens up the possibility to realize a 2D layered magnet, the Rashba effect with an intriguing spin structure, and spin-polarized 2DEG at the interface due to the proximity effect with high perpendicular magnetic anisotropy for future spintronic applications.



## Spinterface-Induced Modification in Magnetic Properties in Co<sub>40</sub>Fe<sub>40</sub>B<sub>20</sub>/Fullerene Bilayers

Purbasha Sharangi<sup>1</sup>, Esita Pandey<sup>1</sup>, Shaktiranjan Mohanty<sup>1</sup>, Sagarika Nayak<sup>1</sup> and Subhankar Bedanta<sup>1,2</sup>

<sup>1</sup>Laboratory for Nanomagnetism and Magnetic Materials (LNMM), School of Physical Sciences, National Institute of Science Education and Research (NISER), HBNI, P.O.- Bhipur Padanpur, Via Jatni, 752050, India

<sup>2</sup>Center for Interdisciplinary Sciences (CIS), National Institute of Science Education and Research (NISER), HBNI, Jatni, 752050 India  
Email: purbasha@niser.ac.in

**Abstract:** Organic semiconductor/ferromagnetic bilayer thin films can exhibit novel properties due to the formation of spinterface at the interface. Buckminsterfullerene (C<sub>60</sub>) has been shown to exhibit ferromagnetism at the interface when it is placed next to a ferromagnet (FM) such as Fe or Co. Formation of spinterface occurs due to the orbital hybridization and spin polarized charge transfer at the interface. In this work, we have demonstrated that one can enhance the magnetic anisotropy of the low Gilbert damping alloy CoFeB thin film by introducing a C<sub>60</sub> layer. We have shown that anisotropy increases by increasing the thickness of C<sub>60</sub> which might be a result of the formation of spinterface. However, the magnetic domain structure remains same in the bilayer samples as compared to the reference CoFeB film.

### 1. INTRODUCTION

In organic spintronics, organic semiconductors (OSCs) (e.g., C<sub>60</sub>, Alq<sub>3</sub>, Ruberene etc.) are used to transport or control spin polarized signals. The main advantages of OSCs are their low production cost, light weight, flexible and chemically interactive nature. There are several reports on organic spin valves, organic light emitting diodes (OLED) using C<sub>60</sub> as a spacer layer. It has been shown that C<sub>60</sub> (~2 nm) can be magnetized when it is placed next to a ferromagnetic (FM) layer.<sup>1</sup> d-p hybridization at the interface of FM/C<sub>60</sub> modifies the density of states (DOS) and exhibits room temperature ferromagnetism. Such kind of interface is known as spinterface.<sup>2</sup> It has been found that ~ 2 nm of C<sub>60</sub> exhibits magnetic moment ~ 3μ<sub>B</sub>/cage at the epitaxial Fe/C<sub>60</sub> interface.<sup>1</sup> There is a decrement in anisotropy in polycrystalline Fe/C<sub>60</sub> system whereas for polycrystalline Co/C<sub>60</sub> system anisotropy got enhanced.<sup>3,4</sup> However, to the best of our knowledge no such basic study has been performed on CoFeB system. For spintronic application a low damping material is always desired as it directly affects the speed of a device. The main advantage of taking CoFeB as a ferromagnet is that it exhibits low Gilbert damping parameter and it is amorphous in nature. In this regard, we have prepared CoFeB/C<sub>60</sub> bilayer films and compared the magnetic properties to its reference CoFeB film.

### 2. EXPERIMENTAL METHODS

CoFeB reference film with 5 nm thickness and bilayer (CoFeB/C<sub>60</sub>) samples have been deposited on Si (100) substrate in a multi-deposition high vacuum chamber. The samples are named as S1, S2, S3, S4 and S5 for the thickness of C<sub>60</sub> (tC<sub>60</sub>) taken as 0, 1.1, 2, 5, 15 nm, respectively. CoFeB, C<sub>60</sub> and MgO layers have been deposited using DC sputtering, thermal evaporation and e-beam evaporation techniques, respectively.

### 3. RESULTS AND DISCUSSION

We have measured hysteresis loops along with domain images using MOKE based microscopy in longitudinal mode for all the samples. It has been

observed that the change in domain structure is not significant between the single layer CoFeB and the bilayer CoFeB/C<sub>60</sub> samples.

Further, to calculate the anisotropy of the system we have performed angle dependent ferromagnetic resonance (FMR) measurements. The measurement was performed at room temperature and a fixed frequency of 7 GHz. Figure 1 shows the  $H_{res}$  vs  $\phi$  plots. The open circles represent the raw data and the solid lines are the best fits. The experimental data is fitted using Landau-Lifshitz-Gilbert (LLG) equation:<sup>5</sup>

$$f = \frac{\gamma}{2\pi} \left( \left( H + \frac{2K_2}{M_S} \cos \phi \right) \left( H + 4\pi M_S + \frac{2K_2}{M_S} \phi \right) \right) \quad (1)$$

where,  $K_2$  is the in-plane uniaxial anisotropy constant,  $\phi$  is the in-plane angle between the easy axis w.r.t the applied magnetic field direction and  $M_S$  is the saturation magnetization.

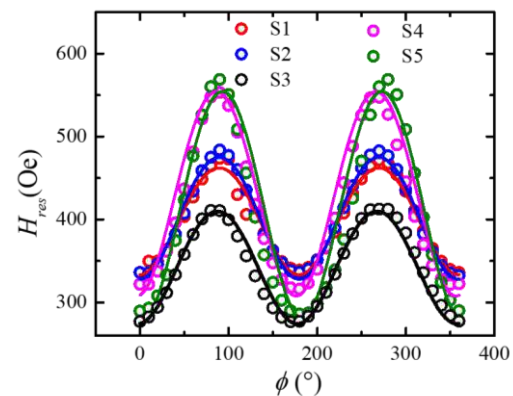


**Fig.1.** Angle dependent resonance field ( $H_{res}$ ) plot for all the five samples to calculate the anisotropy constants of the system. Open circles represent the experimental data, while the solid lines are the best fits. The extracted values of  $K_2$  from the fitting of equation (1) for all the samples are shown in table 1. It has been observed that the anisotropy of the system increases after inserting a C<sub>60</sub> layer. The possible reason for this

increment in the anisotropy might be due to the hybridization between  $d$  orbital of Co, Fe, and  $p$  orbital of C. Due to d-p hybridization at the interface, DOS of  $C_{60}$  is modified and forms a spinterface.

**Table 1.** The values of  $K_2$  extracted from the fitting of LLG equation for all the samples.

Samples	$K_2$ (erg/cc)
S1	$2.56 \times 10^4$
S2	$2.89 \times 10^4$
S3	$3.12 \times 10^4$
S4	$4.10 \times 10^4$
S5	$4.31 \times 10^4$

#### ACKNOWLEDGEMENT

We would like thank DAE, DST-SERB, Govt. of India for funding.

#### REFERENCES

1. S. Mallik, et. al., Sci. Rep. **2018**, 8, 5515.
2. S. Sanvito, Nat. Phys **2010**, 6, 562-564.
3. S. Mallik, et. al., Nanotechnology, **2019**, 30, 435705.
4. S. Mallik, et. al, App. Phys. Lett., **2019**, 115, 242405.
5. S. Pan, et. al., Phys. Rev. Appl., **2017**, 7, 064012

## Nonlinear dynamics of two pinned Bloch domain walls inside an optical cavity

Rahul Gupta<sup>1</sup>, Huaiyang Yuan<sup>2</sup> and Himadri Shekhar Dhar<sup>3</sup>  
 Indian Institute of Technology Bombay, Powai, Mumbai-400076, India<sup>1,3</sup>  
 Utrecht University, Heidelberglaan 8, 3854 CS Utrecht, Netherlands<sup>2</sup>  
 Email: [rahul.quantumfield@iitb.ac.in](mailto:rahul.quantumfield@iitb.ac.in)

**Abstract:** We study the dynamics of a pair of pinned Bloch domain walls coherently coupled with photonic field inside an optical cavity. Under certain conditions we observe that the dynamics is nonlinear and has a stable limit cycle under which the system oscillates with a collective but highly tunable frequency. Preliminary studies seem to suggest that oscillations remain robust under change of parameter values implying possibility for existence of continuous time crystal phase.

### 1. INTRODUCTION

It has been shown [1] that pinned magnetic Bloch domain wall (DW) can be treated as a quantum mechanical oscillator when placed inside an optical cavity, interacting with light via an inverse Faraday effect, and microscopic Hamiltonian is analogous to the optomechanical systems. However, the dynamics when a greater number of such DWs are coupled with a single coherent cavity mode is still unknown.

We study the dynamics of two DWs coherently coupled with single cavity mode and obtain steady-state solutions under different resonance conditions. We find the existence of an unstable steady state for blue resonance around which the system orbits in a stable LC (limit cycle) with a frequency that is larger than the applied laser detuning. Such feature seems to suggest a TTS (Time Translation Symmetry) breaking in the dynamics. We find that the collective frequency depends directly on the amplitude of the applied laser field, coupling, and detuning strength and thus can be tuned easily. It is remarkable that similar phenomenon was also observed in BEC inside an optical cavity [2] despite having a quite different Hamiltonian.

Pinned DWs are already used in several spintronic based applications, but controlling and synchronizing them coherently in quantum/semiclassical regime with laser light opens up several new possibilities including application to quantum information processing.

### 2. PROPOSED SETUP AND MODELLING

The setup we use is analogous to [1] except we now place two pinned DWs in the cavity as shown in Fig.1.

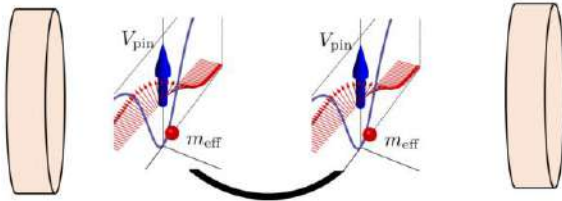


Fig.1. Two pinned Bloch DW inside an optical cavity. Each of them behaves as a massive particle trapped in H.O. and are coupled by the cavity photons.

The microscopic Hamiltonian can be written as  

$$\mathcal{H} = \omega_a a^\dagger a + \omega_1 b_1^\dagger b_1 + \omega_2 b_2^\dagger b_2 + g_1 (b_1 + b_1^\dagger) a^\dagger + g_2 (b_2 + b_2^\dagger) a^\dagger a + \xi (a e^{-i\omega t} + a^\dagger e^{i\omega t}) \quad (1)$$

where  $a$ ,  $b_1$ ,  $b_2$  are the cavity and DW modes respectively and  $g_1$ ,  $g_2$  are the coupling strength and the laser amplitude and frequency being  $\xi$  and  $\omega$  respectively. The eqn.(1) can be made time independent by shifting in driving frame and applying RWA. We obtain the non-linear mean field Quantum Langevin Equations (QLEs) and add incoherent cavity losses and gilbert damping terms to obtain the dynamics and also analytically obtain the steady state solution.

### 3. DYNAMICAL SOLUTIONS AND TTSB

Using standard RK4 method, we obtain the solution to QLEs in the blue resonance regime which exhibits limit cycle dynamics which is robust against minor perturbations of driving strength, dissipation or coupling strengths. The DW modes and photon modes oscillates with a collective frequency which is larger than the resonant detuning value. These are signatures for the presence of a continuous time crystal which brakes TTS as seen in Fig.2.

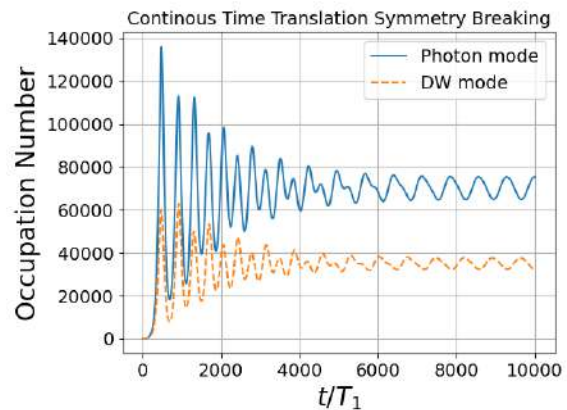


Fig.2. Initially out of phase oscillations synchronizes to oscillate at a single frequency in steady state along a limit cycle, thus breaking time translation symmetry.

### ACKNOWLEDGEMENT

RG acknowledges the support from CSIR-NET JRF.

### REFERENCES

- [1]. I. Proskurin *et al.*, Physical Review B **98**, (2018).
- [2]. H. Keßler *et al.*, Physical Review A **99**, (2019).

## Understanding thermally assisted diffusion and phase transition in FePt/Si Thin Films

Smridhi Chawla, Kapil Dev, Garima Vashisht, S. Annapoorni

Department of Physics and Astrophysics, University of Delhi, Delhi-110007

[smridhi.chawla@mirandahouse.ac.in](mailto:smridhi.chawla@mirandahouse.ac.in)

**Abstract:**  $L1_0$ -FePt is a superior material for ultrahigh density hard-disk drive application because of its extremely high-magnetic-anisotropy ( $\sim 7 \text{ MJ/m}^3$ ) at room temperature. The present work aims to enhance the anisotropy in FePt thin films sputtered over Si substrate. The expected change has been witnessed by recording M-H curves using Vibrating Sample Magnetometer (VSM) as well as by performing micromagnetic simulations via OOMMF. The theoretical results fit well with the experimental results of FePt films annealed at different temperatures. For  $500^\circ\text{C}$ , the simulated model with minor diffusion of FePt (4 nm) into Si substrate exhibits comparatively lesser coercivity as compared to pure FePt film with no diffusion on substrate, which indicates a drawback of annealing at high temperatures.

### 1. INTRODUCTION

FePt is one such interesting material that has large number of applications because of its existence in both the soft as well as hard phase which has their respective advantages [1]. Deposition of FePt thin films at room temperatures results in the formation of the chemically disordered A1(FCC) structure which exhibits soft magnetic properties [2]. Annealing at temperatures  $400^\circ\text{C}$  -  $500^\circ\text{C}$  is essential to obtain the hard magnetic  $L1_0$  (FCT) ordered phase which shows better stability in high density storage applications [3,4].

An attempt is made to modify the magnetic properties of FePt films as an impact of varying the annealing temperature, and consequently study its effect on diffusion at film/substrate interface. In addition, micromagnetic simulations were performed to investigate the effect of annealing on anisotropy, coercivity and the role of diffusion on these parameters.

### 2. METHODOLOGY

FePt thin films of thickness  $\sim 24 \text{ nm}$  was deposited using DC magnetron sputtering at room temperature on Si (100) substrate. They were annealed at  $300^\circ\text{C}$ ,  $400^\circ\text{C}$  and  $500^\circ\text{C}$  in the reducing atmosphere (95% Ar + 5%  $\text{H}_2$ ). M-H curves for in-plane as well as out of plane configuration for the as-prepared and the annealed samples were recorded using VSM. Micromagnetic simulations through OOMMF software were performed to reciprocate the hysteresis curves of fabricated films and investigate the anisotropy constant (K), exchange stiffness constants (A) for soft and hard phase of FePt are estimated considering sample size of (500 x 500) nm and thickness 24 nm.

### 3. RESULTS AND CONCLUSIONS

Fig. 1 shows the experimental as well as simulated M-H curves for the as-deposited and thermally annealed FePt films. An increase in the coercivity was observed from  $\sim 60 \text{ Oe}$  for the as-prepared FePt to 6300 Oe and 9700 Oe in the films annealed at  $400^\circ\text{C}$  and  $500^\circ\text{C}$  respectively. This enhancement in coercivity after annealing is ascribed to the phase transformation of FePt to the ordered  $L1_0$  structure [3]. For  $500^\circ\text{C}$  annealed sample two models were considered for simulations, one having pure FePt film with no diffusion and the other having a diffused interface

between FePt film and the substrate. The simulated model considering diffusion fits well with the experimental result which confirms the reduction of coercivity due to diffusion at higher temperature as compared to the model without diffusion [5]. The parameters used in simulations are given in Table 1.

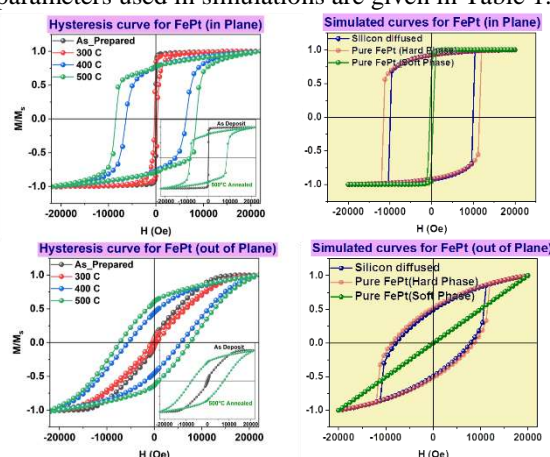


Figure 1:(left) M-H curves for as deposited and annealed FePt thin films, (right) Simulation curves.

Table 1. Simulation Results:

FePt	As Deposit	400 °C	500 °C	500 °C Diffused
$M_s(\text{A/m})$	$10^6$	$10^6$	$10^6$	$10^6$
$A(\text{J/m})$	$5 \times 10^{-11}$	$2 \times 10^{-10}$	$5 \times 10^{-9}$	$5 \times 10^{-9}$
$K(\text{J/m}^3)$	$10^3$	$5 \times 10^5$	$10^6$	$10^6$
InPlane $H_c(\text{Oe})$	100	6300	11500	9700
OutPlane $H_c(\text{Oe})$	60	5520	9630	7400

### 4. ACKNOWLEDGEMENT

University Science Instrumentation Centre (USIC), University of Delhi, India for VSM Measurements.

### 5. REFERENCES

- [1]. Guo et al., Chem. Int. Ed. 52 (2013),8526.
- [2]. R Goyal et al., J. Mag.Mag.Matr., 418(2016), 200.
- [3]. S.H. Sun et al., Adv. Mater. 18 (2006) 393.
- [4]. H. Gu et al., Chem. Commun. 1966 (2003).
- [5]. Shu Chen, et al, J.Mag.Mag.Matr., 417(2016), 442.

## Inverse spin Hall effect in sputter deposited MoS<sub>2</sub>/CoFeB bilayers

Abhisek Mishra\*, V.Thiruvengadam, Pushpendra Gupta, Koustuv Roy, Braj Bhusan Singh, Subhankar Bedanta

Laboratory for Nanomagnetism and Magnetic Materials (LNMM), School of Physical Sciences, National Institute of Science Education and Research (NISER), HBNI, Jatni-752050, Odisha, India  
Email:abhisek.mishra@niser.ac.in

**Abstract:** Two dimensional (2D) transition metal dichalcogenides are known to possess high spin orbit coupling that make them promising candidates for emerging spintronic devices. Here we report the measurement of spin to charge conversion in sputter deposited MoS<sub>2</sub> by inverse spin Hall effect (ISHE). Angle dependent measurements of ISHE are performed to identify various galvanometric rectification effects.

### 1. INTRODUCTION

Pure spin current is the key factor for development of next generation fast and power efficient spintronic devices [1]. Spin pumping is an established method to generate spin current via precessing magnetization from a ferromagnetic (FM) layer by microwave driven ferromagnetic resonance (FMR) in a ferromagnetic-nonmagnetic (FM/NM) system [2]. Heavy metals like Pt, Pd, Ta etc. having high spin orbit coupling (SOC), are crucial for the spin to charge conversion efficiently. However, for fabrications of power efficient and fast spintronic devices at commercial level, new material engineering is required. In this context, transition metal dichalcogenides (TMD) have shown potentials for spin-charge conversion due to their high SOC at atomically thin layer. Their layered structure can lead to formation of atomically flat surfaces thereby facilitating the transport properties to be tuned easily [3]. However, fabrication of 2D materials in large area is still a challenge. Therefore, it requires a high throughput technique like sputtering.

Here we report the spin-charge conversion by observing ISHE in sputtered MoS<sub>2</sub> thin films through the spin pumping from amorphous CoFeB.

### 2. EXPERIMENTAL TECHNIQUE

Thermally oxidized Si (100) substrate was used to grow 28 nm thick MoS<sub>2</sub> thin film, which is deposited by radio frequency (rf) magnetron sputtering. On top of it, CoFeB (6 nm) was grown by dc magnetron sputtering. To avoid oxidation, MgO layer was grown as a capping layer by electron beam evaporation. The sample was kept in a flip chip manner on a coplanar wave guide for the measurement of ISHE in a home modified FMR setup [4].

### 3. RESULT AND DISCUSSION

Angle dependent measurements of ISHE were performed to measure the spin pumping voltage at +15 dBm power of radio frequency field transmitted in the coplanar waveguide. Fig.1 shows the measured voltage signal ( $V_{meas}$ ) for the sample MoS<sub>2</sub>(28nm)/CoFeB(6nm)/MgO(2nm) at an in-plane angle of  $\varphi = 36^\circ$  with applied dc magnetic field ( $H$ ). For this sample the spin pumping voltage was found

to be 1.58  $\mu$ V. Frequency dependent damping studies and power dependent studies were carried out to understand the origin of the voltage signals obtained.

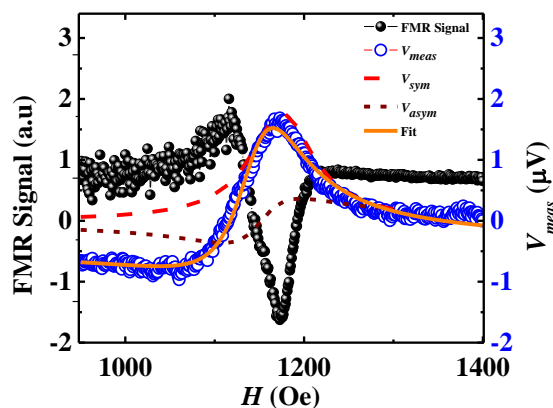


Fig.1. Voltage ( $V_{meas}$ ) measured along with FMR signal for sample with MoS<sub>2</sub> (28 nm) at the  $\varphi$  value of 36°.

### ACKNOWLEDGEMENT

The authors acknowledge the financial support by the Department of Atomic Energy (DAE) and Department of Science and Technology (DST-SERB) of Government of India for the DST-Nanomission [project sanction No. SR/NM/NS-1018/2016(G)]. PG and KR thank UGC and CSIR respectively for SRF fellowship. BBS acknowledges DST for INSPIRE Faculty fellowship.

### REFERENCES

- [1]. T.P.Pareek, Phys. Rev. Lett. 92, 076601 (2004).
- [2]. B. Heinrich *et al.*, Phys. Rev. Lett. 90, 187601 (2003).
- [3]. Z.Hu *et al.*, Chem. Soc. Rev., 2018, 47, 3100
- [4]. B.B.Sigh *et al.*, Phys. Status Solidi RRL 2019, 13, 1800492



## Superconductivity in nickelates via increasing c-axis in films

Akariti Sharma<sup>1,\*</sup>, Navinder Singh<sup>1</sup>

<sup>1</sup> Theoretical Physics Division, Physical Research Laboratory, Navrangpura Ahmedabad, India - 380009

\*Email: akaritisharma@gmail.com

**Abstract:** Nickelates high-temperature superconductivity (HTS) is in picture now. This raises new questions for theoreticians about the mechanism of its superconductivity. From electronic structure calculations of NdNiO<sub>2</sub>, it seems that nickelate superconductivity requires consideration of dz<sup>2</sup> orbital. Comparison of actual NdNiO<sub>2</sub> film with the increased c-axis NdNiO<sub>2</sub> film has framed the main part of this work revealing the importance of enhanced contribution of dz<sup>2</sup> orbital in increased c-axis films of NdNiO<sub>2</sub>.

### 1. INTRODUCTION

To understand how superconductivity (SC) emerges in NdNiO<sub>2</sub> is a crucial step toward the physical understanding of nickelate superconductivity [1–3]. Since the SC mechanism is rooted in different origins of the correlation in NdNiO<sub>2</sub>, the exploration of multiple orbital contributions for SC is of great importance, which could further enrich the subject of SC in NdNiO<sub>2</sub>. The experimental findings of SC in infinite-layer nickelates RNiO<sub>2</sub> (R=La, Pr, Nd) offers a new bench for researchers to explore the hidden mechanism behind unconventional SC. A possible route to address the origin of high-temperature superconductivity is to find the contribution of multi orbitals at Fermi-level, which might help unveil what is relevant for HTS. One plausible strategy to find cuprate analogs is to replace Cu<sup>2+</sup> with iso-electronic Ni<sup>1+</sup>: d<sup>9</sup>. This oxidation state formally takes place in infinite-layer nickelates which is the topic of interest.

### 2. ELECTRONIC STRUCTURE AND COMPUTATIONAL DETAILS

We have performed calculations in both actual NdNiO<sub>2</sub> film (with a = 3.962 Å and c = 3.629 Å), and increased NdNiO<sub>2</sub> film (a = 3.962 Å and c = 3.737 Å), experimentally available parameters of the infinite-layer nickelates family. The primitive P4/mmm cell was employed to study the electronic structure. The corresponding structures for films are shown in Fig.1. The structures of the bulk and layered NdNiO<sub>2</sub> were fully relaxed using the QUANTUM ESPRESSO code within the Perdew-Burke-Ernzerhof version of the generalized gradient approximation. In spin-polarized calculations both ferromagnetic (FM) and antiferromagnetic (AFM) orders were considered.

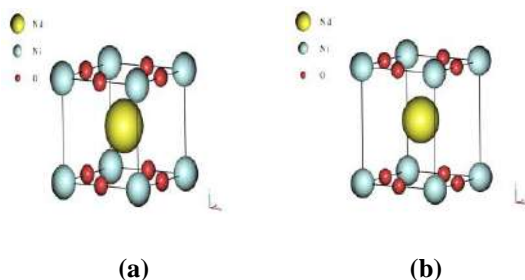
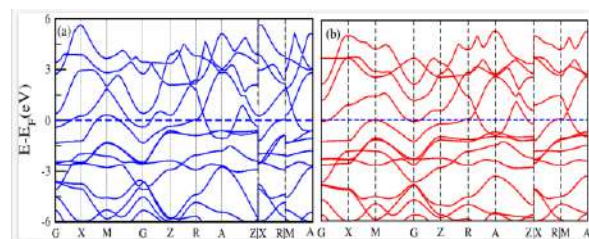


Fig.1. NdNiO<sub>2</sub> films (a), and increased c-axis NdNiO<sub>2</sub> films (b).

### 1. RESULTS

Extraction of layers of oxygen from thin films of Sr doped perovskite structure NdNiO<sub>2</sub> has led to emergence of superconductivity in nickelate. Comparison of the electronic band structure in actual NdNiO<sub>2</sub> films and increased c-axis in NdNiO<sub>2</sub> films are shown in Fig. 2. There is the formation of electron pockets at G- and A-points (see Fig. 2 (a)) whose size decreases with increase in c-axis, which indicates the weakening of crystal field effect due to Nd. Our density of state observations in Fig. 3 point toward a new Ni dz<sup>2</sup> orbital dominance in NdNiO<sub>2</sub> film, with its role enhanced in the increased c-axis case. In contrast to this the dx<sup>2</sup>-y<sup>2</sup> orbital has dominance in cuprates.

Fig.2. Electronic band structure of NdNiO<sub>2</sub> films (a),



and increased c-axis NdNiO<sub>2</sub> films (b).

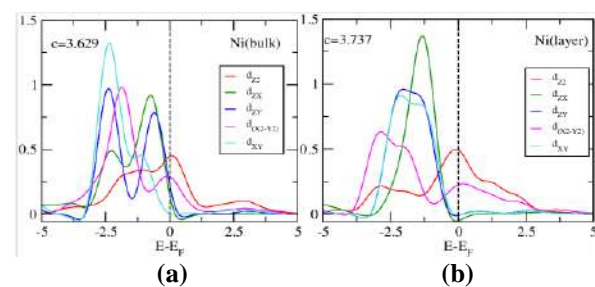


Fig.3. Multi-orbital contribution of Ni in NdNiO<sub>2</sub> films (a), and increased c-axis NdNiO<sub>2</sub> films (b).

### ACKNOWLEDGMENT

I wish to acknowledge HPCC, PRL, Ahmedabad.

### REFERENCES

- [1]. D. Li, et al. Nature **572** (2019) 624.
- [2]. A. S. Botana and M. R. Norman, Phys. Rev. X. **10** (2020) 011024.
- [3]. W. E. Pickett, Nat. Rev. **8** (2021) 1-2.

## Transition Metal Substituted TMDC ( $\text{MoS}_2/\text{WS}_2$ ) Heterostructure for Realization of Dilute Magnetic Semiconductors

Neha Kapila Sharma,<sup>1,2</sup> Sameer Kumar Mallik,<sup>1,2</sup> Anjan Kumar Jena,<sup>1,2</sup> Sandhyarani Sahoo,<sup>1,2</sup> Mousam Charan Sahu,<sup>1,2</sup> Sanjeev K. Gupta,<sup>3</sup> Rajeev Ahuja,<sup>4,5</sup> Satyaprakash Sahoo<sup>1,2</sup>

1. Laboratory for Low Dimensional Materials, Institute of Physics, Bhubaneswar 751005, India

2. Homi Bhabha Training School Complex, Anushakti Nagar, Mumbai, 400094, India

3. Computational Materials and Nanoscience Group, Department of Physics and Electronics, St. Xavier's College, Ahmedabad 380009, India

4. Condensed Matter Theory Group, Department of Physics and Astronomy, Uppsala University, S-75120 Uppsala, Sweden,

5. Department of Physics, Indian Institute of Technology Ropar, Rupnagar, Punjab- 140001, India

Email: (kapilaneha5@gmail.com)

**Abstract:** 2Dimensional(2D) materials manifest excellent magnetic feature, beneficial to the potential applications in spintronics. Using first principles calculations we demonstrate the  $\text{MS}_2$  ( $M = \text{Mo}, \text{W}$ ) monolayers, and their hetero-bilayers as promising 2D dilute magnetic semiconductors with the incorporation of Mn and Co dopants. The electronic and magnetic properties with various pairwise doping configurations have been studied. The magnetic coupling among the dopant pairs can be tuned between FM and AFM orderings via suitable dopant sites. The developed interlayer exchange coupling between the layers leads to strong and long-ranged ferromagnetic interactions which unleash robust magnetic moments with stable doping configurations.

### 1. INTRODUCTION

Dilute magnetic semiconductors (DMS)<sup>1</sup> based on magnetic/non-magnetic ion doping in two-dimensional (2D) materials such as graphene,<sup>2,3</sup> phosphorene,<sup>4</sup> h-BN,<sup>5</sup> and transition metal dichalcogenides (TMDCs)<sup>6</sup> has proven potential applications in spintronics. The doping of TM elements such as Mn, Co, Fe, etc. is proved to be the most efficient and facile one when it comes to the realization of DMS. With the possibility to seek electrical control over magnetism and thus exploit spintronics applications, scalable approaches have been made to engineer these materials to introduce a stable magnetic phase. Herein, with the help of first principles calculations, we demonstrate a 2D DMS consisting of TM doped  $\text{MoS}_2/\text{WS}_2$  hetero-BL. The Mn and Co doping attribute the consequential change in magnetic properties giving rise to excellent magnetic moments with dilute doping concentration.

### 2. RESULTS AND DISCUSSION

#### 2.1. TM dopants in monolayer $\text{MS}_2$ ( $M = \text{Mo}, \text{W}$ )

A pair of host Mo and W atoms have been replaced with two TM elements in a  $5 \times 5 \times 1$  supercell of  $\text{MoS}_2$  and  $\text{WS}_2$  MLs respectively, representing a doping concentration of about 8%, which is sufficient to study the DMS behaviours in view of previously reported results.<sup>6</sup> Depending upon the separation, the two TM atoms are substituted at different M-sites generating 3 configurations (a) first nearest neighbour (NN) (b) second nearest neighbour (NNN), and (c) third nearest neighbour (NNNN). The NN configurations are quite stable with the lowest energies which explain the preference for cluster formation of the dopants in all the cases. However the magnetic moment is highest when the dopants are placed apart as shown in figure-1

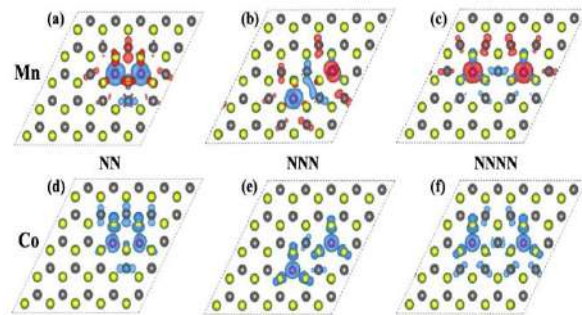


Fig-1 Spin density distribution around impurity atoms

#### 2.2. TM dopants in $\text{MS}_2$ hetero-BLs ( $M = \text{Mo}, \text{W}$ )

Mn and Co pairs at Mo or W sites in the  $\text{MoS}_2/\text{WS}_2$  are most stable at NN site preferring the cluster formation of the dopant pairs.

### 3. Conclusion

Mn and Co show significant change in magnetic behaviour of host layers. The switching between the FM and AFM ordering among the dopant pairs is observed with the dopant pair separation leading to tunable magnetism.

### REFERENCES

- [1]. Sato K et al. Rev. Mod. Phys. 2010, 82 (2), 1633-90
- [2]. Krasheninnikov, A. V et al. Phys. Rev. Lett. 2009, 102 (12), 126807.
- [3]. Santos E.J. G. et al. Phys. Rev. B 2008, 78 (19), 195420.
- [4]. Yu, W et al. Nanoscale Res. Lett. 2016 111 2016, 11 (1), 1–9
- [5]. Ataca, C. et al. Phys. Rev. B - Condens. Matter Mater. Phys. 2010, 82 (16), 165402.
- [6]. Cheng, Y. C. et al. Phys. Rev. B - Condens. Matter Mater. Phys. 2013, 87 (10), 100401.

## **SYNTHESIS OF NANOSTRUCTURED MAGNESIUM OXIDE BY SOL GEL METHOD AND ITS CHARACTERIZATION**

P.Kavitha<sup>1</sup>, V. Ramadevi<sup>1</sup>, Monalisa Hazarika\*<sup>1</sup>

<sup>1</sup>Department of Electronics & Communication Engineering,  
Chaitanya(Deemed to be University), Warangal, Telangana, INDIA

Email: [monalisahzri.tezu@gmail.com](mailto:monalisahzri.tezu@gmail.com)

### **Abstract:**

Metals are able to form a large number of oxides. An important metal oxide known as magnesium oxide (MgO) having good reactivity is widely used in producing electronics, catalyst, ceramics, oil, paint *etc.* Magnesium oxide nanoparticle is non-toxic and need a small amount, so it is suitable for the development of flame-retardant fiber additives. In addition, nano magnesium oxide added in fuel can inhibit corrosion. Spherical shaped Magnesium oxide nanoparticles were successfully synthesized by sol-gel technique at room temperature using magnesium nitrate and sodium hydroxide as a precursor. The morphological investigation of MgO nanoparticles was done by various analytical techniques. X-ray Diffraction (XRD) indicates the crystallinity and crystal size of MgO nanoparticle. Transmission electron microscopy (TEM) tells about the particle size and morphology. Fourier transform infrared microscopy was used to get the infrared spectrum of the sample indicating powdered composition of the sample. UV-Visible spectroscopy was used to know the optical properties of the sample.

### **Reference:**

[1] Gray JE and Luan B: Protective coatings on magnesium and its alloys- a critical review. Journal of Alloys and Compounds 2002; 336: 88-113.



## Effect of Zn<sup>2+</sup>-Zr<sup>4+</sup> Substitution on Magnetic Properties M-type Strontium Hexaferrite

Swati Verma<sup>1\*</sup>, Sachin Godara Kumar<sup>2</sup>, Mandeep Singh<sup>1</sup>

<sup>1</sup>Department of Physics, Guru Nanak Dev University, Amritsar 143005, Punjab, India

<sup>2</sup>Department of Chemistry, UGC Center for Advanced Studies-II, Guru Nanak Dev University, Amritsar, Punjab, India-143005

Email: [swati.phy123@gmail.com](mailto:swati.phy123@gmail.com)

**Abstract:** The aim of this work is to investigate the effect of Zn<sup>2+</sup>-Zr<sup>4+</sup> dopants on M type Strontium hexagonal ferrites (SrM) on structure and properties. In the present work, we have synthesized a series of SrZn<sub>x</sub>Zr<sub>x</sub>Fe<sub>12-2x</sub>O<sub>19</sub> (x= 0.00, 0.01, 0.02, 0.05, 0.10 and 0.15) using solid-state method. Magnetic measurements reveal that the values of coercivity ranges from 5164Oe (x = 0) to 6210Oe (x=0.15). The saturation magnetization (*M<sub>s</sub>*) values are in the range of 66.42 to 86.27 emu/g. The enhanced magnetic properties of Zn<sup>2+</sup>-Zr<sup>4+</sup>doped SrM hexaferrites samples over undoped samples could be vital for permanent magnets and EMI shielding.

### 1. INTRODUCTION

M-type hexaferrite (Ba, Ca, Pb and Sr) have gained significant attention since the last few decades because of their exceptionally high magnetic properties. These materials are used in all areas of life, including simple loud speaker magnets, transformers, radiofrequency coils, microwave devices, electromagnetic shielding devices, memory cells, recording media and supercapacitors [1-3]. In the present study, Zn<sup>2+</sup>-Zr<sup>4+</sup> doped SrM have been synthesized using sol-gel-auto-combustion technique using tartaric acid as fuel. The synthesized solid solutions have been characterized using Vibrating sample magnetometer (VSM) technique to study about the magnetic properties of the synthesized samples. The prepared samples have better magnetic properties and may thus find applications in permanent magnets, data storage devices and EMI shielding.

### 2. STRUCTURAL STUDIES

The X-ray diffractograms of SrZn<sub>x</sub>Zr<sub>x</sub>Fe<sub>12-2x</sub>O<sub>19</sub> (x = 0.00, 0.01, 0.02, 0.05, 0.10, 0.15) samples reveals that all the samples are highly crystalline in nature. A comparison of literature with measured peak positions shows that all the peaks position can be indexed to a single hexagonal unit cell (SrFe<sub>12</sub>O<sub>19</sub>). The comparison of all the peak positions with a single (ICSD 98-011-0455) data card indicates that Zn and Zr cations have been replaced with Ferric ions into the lattice and all the samples are phase pure. Fig. 1 shows Rietveld refined data for x = 0.15 sample.

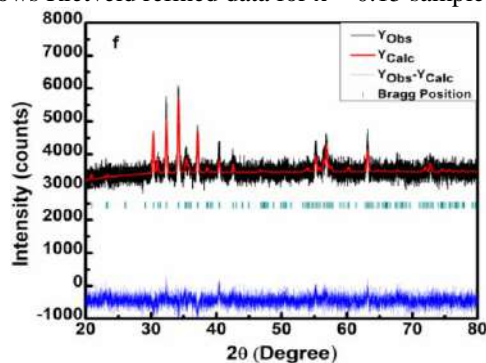


Fig.1: X-ray diffractograms of x=0.15 SrZn<sub>x</sub>Zr<sub>x</sub>Fe<sub>12-2x</sub>O<sub>19</sub> sample.

### 3. MAGNETIC STUDIES

The magnetization (*M*) vs. magnetic field (*H*) plots of SrZn<sub>x</sub>Zr<sub>x</sub>Fe<sub>(12-2x)</sub>O<sub>19</sub> samples (x= 0.00 to 0.15) were shown in Fig. 2. The figure clearly shows that all the samples display non saturating hysteresis loops signifying the presence of strong magnetic ordering. The *M* vs. 1/*H*<sup>2</sup> data was plotted in this range which exhibited almost straight line behavior. The intercept of straight line fit to this data (as shown in Fig. 3 for a typical sample (x=0.00)) on y-axis yielded *M<sub>s</sub>*.

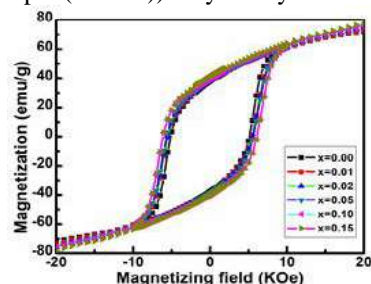


Fig.2: a) The *M* vs. *H* loops of x = 0.00, 0.01, 0.02, 0.05, 0.10 and 0.15 SrZn<sub>x</sub>Zr<sub>x</sub>Fe<sub>12-2x</sub>O<sub>19</sub> samples recorded at 300 K.

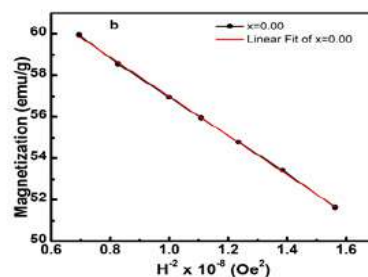


Fig.3: Linear fitting of *M* vs. 1/*H*<sup>2</sup> data to determine *M<sub>s</sub>* for a typical (x=0.00) SrZn<sub>x</sub>Zr<sub>x</sub>Fe<sub>12-2x</sub>O<sub>19</sub> sample.

### ACKNOWLEDGEMENT

The authors gratefully thank Centre for Emerging Life Sciences (GNDU, Amritsar) for providing access to various characterization facilities.

### REFERENCES

- [1]. Bhattacharya et al, *RSC Adv.*, 4 (2014).
- [2]. Qiu et al, *J. Appl. Phys.*, 98, 103905, (2005).
- [3]. Kaur et al, *J. Magn. Magn. Mater.*, 420 (2016).

## Effect of Ir spacer layer on perpendicular synthetic antiferromagnetic coupling in Co/Pt multilayers

Shaktiranjana Mohanty\*, Minaxi Sharma, Brindaban Ojha, Ashish K moharana, Esita Pandey, Braj Bhusan Singh, Subhankar Bedanta

Laboratory for Nanomagnetism and Magnetic Materials (LNMM), School of Physical Sciences,

National Institute of Science Education and Research (NISER), HBNI, Jatni-752050, Odisha, India

Email: [shaktiranjana.mohanty@niser.ac.in](mailto:shaktiranjana.mohanty@niser.ac.in)

**Abstract:** Tunability, miniaturization and functionality of spintronics devices depend on the interface engineering of ferromagnetic (FM) and nonmagnetic (NM) ultrathin layers. In this context, synthetic antiferromagnets (SAFs), which consists of two or more FM layers separated by a spacer layer that may be metallic or a tunnel barrier, having antiparallel magnetization in the consecutive FM layers. Such kinds of SAFs gives extra degree of freedom over antiferromagnetic materials for the, measurements, manipulation of stray field, which helps to tune stability and sensitivity of the devices. Here we show the study of SAF nature in Co/Pt multilayers separated by Ir as a spacer. We have also studied the strain induced modification of the coupling strength of SAF structure.

### Introduction

Development of next generation spintronics devices require the novel interface engineering of ferromagnetic (FM) layers to overcome the requirement of low current density to switch magnetization, high thermal stability, and fast speed of data writing reading etc. Magnetic tunnel junctions (MTJs) already established a jump in the enhancement of data storage capacity. [1]. Synthetic antiferromagnets (SAF) are the key part of these MTJs devices for better data retaining and thermal stability due to the absence of stray field. SAFs are basically with Ferromagnetic (FM) layers periodically interleaved with metallic or insulating spacers, where the magnetization of adjacent FM layers alternates owing to the antiferromagnetic (AF) interlayer exchange coupling (IEC). For metallic spacers, IEC is achieved via Ruderman-Kittel-Kasuya-Yosida (RKKY) type exchange interaction mediated by spin polarized charge carriers in the spacer [2]. By changing the thickness of non-magnetic material between two magnetic layers one can therefore tune the interaction from ferromagnetic preferring parallel alignment to antiferromagnetic, preferring antiparallel alignment, whereas for thick spacers the interlayer exchange coupling is suppressed. Using a SAF structure as either the free layer or the pinned layer, has the advantage of producing an adjustable net magnetic moment and reduced magnetostatic interaction between the layers and also provides a good field sensitivity [3].

Here fabricated SAF samples with Co as FM layer and Ir as a spacer layer and studied the magnetic properties. We then prepared the similar structure taking one FM layer both below and above the Ir spacer on a flexible polyimide substrate. With the application of both compressive and tensile stress, we observed a substantial change in the interlayer exchange coupling of the SAF layers.

### Experimental Details

All the samples were prepared using the multi deposition sputtering system manufactured by Mantis Deposition Ltd. For all the samples deposition, the chamber was maintained at a base pressure of  $\sim 2 \times 10^{-7}$  mbar. During deposition, the substrate table was rotated at 15 rpm for all the layers. Domain imaging and hysteresis loop

measurements have been performed by using magneto optic Kerr effect (MOKE) microscopy. Magnetization vs field was measured in a SQUID (Superconducting Quantum Interference Device) VSM. The sample structures are Si/Ta(3 nm)/ [Pt(3.5 nm)/Co(0.8 nm)]<sub>2</sub>/Ir( $t_{Ir}$  = 0.5, 1.0 1.5, 2 nm)/Co(0.8 nm)/ Pt(3.5 nm). Also one reference sample was prepared without the Ir spacer layer. The sample structure of the reference sample is Si/Ta(3 nm)/[Pt(3.5 nm)/Co(0.8nm)]<sub>2</sub>/Ta(3 nm).

### Result and Discussion

Among all the above mentioned structures, samples with Ir thickness 0.5 nm and 1.5 nm show AFM coupling between the Co layers. The samples with Ir thickness shows FM coupling. Sample with 1.5 nm Ir thickness shows a strong AFM interlayer exchange coupling (Fig.1).

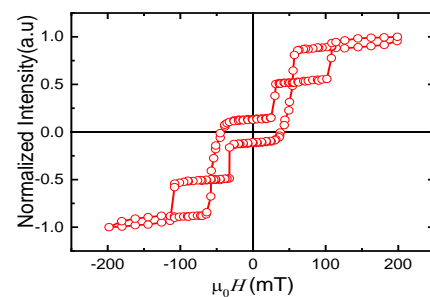


Fig. 1: Hysteresis loop obtained from the Kerr Microscopy measurement for the SAF sample with Ir thickness 1.5 nm

### Acknowledgement

Authors would like to thank DAE & DST, Govt. of India for the financial support to carry out the experiments. BBS acknowledges DST for INSPIRE Faculty fellowship.

### Reference

1. Chatterjee, J., Auffret, S., Sousa, R. *et al. Sci Rep* 8, 11724 (2018)
2. Kay Yakushiji *et al* 2015 *Appl. Phys. Express* 8 083003
3. Duine, R.A., Lee, K., Parkin, S.S.P. *et al., Nature Phys* 14, 217–219 (2018)

## Structural changes on the post annealing of Ta/Co<sub>60</sub>Fe<sub>20</sub>B<sub>20</sub>/Ta heterostructures: Effects on static and dynamics magnetization properties

**Nanhe Kumar Gupta,<sup>1,\*</sup> Sajid Husain<sup>2</sup>, Vineet Barwal,<sup>1</sup> Soumyarup Hait,<sup>1</sup> and Sujeet Chaudhary,<sup>1</sup>**

*Thin Film Laboratory, Department of Physics, Indian Institute of Technology Delhi, New Delhi-110016, India*

*<sup>2</sup>Unité Mixte de Physique, CNRS, Thales, Université Paris-Saclay, 91767 Palaiseau, France*

\* Corresponding author: [nanhekg@gmail.com](mailto:nanhekg@gmail.com)

The CoFeB alloy has been recognized as potential material system for the ferromagnetic electrode in spin torque-based devices. In the device fabrication, one of the most crucial process steps is the post-annealing treatment of the heterostructure as it majorly governs the performance of the device. In this work, we have systematically investigated the critical role of annealing treatment on the structural and magnetic (both static as well as dynamic) properties of the Ta/CoFeB/Ta heterostructures by varying the annealing temperature ( $T_A$ ). The dependence of damping parameter ( $\alpha$ ), saturation magnetization, and coercive field on  $T_A$  is thoroughly studied. Notably, these parameters show abrupt changes at  $T_A=400^\circ\text{C}$  which are strongly correlated with the structural properties of CoFeB. Interestingly, the damping constant is initially found to decrease with  $T_A$  up to  $400^\circ\text{C}$ , followed by a sharp enhancement at  $415^\circ\text{C}$ . The damping variation is found to be robust in a range of thicknesses from 28nm to 5nm of CoFeB. A slow reduction of  $\alpha$  occurs due to an early stage of crystallization and a record low value of  $\alpha \sim 3.46(0.06) \times 10^{-3}$  is achieved at  $400^\circ\text{C}$ . A sharp transition in electrical resistivity at  $400^\circ\text{C}$  reveals the onset of modification in the microstructure of CoFeB. The coercivity, crystallite size, surface roughness, and magnetic anisotropy are found to be highly sensitive to the  $T_A$  dependent changes during the post-annealing of the stacks. The work substantiates the deterministic role of the appropriate choice of annealing temperature on the microstructure of our unique composition of CoFeB that paves the way to consider it for future spintronic research.

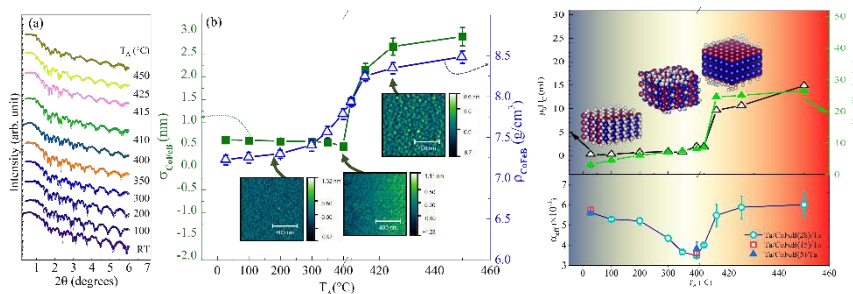


**Figure 1** (a) X-ray reflectivity profiles recorded on Si/SiO<sub>2</sub>/Ta/CoFeB/Ta heterostructure annealed at various  $T_A$ . The symbols represent the experimental data, and solid lines are simulated fits. (b) Variation of the estimated values of the *rms* roughness of the upper CoFeB/Ta interface (solid squares) in the heterostructure and density (open triangles) of CoFeB layer evaluated from XRR simulated fitting, with  $T_A$ . The line connecting the symbols are guide to the eye. The 3 AFM images shown within the panel of Fig. 1(b) correspond to the uncapped CoFeB (28 nm) films annealed at  $T_A=200, 410$  and  $415^\circ\text{C}$ , and Fig.1(c) summarize the effect of  $T_A$  on crystallite size, coercivity and damping constant.

[1] A. Conca, E. Th. Papaioannou, S. Klingler, J. Greser, T. Sebastian, B. Leven, J. L€osch, and B. Hillebrands, Applied Physics Letter 104, 182407 (2014)

## Reconfigurable logic operations via gate controlled skyrmion motion in a nanomagnetic device

Bibekanda Paikaray<sup>1</sup>, Mahathi Kuchibhotla<sup>2</sup>, Arabinda Haldar<sup>2</sup>, and Chandrasekhar Murapaka<sup>1</sup>

<sup>1</sup>Department of Materials Science and Metallurgical Engineering, Indian Institute of Technology Hyderabad, Kandi 502284, Telangana, India

<sup>2</sup>Department of Physics, Indian Institute of Technology Hyderabad, Kandi 502284, Telangana, India

Email: (Times New Roman 10 point)

**Abstract:** Magnetic skyrmion is a topological object having particle-spin like configuration, which can be stabilized in ferromagnetic systems with Dzyaloshinskii-Moriya interaction. We have proposed a reconfigurable skyrmion-based two-input logic device architecture as shown in Figure 1(a). Using micromagnetic simulations, we have demonstrated that the device is capable of performing both OR & AND logic gate functionalities in a reconfigurable manner.

### 1. INTRODUCTION

Magnetic skyrmions are particle like whirling spin texture with topological protection. Skyrmions have attracted much attention recently in the field of spintronics, due to their nanoscale size  $\sim(10-100\text{ nm})$ , high speed  $\sim(10-100\text{ m/s})$  and relatively low driving current density  $\sim(10^6\text{ A/m}^2)$  as compared to domain walls [1,2]. Thus, it acts as a promising candidate for low power consumption, fast processing, and high-density spintronic-based memory and logic applications [3]. The spin texture of magnetic skyrmions is a stable configuration, which originates from an anti-symmetric exchange interaction known as Dzyaloshinskii-Moriya interaction (DMI). In addition to DMI, various other internal magnetic energies such as exchange interaction, demagnetization energy and anisotropy energy play a vital role in the formation of twisted magnetic textures and make the skyrmion topologically stable.

### RESULTS AND DISCUSSION

In this work, we have proposed a simple architecture for reconfigurable skyrmion-based nanomagnetic devices (see Fig.1(a)) which are capable of performing both OR & AND logic operations in a single magnetic nanostructure as shown in Fig. 1(b,c). To demonstrate the concept, we have used the micromagnetic simulations which is a powerful technique for investigations before any practical implementations. The skyrmion in the device is driven by the SOT and a current-induced Oersted field through a non-magnetic metallic gate controls the skyrmion trajectory in the device. By simply switching ON and OFF the current at the metallic gate, we can toggle between OR & AND logic operations. Furthermore, to understand the motion of the skyrmions and the effect of different forces on the skyrmion, we have estimated the  $\phi_{SkH}$  and the size of the skyrmion at different positions of the nanodevice. The performance and a robust operation of the logic device have been investigated in detail by systematically varying the driving current density ( $j$ ) and Oersted field (see Fig.1(d)), DMI ( $D$ ) constant, anisotropy constant ( $K_u$ ) and geometrical parameters.

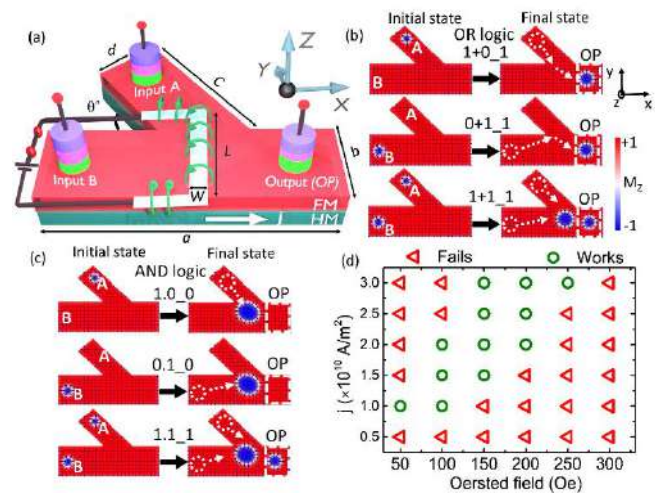


Fig.1.(a)Schematic device structures of the proposed reconfigurable skyrmion based logic gate with two inputs A, B and one output (OP). Initial and final magnetic states of skyrmion motion in FM film for the inputs in logic (b) OR gate (c) AND gate (d) Working window of the AND logic operation as a function of Oersted field (Oe) generated by the metallic gate and the current density ( $j$ ).

### ACKNOWLEDGEMENT

CM would like to acknowledge funding from SERB-Early Career Research Award (ECR/2018/002664). BP would like to acknowledge fellowship from the Department of science and Technology, India (DST/INSPIRE Fellowship/ [IF180927]).

### REFERENCES

- [1] A. Fert, et.al.Nature Nanotechnology8, 152 (2013)
- [2] Luo S et la., APL Materials 9, 050901 (2021).
- [3] Sampaio, S et al.,Nature Nanotechnology,8, 839844 (2013).



## Effect of Calcination Temperature on the Structural, Surface Morphology and Magnetic Properties of M-type Barium Strontium Hexaferrite

Sachin Kumar Godara<sup>1</sup>, Vishal Kumar<sup>2</sup>

<sup>1,2</sup>Department of Chemistry, UGC Center for Advanced Studies-II, Guru Nanak Dev University, Amritsar, Punjab, India-143005  
Email: vishalchalotra00@gmail.com

**Abstract:** In the current study, the synthesis of  $Ba_{0.5}Sr_{0.5}Fe_{12}O_{19}$  samples using the sol-gel auto-combustion method was carried out. XRD spectra indicate pure phase formation  $\geq 900^\circ C$  calcined sample. FESEM micrographs reveal an increase in grain size with an increase in calcination temperature. Raman peaks broadening without any peak shift at  $1200^\circ C$  calcined samples may be due to slight crystal straining. Magnetic studies reveal that the maximum value of saturation magnetization ( $M_s$ ) is 68.44 for a  $1200^\circ C$  calcined sample. The coercivity ( $H_c$ ) monotonically increases from 4099 to 5190 Oe with increasing calcination temperature up to  $1100^\circ C$  and then decrease drastically to 2377 Oe.

### 1. INTRODUCTION

Since the last few decades, a lot of work has been carried out to tune the magnetic, dielectric, optical, and microwave properties of M-type hexaferrite (like BaM, SrM, etc.). Hexaferrites have excellent magnetic properties, high Curie temperature, good microwave absorption properties, high chemical stability, high corrosion resistance, and lower cost as compared to conventional magnetic materials[1-2]. These materials have many applications such as in data recording devices, electronic devices, in the medical sector etc [3]. Further, the properties of M-type hexagonal ferrites are known to depend upon external dopants, crystallite/grain size, calcination temperature, and synthesis method [4]. Optimization of calcination temperature is most widely studied for BaM. However, not much work has been reported on the optimization of calcination of  $Ba_{0.5}Sr_{0.5}Fe_{12}O_{19}$  and studied its impact on the structure, morphology, and magnetic properties.

### 2. EXPERIMENTS AND RESULTS

#### 2.1. Experiment

Barium-Strontium M-type hexaferrite (BaSrM) was synthesized by sol-gel auto combustion method using metal nitrate to fuel (Citric acid) ratio of 1:1. Analytical grade chemicals such as ferric nitrate, Barium nitrate, strontium nitrate and citric acid were used. The prepared material was grounded into a fine powder and then calcined at different temperatures  $500-1200^\circ C$  for 6 hours furnace using a heating rate of  $100^\circ C/hr$ .

#### 2.2. Results

Figure 1a-d shows the FESEM micrographs of typical  $Ba_{0.5}Sr_{0.5}Fe_{12}O_{19}$  samples (calcined at  $900, 1000, 1100$  and  $1200^\circ C$ ). The micrographs reveal that these samples consist of polygon shaped isolated and agglomerated particles. The samples exhibit a lot of polydispersity and the particle size appear to increase with increasing calcination from  $900$  to  $1200^\circ C$ .

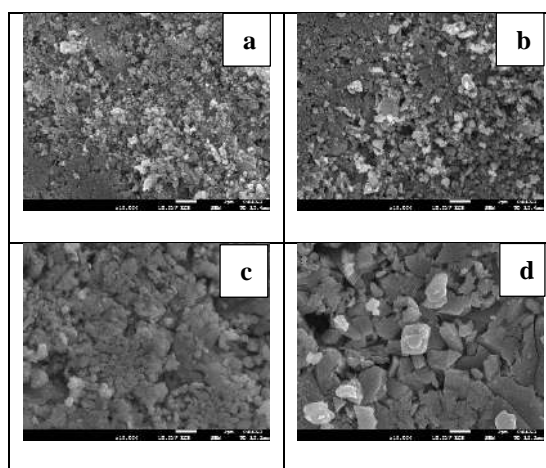


Fig.1: FESEM micrographs of a) 900 b) 1000, c) 1100 and d) 1200  $Ba_{0.5}Sr_{0.5}Fe_{12}O_{19}$  samples

Table 1: Average grain size of  $Ba_{0.5}Sr_{0.5}Fe_{12}O_{19}$  samples calcined at different temperatures

Calcination temperature	Average grain size in nm
$900^\circ C$	100
$1000^\circ C$	202
$1100^\circ C$	325
$1200^\circ C$	1022

### 3. REFERENCES

- T. Kaur et al, Cryst. Res. Technol., 52 (2017).  
 J. Mohammed et al, Mater. Res. Express, 5 (2018) 86106  
 S.K. Godara et al, Results in Physics., 22 (2021) 103892  
 J. Mohammed et al., *J. Mater. Sci. Mater. Electron.*, 30 (2019) 4026.  
 J. Mohammed et al., *J. Phys. Chem. Solids*, vol. 126, (2019).

## Thickness dependent structural and magnetic properties investigation of CoFeB films interfaced with 4d (Ru) and 5d (Ta) heavy metals

Harsh Vardhan<sup>1,2\*</sup>, Gagan Sharma<sup>1,2</sup>, Kavita Sharma<sup>1,2</sup>, Mukul Gupta<sup>3</sup>, Anil Gome<sup>3</sup>, V. R. Reddy<sup>3</sup>

<sup>1</sup>Amity Center for Spintronic Materials, Amity University UP, Sector-125, Noida 201313, India

<sup>2</sup>Amity Institute of Applied Sciences, Amity University UP, Sector-125, Noida 201313, India

<sup>3</sup>UGC-DAE CSR, University Campus, Khandwa road, Indore 452001, India

Email: ([hvardhan1@amity.edu](mailto:hvardhan1@amity.edu))\*

**Abstract:** In the present work, wedge shaped CoFeB film interfaced with Ta and Ru were deposited using ion beam sputtering. Structural magnetic properties of deposited multilayer structure were investigated using X-Ray reflectivity (XRR) and magnetic optical Kerr effect (MOKE).

### 1. INTRODUCTION

Extensive studies have been reported in recent literature on investigation of the structural and magnetic properties of ferromagnetic films interfaced with heavy metals. In fact, ferromagnetic films interfaced with heavy metals exhibits a number of important phenomenon like spin-orbit torque[1], interfacial perpendicular magnetic anisotropy[2] and Dzyaloshinskii-Moriya interaction (DMI) which are crucial for next generation spintronic devices[3]. However, the strength of such phenomenon is significantly affected by the degree of alloying of ferromagnetic films at interface. Therefore, detailed study is to be done in this direction and exploring the interfacial magnetism.

### 2. EXPERIMENTAL

Two different samples were prepared on Si (111) wafer with wedge of CoFeB<sub>(0-18 nm)</sub> with thickness gradient of 0.3 nm/mm. Magnetic layer was interfaced with different heavy metals i.e., Ru<sub>(4d)</sub> and Ta<sub>(5d)</sub>, with the base layer of 10 nm and the capping layer of 3 nm, using ion beam sputtering in ultra-high vacuum to study role of thickness on magnetic properties, particularly in plane magnetic anisotropy, coercivity, magnetic Kerr intensity.

Magnetic hysteresis loops were measured using longitudinal magnetic optical Kerr effect (MOKE), with He-Ne laser having a spot size of 1.5 mm. A pair of Helmholtz coils was used to apply magnetic field in the film plane in the range of  $\pm 75$  Oe. MOKE measurements were carried out as a function of CoFeB film thickness by moving the sample vertically with respect to the laser spot using a linear stage with an accuracy of 0.1 mm. For magnetic anisotropy studies loops were taken as a function of azimuthal angle for different CoFeB thickness, and corresponding azimuthal angle dependence of remanent magnetization were obtained.

X-ray reflectivity (XRR) was done to elucidate structural properties like interface and surface roughness, electron density and thickness.

### 3. RESULT

The quality of samples along with thickness variation was confirmed using X-ray reflectivity, as shown in Figure 1. The variation of MOKE shows increasing Kerr signal with increasing thickness of magnetic film. Figure 2 represents the MOKE hysteresis loops as a function of azimuthal angle and corresponding azimuthal angle dependence of remanent magnetization at low and high CoFeB thickness

indicating the presence of weak four-fold magnetic anisotropy, which enhance with increasing thickness. In previous studies it is reported that CoFeB exhibit a strong in-plane uniaxial magnetic anisotropy due to long range quenched-in stress [4], which modifies in presence of 4d/5d heavy metals at interface. Detailed analysis of present work is under process.

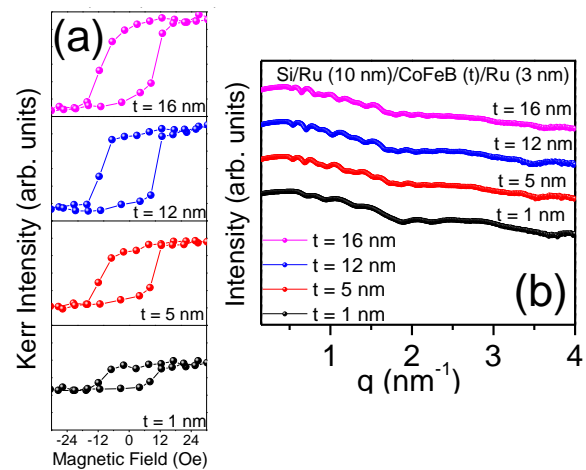


Fig.1. (a) MOKE and (b) XRR obtained at different thicknesses for Ru/CoFeB/Ru.

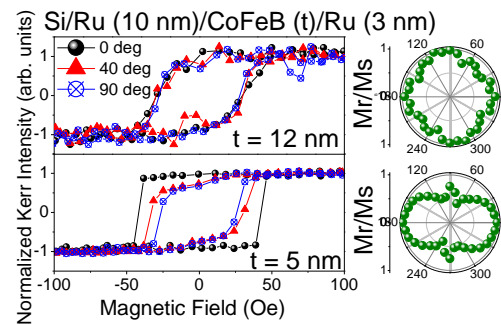


Fig.2. MOKE loops and corresponding polar plot for anisotropy obtained at different thicknesses for Ru/CoFeB/Ru

### ACKNOWLEDGEMENT

Financial support from the Board of Research in Nuclear Sciences (BRNS) (project no. 58/14/07/2019-BRNS/10381). is thankfully acknowledged

### REFERENCES

- [1]. G. Yu et al, Appl. Phys. Lett. **105** (2014) 102411.
- [2]. B. Dieny, Rev. Mod. Phys. **89** (2017) 025008
- [3]. Syamlal S. K et al, Mater. Sci. Eng. B. **272** (2021) 115367.
- [4]. J.Dwivedi, et al, Appl. Surf. Sci **5** (2021) 100113.

## Magnetic properties investigation of ferromagnetic films on ion irradiated Si

Yasmeen Jafri<sup>1,2,\*</sup>, Aastha Vasdev<sup>3</sup>, Goutam Sheet<sup>3</sup>, Kavita Sharma<sup>1,2</sup>, Gagan Sharma<sup>1,2</sup>

<sup>1</sup>Amity Center for Spintronic Materials, Amity University, Sec-125, Noida - 201313, India

<sup>2</sup>Amity Institute of Applied Sciences, Amity University, Sec-125, Noida - 201313, India

<sup>3</sup>Indian Institute of Science Education and Research, Sec- 81, Mohali - 140306, India

\* Email: yjafri@amity.edu

**Abstract:** In the present work, investigation of magnetic properties of ferromagnetic (Fe, Co) films deposited on polished and ion irradiated Si substrates have been carried out. Influence of ion beam parameters such as ion beam incidence angle and irradiation time on surface nano-structuring of Si and magnetic properties of ferromagnetic films have been studied.

### 1. INTRODUCTION

Nanostructured surfaces produced by low energy ion beam irradiation have attracted immense attention in recent times due to their wide range of technological applications [1]. In particular, uniaxial magnetic anisotropy (UMA) generated by nanoscale patterning of the surfaces has been the topic of immense interest in spintronics [2]. Different ion beam parameters such as incidence angle, ion fluence, ion energy, ion species etc., significantly influence the formation of nanopatterns on the surface. Such surfaces also act as template to grow and modify the functional properties of thin films in controlled manner.

In the present work, optimization of ion beam parameters for surface nano-structuring and influence of the same on the magnetic properties of ferromagnetic (FM) films have been studied.

### 2. EXPERIMENTAL

Ion irradiation of Si substrates were done using ion beam sputtering technique with Ar ions of energy 600 eV, for varying incidence angle ( $\theta$ ) and irradiation time. Further, thin films of Fe and Co were deposited on irradiated Si along with polished Si substrates. X-ray reflectivity (XRR), atomic force microscopy (AFM) and magneto optical Kerr effect (MOKE) measurements were carried out for investigating the Si surfaces and magnetic properties of the deposited FM films respectively.

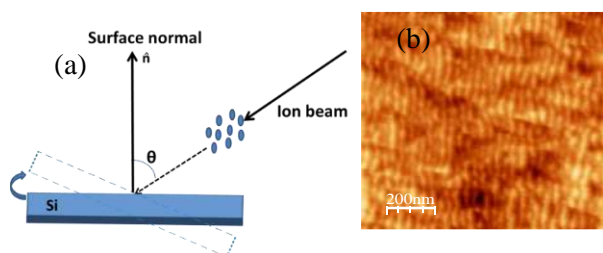


Fig.1. (a) Geometric representation of ion-irradiation on Si substrate (b) Si substrate with ripple patterns.

### 3. RESULTS AND DISCUSSION

X-ray reflectivity measurements on different Si substrates (polished and irradiated) showed variation in surface roughness with varying ion beam

parameters. Irradiated Si possessed higher surface roughness as compared to polished Si which further enhances with increasing incidence angle and irradiation time. AFM suggest the formation of wave like periodic ripple patterns only for the surfaces irradiated at  $\theta = 65^\circ$ . The wavelength of these ripple patterns as calculated from the line profiles of the surface observed to increase as function of irradiation time [3]. MOKE measurements suggests that Fe films on rippled Si surfaces possess uniaxial magnetic anisotropy whereas no such anisotropy has been observed for Fe films on other Si substrates. Moreover, in case of Co films, higher magnetic anisotropy was observed for film deposited on rippled Si, as compared to other Si surfaces. Increase in magnetic coercivity of both Fe and Co films on irradiated Si were observed as function of ion beam incidence angle. Higher magnetic coercivity in Fe than Co was observed while deposited on polished Si.

### 4. CONCLUSIONS

Magnetic properties investigation of Fe and Co films on polished and ion irradiated Si were carried out. Periodic ripple patterns were observed for Si irradiated at  $\theta = 65^\circ$ . These periodic patterns were significantly enhancing the magnetic anisotropy in FM films. Magnetic coercivity of Fe and Co were also observed to influence by the variation in ion beam parameters. Fe films on polished Si possessed higher coercivity than Co. The present study is helpful in optimization of ion beam parameters for achieving desired magnetic properties in ferromagnetic films.

### ACKNOWLEDGEMENT

Thanks are due to UGC-DAE CSR, Indore for experimental and financial support through project (CSR-IC/TIMR-04/CRS-271).

### REFERENCES

- [1]. J. M.-Garcia et al., Materials Science and Engineering: R: Reports **86** (2014) 1- 44.
- [2]. S.A. Mollick et al., Nanotechnology **29** (2018) 125302.
- [3]. A. Keller et al., Materials **3** (2010) 4811-4841.

**Esita Pandey, Brindaban Ojha, Subhankar Bedanta**

*Laboratory for Nanomagnetism and Magnetic Materials, School of Physical Sciences, National Institute of Science Education and Research (NISER), HBNI, Jatni-752050, India*

\*Email: sbedanta@niser.ac.in

**Abstract:** Spin dependent hybridization at the ferromagnet/organic semiconductor interface is very promising for fabricating highly efficient spintronic device. However, the ability of such spin polarized interface on tailoring domain wall dynamics and interfacial DM interaction is not understood well. In this context, we have studied the effect of inserting a low spin orbit coupling organic molecule (C<sub>60</sub>) on the magnetic properties of PMA Pd/Co/Pd sample. The coercivity of the samples reduced systematically by increasing the thickness of the molecular layer. But a significant reduction of bubble domain size is found for a 0.5 nm thin layer of C<sub>60</sub>. Magnetization relaxation mechanism became much faster in the Pd/Co/C<sub>60</sub>/Pd samples due to the enhanced domain wall velocity measured by applying pulsed magnetic field. It reflects that the formation of a spin polarized interface (at Co/C<sub>60</sub> interface), has reduced the magnetic anisotropy of the sample and enhanced the DW velocity in the creep region. The interfacial DM constant deduced by asymmetric DW expansion method shows an increase in DMI constant possibly due to the curvature enhanced spin orbit coupling in C<sub>60</sub>.

## 1. INTRODUCTION

Interfacial Dzyaloshinskii-Moriya interaction (iDMI) plays a crucial role for stabilizing chiral domain walls (DW) [1]. The strength of iDMI can be tuned by inserting different heavy metals (HM) in a symmetric PMA system [2]. As, organic molecules have recently shows an excellent tunability of PMA, hence in our work we have used an organic semiconductor (OSC) fullerene (C<sub>60</sub>) to break the symmetry of an originally symmetric Pd/Co/Pd system [3]. As C<sub>60</sub> exhibits a curvature enhanced spin orbit coupling [4], hence, the effect of introducing such OSC may significantly tailor effective iDMI constant and DW dynamics of the Pd/Co sample, which will be very promising from application viewpoint. A series of samples have been prepared by varying the thickness of C<sub>60</sub> and their magnetic properties have been studied in detail.

## 2. EXPERIMENTAL DETAILS

We have prepared Pd/Co/C<sub>60</sub>(t)/Pd samples, where only the thickness of C<sub>60</sub> is varied in the series. Hysteresis loops and domain images have been recorded for all the samples using Kerr microscopy, whereas magnetic anisotropy is calculated using SQUID magnetometry. Magnetization relaxation measurements have been performed at sub-coercive field values by Kerr microscopy. DW velocity is measured at the creep region of the sample by symmetric domain expansion method whereas iDMI constants are evaluated by asymmetric domain expansion method.

## 3. RESULTS AND DISCUSSIONS

A decrease in coercivity ( $\mu_0 H_c$ ) of the samples have been observed with increasing thickness of C<sub>60</sub>. After a certain thickness of C<sub>60</sub> (~1.6nm) there are no further significant changes in  $\mu_0 H_c$  has been observed, which gives an insight about the spinterface thickness of the sample. Bubble domain size is reduced significantly in the sample with 0.5 nm thickness of C<sub>60</sub> from its

reference sample. Such reduction might be attributed as a result of change in PMA and iDMI of the sample. Relaxation measurements revealed a faster relaxation phenomena while insertion of C<sub>60</sub> which indicates an effect of increased DW velocity. Thus, DW velocity is measured for all the samples and found that the velocity has increased by one order of magnitude in the sample with higher thickness of C<sub>60</sub> than the reference sample, as shown in fig. 1. The experimental data are fitted by creep law written in following:

$$v = v_0 e^{\left[ -\frac{T_d}{T} \left( \frac{H}{H_d} \right)^{-\frac{1}{4}} \right]} \quad (1)$$

where,  $v_0$  is a constant,  $T_d$  is the depinning temperature and  $H_d$  is the depinning field.

Such enhancement is further supported by a decrease in PMA and increase in iDMI strength in the samples with C<sub>60</sub>. Thus, insertion of fullerene in Pd/Co/Pd helps to tune basic magnetic properties significantly due to interfacial hybridization at the Co/C<sub>60</sub> interface.

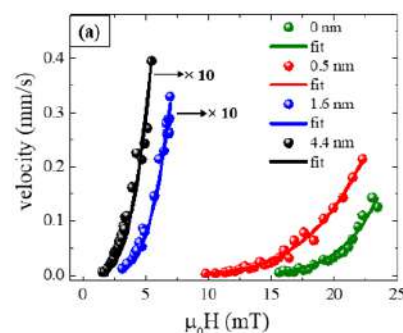


Figure 1. Velocity vs.  $\mu_0 H$  plot for the Pd/Co/C<sub>60</sub>(t)/Pd samples with varied  $t_{C_{60}}$ .

## 4. REFERENCES

1. A. Thiaville et al., EPL **100**, 57002 (2012)
2. K. Shahbazi et al., Phys. Rev. B **99**, 094409 (2019)
3. K. Bairagi et al., Phys. Rev. Lett. **114**, 247203 (2015).
4. S. Liang et al., Sci. Rep. **6**, 19461 (2016)



## Driving skyrmions with low threshold current density in Pt/CoFeB thin film

Brindaban Ojha,<sup>1</sup> Sougata Mallick,<sup>2</sup> Sujit Kumar Panigrahy,<sup>2</sup> Minaxi Sharma,<sup>1</sup> Andr e Thiaville,<sup>2</sup> Stanislas Rohart,<sup>2</sup> and Subhankar Bedanta<sup>1</sup>

<sup>1</sup>Laboratory for Nanomagnetism and Magnetic Materials (LNMM), School of Physical Sciences, National Institute of Science Education and Research (NISER), An OCC of Homi Bhabha National Institute (HBNI), Jatni 752050, Odisha, India

<sup>2</sup>Laboratoire de Physique des Solides, Universit e Paris-Saclay, CNRS UMR 8502, F-91405 Orsay Cedex, France  
Email: sbedanta@niser.ac.in

**Abstract:** We have studied Pt/CoFeB/MgO heterostructures in which skyrmions have been stabilized at room temperature (RT). It has been observed that the shape of the skyrmions are perturbed even by the small stray field arising from low moment magnetic tips while performing the magnetic force microscopy (MFM), indicating presence of low pinning landscape in the samples. This hypothesis is indeed confirmed by the low threshold current density to drive the skyrmions in our sample, at velocities of few 10 m/s.

### 1. INTRODUCTION

Skyrmions are nano-scale sized, topologically protected spin configurations [1]. Further, the solitonic nature of the skyrmions allows them to behave like particles under the influence of electrical excitations. These properties make them promising candidates for logic and storage technology [2, 3]. Competition between Heisenberg exchange interaction, Dzyaloshinskii-Moriya interaction (DMI) and perpendicular magnetic anisotropic energy can lead to stabilization of non-collinear spin textures viz. skyrmions [2, 3]. The most widely used combination for such a system is a heterostructure of heavy metal (HM)/ferromagnet (FM)/oxide (O). In this context, we chose the combination of Pt/Co<sub>40</sub>Fe<sub>40</sub>B<sub>20</sub>/MgO to investigate the current-driven dynamics of the skyrmions under the influence of SOT. We show that the threshold current density to drive the skyrmions is significantly lower than the existing literature.

### 2. EXPERIMENTAL DETAILS

We have prepared Ta (5 nm)/Pt (6 nm)/Co<sub>40</sub>Fe<sub>40</sub>B<sub>20</sub> (*t*<sub>CoFeB</sub>)/MgO (2 nm)/Ta (3 nm) heterostructure on thermally oxidized Si/SiO<sub>2</sub> (100 nm) substrates. The samples are named as S1, S2, S3, S4 and S5 for *t*<sub>CoFeB</sub> = 1.5, 1.6, 1.7, 1.75 and 1.9 nm, respectively. Ta, Pt, and CoFeB layers were deposited using DC magnetron sputtering while e-beam evaporation technique was employed to prepare MgO. Magneto optic Kerr effect-based microscope (MOKE) and superconducting quantum interference device (SQUID) are performed for the magnetization measurements. Magnetic force microscopy (MFM) and electron beam lithography (EBL) is performed for skyrmions imaging and dynamics study, respectively.

### 3. RESULTS AND DISCUSSION

The MOKE measurements confirm that the samples S1, S2, S3 and S4 are out-of-plane (OOP) magnetized while samples S5, S6 and S7 are in-plane (IP) magnetized. We have deduced the effective anisotropy ( $K_{\text{eff}}$ ) constant using the relation  $K_{\text{eff}} = -\frac{1}{2}(H_s M_s)$  (negative sign indicates the IP anisotropy), where  $H_s$  and  $M_s$  are saturation field, and spontaneous magnetization, respectively and spin reorientation transition happens at *t*<sub>CoFeB</sub> = ~1.63 nm. As, *t*<sub>CoFeB</sub> of sample S1 and S2 are near SRT, we have performed

MFM measurements to confirm the existence of skyrmions. We should note that the shape of the skyrmions is significantly perturbed even by the stray field of the lowest moment magnetic tips. This indicates the presence of low pinning landscape in the CoFeB thin film. Sample S3 is selected for the study of current-induced dynamics due to its potentially low pinning energy landscape and better control under applied magnetic field. We have prepared a nanotracks (3 parallel tracks with width ~1.2 nm separated by ~2.8 nm from each other) with Ti/Au contact pads using EBL. The skyrmion velocity as a function of applied current density is measured by calculating the average displacement of all the skyrmions present in the track. Fig. 1(a) and (b) show the skyrmion displacements marked by different colours before and after the application of one current pulse. Beyond a threshold current density of  $\sim 0.8 \times 10^{11}$  A/m<sup>2</sup>, the skyrmions start moving in the track (see Fig. 1(c)). The threshold current density is lower than the previous report.

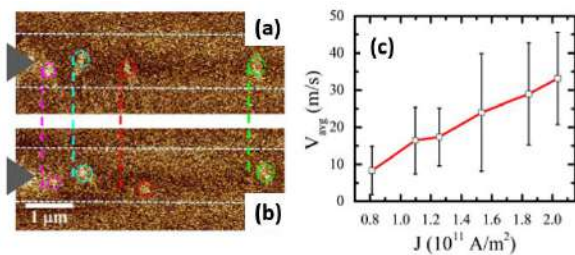


Fig.1 (a) and (b) represents the position of skyrmions before and after applied pulsed current respectively. (c) Av. velocity as a function of current density.

### 5. ACKNOWLEDGEMENTS

The authors thank DAE, Govt. of India and the IndoFrench collaborative project supported by CEFIPRA (IFC/5808-1/2017), and the French National Research Agency (ANR) (Topsky, ANR-17-CE24-0025) for providing the research funding. We would like to thank Dr. Braj Bhusan Singh for valuable discussion. We thank Raphael Weil for his help in microfabrication.

### 6. REFERENCES

- [1]. A. Fert et al., Nature Nanotech, **8**, 152–156 (2013).
- [2]. N. Nagaosa et al., Nature Nanotech, **8**, 899 (2013).
- [3]. A. Fert et al., Nature Rev. Mater., **2**, 17031 (2017).

**180° Magnetization Reversal in Fe/BaTiO<sub>3</sub>(110) Multiferroics**  
**Anupama Swain<sup>1,4</sup>, Katsuyoshi Komatsu<sup>2</sup>, Mitsuru Itoh<sup>2</sup>, Tomoyasu Taniyama<sup>2,3</sup>,**  
**and Venkataiah Gorige<sup>4</sup>**

<sup>1</sup>**School of Physical Sciences, NISER, Jatni 752050, India**

<sup>2</sup>**Laboratory for Materials and Structures, Tokyo Institute of Technology, Midori-ku, Yokohama, Japan**

<sup>3</sup>**Department of Physics, Nagoya University, Furo-cho, Chikusa-ku, Nagoya 464-8602, Japan**

<sup>4</sup>**School of Physics, University of Hyderabad, Hyderabad 500046, India**

Email: swainanupama@niser.ac.in

**Abstract:** Magnetization reversal has been demonstrated in an Fe layer grown on BaTiO<sub>3</sub>(110) single crystal substrate by utilizing the interface magnetic anisotropy induced by lattice strain and a small magnetic field bias. Cooling and heating cycles in the range of 150–325 K in an applied magnetic field of -35 Oe along [-111]pc enable to achieve the deterministic 180° magnetization reversal, where distinct magnetic anisotropies of Fe associated with different structural phases of BaTiO<sub>3</sub> will be the driving force. Electric field dependence of the magnetic coercivity shows hysteric behavior, which is attributed to the combined interfacial effect of magnetization rotation in Fe and ferroelectric polarization switching in BaTiO<sub>3</sub>.

### 1. INTRODUCTION

In crystalline materials, magnetic moments, and electric dipoles are mutually exclusive due to symmetry constraints. Interestingly, the recent discovery of magneto electric (ME) multiferroics gives a ray of hope that leads to the coexistence of magnetic moments and electric dipoles in a single material with weak ME coupling at room temperature (RT) [1]. Alternatively, heterostructures of ferromagnetic (FM) and ferroelectric (FE) components are likely to be promising for device applications in the near future owing to their strong ME coupling at RT, flexibility in materials choice and design. Most importantly, FM/FEs provide a great opportunity for manipulating the magnetic properties by an electric field, which is an alternative approach beyond the traditional electric/spin current control of magnetism [2].

### 2. EXPERIMENTAL

Polycrystalline Fe films of 30 nm thickness with a 5-nm-thick Au cap were grown on a 500- $\mu$ m-thick BTO(110) single crystal substrate at RT by using a molecular beam epitaxy. Ex-situ X-ray diffraction (XRD) measurements were carried out at RT in the  $\theta$ - $2\theta$  scanning geometry. A vibrating sample magnetometer was used to measure the in-plane magnetization as a function of magnetic field orientation and temperature. Electric field (E) dependence of in-plane M-H loops using magneto-optical Kerr magnetometry. The ferroelectric hysteresis loops also were measured by using piezoresponse force microscopy.

### 3. RESULTS AND DISCUSSION

The XRD pattern of Fe/BTO measured at RT shows no prominent peaks corresponding to reflections from Fe, indicating that Fe films grown on BTO are polycrystalline with tiny crystallites since the growth of Fe films was carried out at RT. The in-plane M-H loops were measured with a view to understand the magnetic anisotropies of Fe/ BTO associated with the different ferroelectric phases of BTO at 293, 230, and 175 K that corresponds to the tetragonal (T), orthorhombic (O)

and rhombohedral (R) phases of BTO, respectively. The polar plot of  $M_R/M_S$  in T phase shows isotropic behaviour, while in O and R phases it exhibits uniaxial magnetic anisotropy with the easy axis orientation along [-111]pc of BTO. The results indicate that the remnant magnetization in O and R phases should be almost aligned in the direction of easy axis irrespective of applied field direction and the alignment is much more prominent in R phase [3].

The in plane MT measurements at an applied field of -35 Oe depict that the strain-induced magnetic anisotropy associated with the different ferroelectric phases of BTO along with a small negative applied magnetic field makes it possible to achieve 180° magnetization reversal in Fe/BTO heterostructures. The in-plane M-H loops of Fe/BTO at different E shows that the applied  $E \geq \pm 5$  kV cm<sup>-1</sup> is large enough to bring the ferroelectric domains in the field directions, thereby causing a change in  $H_C$ . This indicates that the magnetization process is strongly coupled to the ferroelectric domain structures.

In summary, we have demonstrated strain mediated 180° magnetization reversal in Fe/BTO heterostructure via thermal and electric means. The magnetization reversal becomes possible with a unique set of magnetic anisotropies associated with the different ferroelectric phases of BaTiO<sub>3</sub> via interface elastic strain and small applied bias field.

### ACKNOWLEDGEMENTS

The present work has been supported by collaborative research project (CRP-2015 & 2016) of Laboratory for Materials and Structures, Tokyo Institute of Technology. One of the authors (V. G.) would like to thank DST, UGC and CSIR of India for financial support.

### REFERENCES

- [1] H. Schmid, *Ferroelectrics* **162** (1994) 317.
- [2] M. Opel et al, *Phys. Status Solidi A* **208** (2011) 232.
- [3] V. Gorige et al, *Phys. Status Solidi RRL* **11** (2017) 1700294

# Spin to charge conversion in IrO<sub>x</sub>/Ni<sub>80</sub>Fe<sub>20</sub> bilayers

Mohammed Azharudheen\*, Pushendra Gupta, Abhisek Mishra, Subhankar Bedanta

Laboratory for Nanomagnetism and Magnetic Materials (LNMM), School of Physical Sciences,  
National Institute of Science Education and Research (NISER), HBNI, Jatni-752050, India

Email: [mohdazharudheen.n@niser.ac.in](mailto:mohdazharudheen.n@niser.ac.in)

**Abstract:** Spin to charge conversion efficiency is one of the exciting topic in spintronics where Ferromagnet (FM)/Non magnet (NM) bilayers were largely explored. Recently, heavy metal oxides like IrO<sub>2</sub> are emerged as potential candidate which can be serve as NM due to their high spin orbit coupling (SOC) and intriguing topological properties. Here we report the spin to charge conversion in IrO<sub>x</sub>/Ni<sub>80</sub>Fe<sub>20</sub> bilayer.

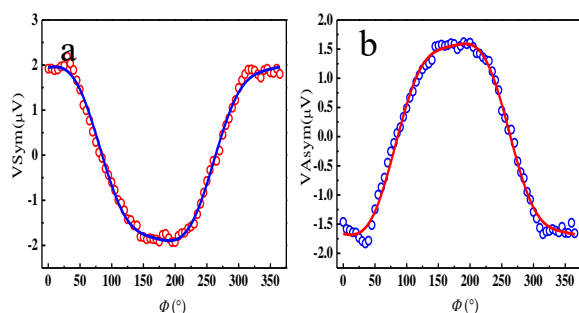
## 1. INTRODUCTION

Spin degree of freedom of electron made new path way for future power efficient storage devices. Inverse spin Hall Effect (ISHE) is a well-established technique to detect spin current since it is difficult to detect pure spin current electrically [1]. The generation and detection of spin current can be done in ferromagnet(FM)/non-magnet(NM) bilayers. The NMs (Pt,Ta,W,Pd etc.) exhibit high spin orbit coupling (SOC), however, these materials are either costly or less abundant. So one has to explore other materials which have high SOC. In this context heavy metal oxides emerge as potential candidates which exhibit high SOC when compared to their parent heavy metal [2]. Here we have chosen IrO<sub>2</sub> as NM which has a SOC strength of  $3.1 \hbar^2$  and Ni<sub>80</sub>Fe<sub>20</sub> as FM which is a soft magnetic as well as a low damping material [3]. The Enhancement of SOC in IrO<sub>2</sub> is due to the 5d conduction [5]. In addition, IrO<sub>2</sub> is a less resistive metal oxide when it is grown in single crystalline phase [6, 7]. Here we study the spin to charge conversion in IrO<sub>x</sub> by spin pumping and ISHE.

## 2. EXPERIMENTAL DETAILS

All the samples were prepared by DC magnetron sputtering with a base pressure better than  $\sim 9.8 \times 10^{-8}$  mbar on top Si(100) substrate. IrO<sub>2</sub> has been prepared by reactive sputtering with Ar:O<sub>2</sub> =3:1 at 70°C.

**Figure 1.** Fitting of symmetric and antisymmetric voltage signal of IrO<sub>x</sub> (3 nm)/ Ni<sub>80</sub>Fe<sub>20</sub> (20 nm)



All the samples in the have been prepare with an argon flow of 15sccm. In order to reduce growth induced anisotropy substrate table was rotated at 25 RPM. Thin layer of Cu having thickness of 3 nm is used to protect the sample from the oxidation. The structural

characterization were done by XRD. Interface quality and the line scan were done with cross sectional TEM. The magnetization dynamics and ISHE studies were carried out with home modified FMR set up with a frequency range of (4-17) GHz [3]. Magnetic hysteresis was done by SQUID.

## 3. RESULTS AND DISCUSSION

The presence of IrO<sub>x</sub> was confirmed from XRD peaks at 32° and 55° corresponding to (101) and (211) respectively [4]. From TEM image it is clear that both Ni<sub>80</sub>Fe<sub>20</sub> and IrO<sub>x</sub> are polycrystalline in nature. The line scan confirms the presence of all the elements. Gilbert damping ( $\alpha$ ) of the samples are evaluated by FMR and its value found to be 0.00825 for reference sample (R1). It can be noticed that there is a significant enhancement in the value of value of  $\alpha$  when compared to R1. This enhancement may be due to spin pumping. In order to confirm the spin pumping we have performed ISHE. Further angle dependent ISHE measurements have been carried out to disentangle spin pumping voltage from other spurious effect like anomalous Hall Effect (AHE) and anisotropic magneto resistance (AMR).

Figure 1 shows the best fit of the  $V_{sym}$  and  $V_{asym}$  Vs angle for R1 and S1. The values of  $V_{sp}$  and  $V_{AHE}$  are listed in Table 1. Further spin mixing conductance found to be in the order of  $10^{19} \text{ m}^{-2}$  which is comparable with traditional heavy metals like Pt, Pd, Ta etc.

**Table 1.** Fitted parameters of angle dependent ISHE

sample		$V_{sp}$ ( $\mu\text{V}$ )	$V_{AHE}$ ( $\mu\text{V}$ )
R1	IrO <sub>3</sub> (3)/Ni <sub>80</sub> Fe <sub>20</sub> (20)	4.59	1.04
S2	Ni <sub>80</sub> Fe <sub>20</sub> (12)/IrO <sub>3</sub> (3)/Cu(3)	0	0

## ACKNOWLEDGEMENT

The authors acknowledge DAE, Govt. of India, for the financial support for the experimental facilities.

## REFERENCES

- [1] E. Saitoh et al. (2006), *Appl. Phys. Lett.* **88**, 182509.
- [2] A. Bose et al. (2020), *ACS Appl. Mater. Interfaces.* **12**, 5541-55416.
- [3] K. Fujiiwara et al. (2013), *Nat. Commun.* **4**, 2893.
- [4] M.A. El khakani et al. (1996), *Appl. Phys. Lett.* **69**, 2027-2029.

## Spinterface modulated magnetic properties of CoFeB/Alq<sub>3</sub> system

Swayang Priya Mahanta, Sagarika Nayak, Mohammed Azharudeen N, Subhankar Bedanta  
*Laboratory for Nanomagnetism and Magnetic Materials (LNMM), School of Physical Sciences, National Institute of Science Education and Research (NISER), HBNI, P.O. Bhipur-Padanpur, Via –Jatni, Odisha-752050, India*

\*Email: sbedanta@niser.ac.in

**Abstract:** The interface between the organic semiconductor (OSC)/ferromagnetic (FM) has attracted much attention recently. Charge/spin transfer may occur from the FM to OSC layer leading to the formation of ‘spinterface’ and can modulate basic magnetic properties e.g., coercivity, domain structure, damping and magnetic anisotropy of the system. Alq<sub>3</sub> is a promising organic molecule for spin transport over a long time. In this regard, we have prepared Co<sub>20</sub>Fe<sub>60</sub>B<sub>20</sub> (CFB)/Alq<sub>3</sub> bilayer system due to low damping of CFB ( $\sim 10^{-3}$ ). We have studied the magnetization reversal dynamics and damping properties of CFB/Alq<sub>3</sub> bilayer systems and observed a significant modifications in comparison to the reference CFB layer. The observed modifications can be attributed to the effect of ‘spinterface’ formed at the CFB and Alq<sub>3</sub> interface.

### 1. INTRODUCTION

Spintronics is one of the emerging field for next generation devices to reduce their power consumption, to increase their memory and processing capabilities [1]. Spintronics has been widely explored in inorganic materials. Very recently, the use of organic molecules in spintronics devices has attracted much attention for future applications like magnetic sensors and memory devices [2]. Organic molecules are basically  $\pi$ -conjugated molecules which are composed of low atomic number elements like carbon (C), Hydrogen (H), Oxygen (O) and Nitrogen (N) etc. They are well-known for their low spin orbit coupling and less hyperfine interactions which makes them best candidates to transport spins over a long distance and long time. There are a number of promising OSCs like C<sub>60</sub>, Alq<sub>3</sub>, Rubrene *etc.* Organic semiconductors could be utilised in novel spintronics devices in the future. As a result, further experimental and theoretical study is required to fully understand the mechanism of spin injection and spin transport.

### 2. EXPERIMENTAL DETAILS

In this study, we have prepared three samples CFB (S1), CFB/Alq<sub>3</sub> (S2), Alq<sub>3</sub>/CFB (S3) on Si (100) substrate. All the samples were capped with 3 nm of Cu layer. CFB and Cu layers were deposited using DC magnetron sputtering and Alq<sub>3</sub> layers were deposited using thermal evaporation technique in a multi deposition high vacuum chamber manufactured by EXCEL instruments, India.

Damping measurements were done using lock-in based FMR. The hysteresis loops and the domain images have been measured at room temperature using magneto-optic Kerr effect (MOKE) based microscopy. The hysteresis measurements have been performed within a field range of 5 mT by varying the angle  $\phi$  in longitudinal modes. Here  $\phi$  denotes the angle between the easy axis and applied field direction.

#### 2.2. Results

We observed magnetic damping of 0.006 for CFB sample. Magnetic damping value increased

significantly in S2 and S3 and the values are 0.01 and 0.009 respectively. A careful investigation of the hysteresis loops indicates the presence of uniaxial anisotropy in all the samples. Branch domains have been observed in the CFB reference sample. Big domains are observed along the easy axis for all the samples and domain size reduced while moving away from easy axis. Domain size and domain type changed when Alq<sub>3</sub> layers were deposited above or below the CFB layers. The domain size got reduced significantly in S2 and S3 as compared to S1 which is because of the nature of the FM/OSC interface in S2 and S3. We have also observed an increment in coercivity as the effect of spinterface in the sample S2 and S3.

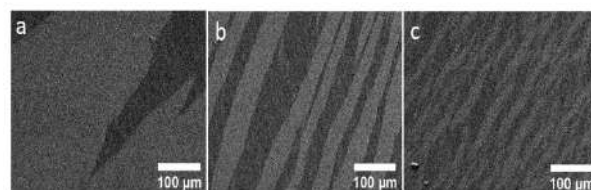


Fig.1. Domain images of the samples S1, S2 and S3 near coercivity are shown in a, b and c, respectively, at an angle of 45° away from easy axis.

### ACKNOWLEDGEMENT

Authors would like to thank the Department of Atomic Energy (DAE) of Govt. of India for providing the funding to carry out the research.

### REFERENCES

- [1]. Atsufumi Hirohata, Keisuke Yamada, Yoshinobu Nakatani, Ioan-Lucian Pre-jbeanu, Bernard Diény, Philipp Pirro, and Burkard Hillebrands. *Journal of Magnetism and Magnetic Materials*, 509:166711, 2020
- [2]. Xiong, Z. H., Wu, D., Vardeny, Z. V. & Shi, J. *Nature* 427, 821–824 (2004).

## Spin Valve effect in FL-MoS<sub>2</sub> and ferromagnetic shape memory alloy based magnetic tunnel junction

Pradeep kumar<sup>1</sup>, and Davinder Kaur<sup>1\*</sup>

<sup>1</sup>*Functional Nanomaterials Research Laboratory, Department of Physics and Centre for nanotechnology, Indian Institute of Technology Roorkee, Roorkee- 247667, Uttarakhand, India*

\*Corresponding author: [davinder.kaur@ph.iitr.ac.in](mailto:davinder.kaur@ph.iitr.ac.in)

Email: pkumar3@ph.iitr.ac.in

### Abstract:

In the last decade, two-dimensional (2D) transition metal dichalcogenides have been introduced with great significance in the spintronic devices for their extraordinary electrical, optical, and spin-dependent properties. In this work, we have fabricated a few-layer molybdenum disulfide (FL-MoS<sub>2</sub>) (~6 nm) as a non-magnetic spacer layer in Ni-Mn-In/FL-MoS<sub>2</sub>/Ni-Mn-In magnetic tunnel junction (MTJ) using DC magnetron sputtering. The magnetic and transport characteristics of the fabricated MTJ have been recorded using physical property measurement system (PPMS, DYNACOOOL). FL-MoS<sub>2</sub> thin film sandwiched between two ferromagnetic (FM) electrodes exhibit semiconducting behavior, confirmed by current-voltage (I-V) characteristics and temperature dependent resistance measurement. The fabricated MTJ shows spin valve effect in the presence of an external magnetic field. The tunneling magnetoresistance (TMR) has been recorded in 10 K to 300 K temperature range. The highest TMR ratio of 0.51% was obtained at a low temperature ~10 K, corresponding to the spin polarization of ~5%. This TMR ratio reduces to its minimum value of 0.032% as the temperature of the device increases up to 300 K. Also, a detailed study of thickness and temperature-dependent magnetization vs magnetic field (M-H) hysteresis loops of Ni-Mn-In thin films has been performed to understand the complex TMR behavior. The present study paves the way for the use of sputtered 2D-transition metal dichalcogenides MoS<sub>2</sub> thin film in ultrafast spintronic devices for the semiconductor industry.

**Keywords:** Thin films, spintronics, sputtering, tunnel magnetoresistance, 2D TMDs



## Effect of Cr doping on the Structural, Surface Morphology, Magnetic and Antimicrobial Properties of Cobalt ferrite

Sachin Kumar Godara<sup>1</sup>, Sukhmanbir kaur<sup>2</sup>

<sup>1,2</sup>Department of Chemistry, UGC Center for Advanced Studies-II, Guru Nanak Dev University, Amritsar, Punjab, India-143005

Email: sukhmanaulakh11@gmail.com

**Abstract:** In the present study, Cr-substituted Cobalt ferrites with composition  $\text{Cr}_x\text{Co}_{(1-x)}\text{Fe}_2\text{O}_4$  ( $x = 0.0, 0.025, 0.05, 0.1, 0.15, 0.2$ ) was synthesized using sol-gel technique. X-ray diffraction spectra reveals that all the synthesized samples were phase pure except  $x=0.2$ . Magnetic studies reveal that the maximum value of saturation magnetization ( $M_s$ ) is 78.90 emu/g for pure cobalt ferrite sample. The coercivity ( $H_c$ ) varies between 619-887 Oe. The prepared nanoparticles shows antimicrobial activity against gram-negative (*Escherichia coli*) and gram-positive bacteria (*Staphylococcus aureus*).

### 1. INTRODUCTION

The use of metal and metal-oxide nanoparticles for antimicrobial performance is gaining popularity, as several of these exhibit superior activity against resistant microorganisms. Ferrites are ferromagnetic compounds that are traditionally transition metal oxides [1]. Ferrites are normally found in powder or ceramic form and are classified into four types: hexagonal ( $\text{MFe}_{12}\text{O}_{19}$ ), garnet ( $\text{M}_3\text{Fe}_5\text{O}_{12}$ ), orthogonal ( $\text{MFeO}_3$ ) and spinel ( $\text{AB}_2\text{O}_4$ ). Spinel ferrite nanoparticles are known for their novel optical, photoelectric, and magnetic properties. Ferrites are commonly classified as soft or hard in phases with magnetic properties, resulting in decreased or increased magnetic coercivity. The spinel composition is found in the majority of ferrites used in the production of magnetic liquids. Furthermore, ferrites are used in a wide range of technological applications, including electrical designs, humidity sensors, microwave reflection, drug delivery techniques, magnetic resonance imaging, and inductors.

### 2. EXPERIMENTS AND RESULTS

#### 2.1. Experiment

The prepared nanoparticles were tested for antimicrobial susceptibility against gram-negative and gram-positive bacteria. A modified agar well diffusion method was used to test antimicrobial activity [2]. Antimicrobial activity was tested against pathogenic bacteria using 100  $\mu\text{l}$  nanoparticles solution (100mg/ml) and 10  $\mu\text{l}$  antibiotic solutions (100mg/ml). Furthermore, ampicilin was used as a positive control whereas, triple distilled water serving as a negative control. The Petri plates were incubated at 37°C for 16-18 hours for the growth of bacteria. All of the tests were carried out in triplicates. Using the HiMedia antibiotic zone scale, the diameters of the inhibition zones obtained around the wells were measured in millimetres (mm)[3].

#### 2.2. Effect of Cr doping on the antimicrobial properties of cobalt ferrite

The synthesized doped nanoparticles showed antimicrobial activity against both the gram positive and gram negative bacteria. The inhibition zones (in mm) of varying sizes were obtained as mentioned in Figure 1. The inhibition zones were measured by taking the amount of 100 $\mu\text{l}$  of nanoparticles solution and ampicilin in a different well. The positive control showed the zone of inhibition against both gram-positive and gram-negative bacteria. In gram-negative *i.e.*, *E. coli*,  **$\text{Co}_{0.8}\text{Cr}_{0.2}$**  showed maximum zone of inhibition ( $17 \pm 0.592$ ) and  **$\text{Co}_{0.95}\text{Cr}_{0.05}$**  showed minimum zone of inhibition ( $14.5 \pm 0.568$ ) whereas,  **$\text{Co}_{0.975}\text{Cr}_{0.025}$** ,  **$\text{Co}_{0.9}\text{Cr}_{0.1}$**  and  **$\text{Co}_{0.85}\text{Cr}_{0.15}$**  showed no zone of inhibition.

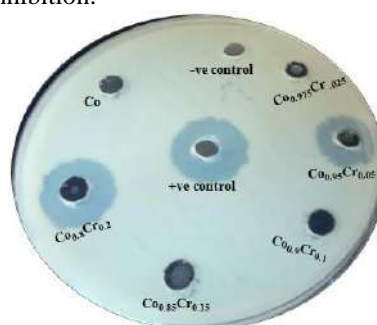


Fig.1: antimicrobial activity shown by Cr-substituted Cobalt ferrites [ $\text{Cr}_x\text{Co}_{(1-x)}\text{Fe}_2\text{O}_4$  ( $x = 0.0, 0.025, 0.05, 0.1, 0.15, 0.2$ )]

### 3. REFERENCES

1. Mmlesi et al., Mater Sci Semicond Process. 123, (2020) 105523.
2. Swati et al., J Environ Chem Eng. 8 (2020) 103730.
3. Morones et al., Nanotechnol. 16 (2005) 2346.

## Role of chemical pressure in spin-disordered $\text{Ho}_2\text{Ge}_x\text{Ti}_{2-x}\text{O}_7$ system

Manjari Shukla and Chandan Upadhyay

School of Materials Science and Technology, Indian Institute of Technology (Banaras Hindu University),  
Varanasi, 221005

Email: manjaris.rs.mst15@iitbhu.ac.in

**Abstract:** Frustrated systems help to discover new states and new properties of matter.  $\text{Ho}_2\text{Ge}_x\text{Ti}_{2-x}\text{O}_7$  series had been synthesized through standard solid-state route.  $\text{Ho}_2\text{Ti}_2\text{O}_7$  crystallizes in cubic  $\text{Fd}\bar{3}\text{m}$  space group, and  $\text{Ho}_2\text{Ge}_2\text{O}_7$  belongs to tetragonal  $\text{P4}_12_12$  space group. The crystal lattice is bipartite consisting of two interpenetrating sublattices.  $\text{Ho}_2\text{Ti}_2\text{O}_7$  and  $\text{Ho}_2\text{Ge}_2\text{O}_7$  magnetically frustrated systems are important due to their exotic spin relaxation phenomenon originating from their ground state degeneracy. The role of quantum fluctuations, along with the correlations within the ground states and low-temperature spin dynamics, had been discussed in details. The effects of chemical pressure upon the band gap tenability, from insulator ( $\text{Ho}_2\text{Ge}_2\text{O}_7$ ) to high band semiconductor ( $\text{Ho}_2\text{Ti}_2\text{O}_7$ ) has been elaborated.

### 1. INTRODUCTION

After the realization of implications of Anderson's resonating-valence-bond (RVB) theory to high-temperature superconductors, frustrated magnetism developed wide-spread recognition. Experimentally, the absence of phase transition at Curie-Weiss temperature signals the possibility of unconventional low-temperature physics.

The Hamiltonian accounting the interaction between magnetic ions is based upon dipolar spin ice model (DSIM) and can be given as:

$$H = -J_{nn} \sum_{\langle ij \rangle} \vec{S}_i \cdot \vec{S}_j + D_{nn} r_{nn}^3 \sum_{\langle ij \rangle} \left[ \frac{\vec{S}_i \cdot \vec{S}_j}{|r_{ij}|^3} - \frac{3(\vec{S}_i \cdot \vec{r}_{ij})(\vec{S}_j \cdot \vec{r}_{ij})}{|r_{ij}|^5} \right], \quad (1)$$

where  $J_{nn}$  and  $D_{nn}$  are the nearest neighbor exchange and dipolar coupling constants, respectively;  $i$  and  $j$  label the sites of pyrochlore lattice;  $\vec{S}_i = \sigma_i \vec{z}_i$ ;  $\sigma_i = \pm 1$  and  $\vec{z}_i$  are four inequivalent unit vectors pointing from one tetrahedral sublattice to other;  $r_{nn}$  indicates nearest neighbor distance on pyrochlore lattice,  $r_{ij}$  is the distance between sites  $i$  and  $j$ .<sup>1,2</sup>

### 2. EXPERIMENT

Synthesis parameters, namely temperature and time, were optimized in order to obtain pure phase  $\text{Ho}_2\text{Ge}_x\text{Ti}_{2-x}\text{O}_7$  through solid-state route. The duration for mechanical mixing (~ 8 Hours) [high energy ball mill], temperature for thermochemical reaction ~ 1300° C, binder removal temperature (~ 600° C), as well as the sintering (~ 1350° C) and annealing temperatures (~ 600° C), were optimized to ensure the maximum reproducibility of the samples.

### 3. RESULT AND DISCUSSIONS

Fig. 1. shows the ac-susceptibility feature of  $\text{Ho}_2\text{Ge}_x\text{Ti}_{2-x}\text{O}_7$ . For the conventional cubic pyrochlore  $\text{Ho}_2\text{Ti}_2\text{O}_7$ , the magnetic ground state is spin-ice (~ 2 K), and this freezing relaxation is robust to the application of positive chemical pressure effect, classifying it as a quantum spin-ice system.<sup>3</sup>

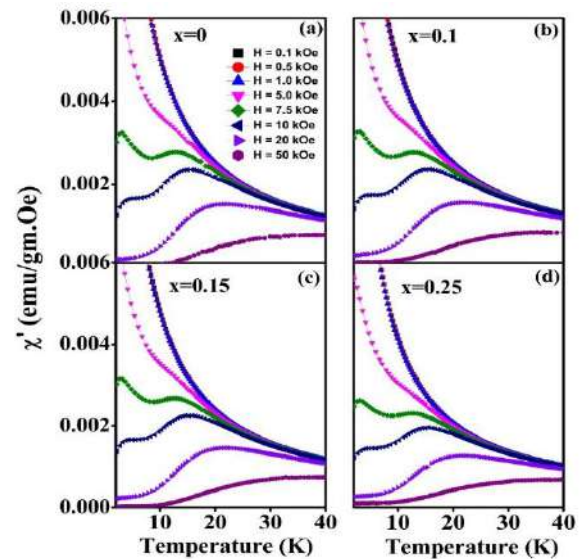


**Fig. 1.** Real part of ac susceptibility of  $\text{Ho}_2\text{Ge}_x\text{Ti}_{2-x}\text{O}_7$  for (a)  $x = 0$  (b)  $x = 0.1$  (c)  $x = 0.15$  (d)  $x = 0.25$  measured at  $H = 0.1, 0.5, 1, 5, 7.5, 10, 20$  and  $50$  kOe at an applied ac-frequency of  $500$  Hz.

### 3. CONCLUSIONS

The robust nature of the spin ice freezing ( $T \sim 2$  K) for conventional cubic pyrochlore has been established in  $\text{Ho}_2\text{Ti}_2\text{O}_7$ . Low-temperature synchrotron x-ray diffraction pattern indicates an anomaly in lattice volume below  $30$  K, the curve of lattice volume vs. temperature when fitted using Debye-Grüneisen equation established crystal field-phonon coupling in  $\text{Ho}_2\text{Ti}_2\text{O}_7$ .

### ACKNOWLEDGEMENT

We acknowledge the support from CIFIC, IIT (BHU) for HRXRD and Magnetic measurements.

### REFERENCES

- [1]. L.D.C. Jaubert et al, J. Phys. Chem. Solids **23** (2011) 1-15.
- [2]. B. Tomasello, et al, Phys. Rev. B **92**, (2015). 1-14.
- [3]. M. Shukla et al, J. Phys. Condens. Matter **32**, (2020) 1-10.

## Signatures of Rashba Effect in Angle Resolved Magnetoresistance

ANSHU GUPTA<sup>1</sup>, SUVANKAR CHAKRAVERTY

<sup>1</sup>Quantum Materials and Devices Unit, Institute of Nano Science and Technology, Sector-81, Punjab, 140306, India.

anshu.ph19221@inst.ac.in

We study the angular dependence of the longitudinal and planar magnetoresistance at the conducting interface of  $\text{LaVO}_3\text{-KTaO}_3$  having strong spin-orbit coupling strength. The system exhibits negative longitudinal magnetoresistance, planar Hall effect and anisotropic magnetoresistance which are the signature of chiral anomaly. The observance of negative magnetoresistance for all in-plane angles is unusual feature. These features are of quantum origin arises from strong spin-orbit coupling and pave a path to engineer non-magnetic materials as sensors for vector magnetic fields.



## Tilted anisotropy induced deterministic magnetization switching in perpendicularly magnetized Ta/Pt/CoFeB/Au multilayer

B. Ravi Kumar, P. S. Anil Kumar\*

Department of Physics, Indian Institute of Science, Bangalore-560012, Karnataka, India

Email: (anil@iisc.ac.in)

**Abstract:** In this communication, we report on deterministic magnetization reversal in the direction perpendicular to a thickness gradient patterned on Ta/Pt/CoFeB/Au multilayer. We attribute this observation to tilted anisotropy produced by thickness gradient in addition to spin-orbit torques.

### 1. INTRODUCTION

Switching of magnetization using current-induced spin-orbit torques (SOT) offers real opportunities for high density and lower power consumption for magnetic memory and logic devices [1]. Though a huge work has been carried out, obtaining deterministic magnetization reversal using low critical current densities ( $< 10^6$  A/cm<sup>2</sup>) remains challenging for applications requirements [2]. Reversing the magnetization without applying an in-plane magnetic field ( $H_{IP}$ ) using lower critical current densities ( $J_c$ ) in a thickness-gradient ferromagnetic layer in heavy metal/ferromagnetic metal bilayers has got huge attention among various attempts [3]. In this work, we follow the same method to achieve a deterministic magnetization reversal.

### 2. EXPERIMENTAL DETAILS

Multilayer with the details: Ta(3 nm)/Pt(3 nm)/CoFeB(0.5)/Au(2 nm) were grown on thermally oxidized Si/SiO<sub>2</sub> substrates of area 4 mm × 3.8 mm using a DC sputtering system with the base pressure of  $7 \times 10^{-7}$  mbar, and a working pressure of  $5 \times 10^{-3}$  mbar using argon gas with a purity of 99.999%. While depositing all the layers except CoFeB, the substrate has been rotated. Whereas the CoFeB layer has been deposited when the substrate was not rotated to ensure a thickness gradient in the direction of deposition. Kerr microscopy has been used to perform the current-induced magnetization reversal measurements.

### 3. RESULTS AND DISCUSSION

Figure 1 (a) illustrates a hysteresis loop when an ac current has been applied to the device when the  $H_{IP}$  was kept zero. Whether the  $H_{IP}$  is finite or zero, the magnetization reversal can occur by SOT produced by heavy metal (in the present study, Pt) while passing an electrical current through it [2,3]. Furthermore, as highlighted in the right panel of this figure where the variation of the  $J_c$  with the  $H_{IP}$  is shown, the peak/valley in the  $J_c$  occurs at finite but not at zero  $H_{IP}$ , which indicates that the critical current needed to switch the magnetization at zero  $H_{IP}$  is less than that needed at the finite  $H_{IP}$ . This is due to a finite *internal* in-plane field arising from a tilted anisotropy produced by a thickness gradient [3]. This highlights a deterministic magnetization reversal at zero  $H_{IP}$  which will be useful to switch a magnetization without an application of magnetic fields but currents in spintronics devices. Although the obtained critical current density is not the

lowest one at zero in-plane fields, there we achieved a deterministic magnetization reversal.

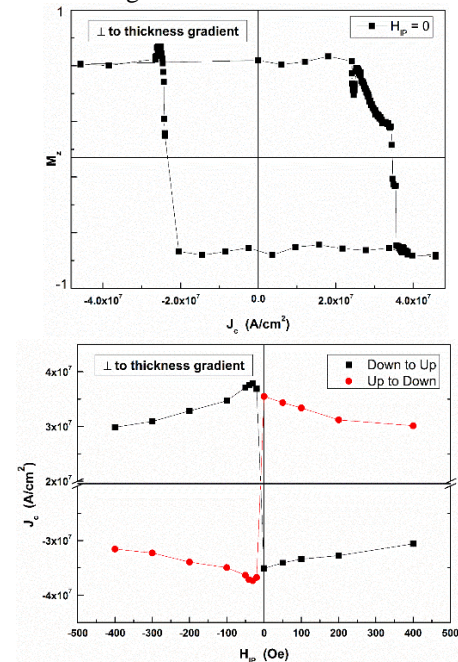


Fig. 1: (top panel) Kerr intensity as a function of  $J_c$  in the absence of  $H_{IP}$ . (bottom panel)  $J_c$  vs  $H_{IP}$ .

### 5. SUMMARY

A thickness gradient is created while depositing CoFeB in a Ta/Pt/CoFeB/Au multilayer using sputtering technique. Current-induced magnetization reversal measurement performed using Kerr-microscopy reveals that a deterministic magnetization switching can occur in the direction perpendicular to a thickness gradient. The deterministic magnetization reversal achieved may be useful in spintronics applications.

### ACKNOWLEDGEMENT

B. R. K. acknowledges Dr. D. S. Kothari post-doctoral fellowship scheme, University Grants Commission, India, with reg. no. PH/17-18/0096 for financial assistance.

### REFERENCES

- [1] I. M. Miron et al., Nature (London) **476** (2011) 189.
- [2] Rowan-Robinson et al., J. Appl. Phys. **124** (2018) 183901.
- [3] Vineeth Mohanan P et al., Phys. Rev. B **96** (2017) 104412.

## Rapid thermal annealing on FePtCu based systems for enhanced transformation kinetics and improved structural properties

Shubham Kumar<sup>\* 1,2</sup>, Atul Tiwari<sup>1,2</sup>, Kavita Sharma<sup>1,2</sup>, Gagan Sharma<sup>1,2</sup>, Mukul Gupta<sup>3</sup>, V. Raghavendra Reddy<sup>3</sup>, Ajay Gupta<sup>4</sup>

<sup>1</sup>Amity Centre for Spintronic Materials, Amity University, Noida, India-201313

<sup>2</sup>Amity Institute of Applied Sciences, Amity University, Noida, India-201313

<sup>3</sup>UGC-DAE Consortium for Scientific Research, Khandwa Road, Indore, India-452017

<sup>4</sup>Department of Physics, University of Petroleum and Energy Studies, Dehradun 248007, India

\*Email: skumar54@amity.edu

**Abstract:** L<sub>10</sub> ordered FePt thin films are highly anisotropic and considered as the potential candidate for future magnetic recording media. Achieving L<sub>10</sub> phase at viable conditions is the key task for manufacturing purposes. In our present work, we attempted to achieve L<sub>10</sub> ordering in FePt based systems with enhanced transformation kinetics and lower grain size. Rapid Thermal Annealing (RTA) has been done on Fe multilayer doped with optimum concentration of Cu. Structural and magnetic properties were studied using x-ray diffraction, and magneto optical Kerr effect measurements.

### 1. INTRODUCTION:

L<sub>10</sub> ordered FePt is a potential candidate for future magnetic recording media[1]. FCT L<sub>10</sub>FePt phase is obtained from high temperature post deposition treatments of FCCFePt. The mechanism of mixing of Fe and Pt and formation of L<sub>10</sub> involves transformation kinetics that depends on various parameters like annealing time, temperature rate of heating etc[1]. Moreover these parameters have also impact on the grain size of the final phase which is another perspective that need to be optimized for practical applications of these systems. In present work we attempted to achieve L<sub>10</sub> phase in FePt with enhance diffusion kinetics and low grain size. For this we use Rapid thermal annealing as a tool for intermixing Fe, Pt and Cu in FePt based systems with different initial configurations and investigated the effect of Rapid thermal annealing on the structure and magnetic properties of these system.

### 2. EXPERIMENTAL

Three films [Fe(19Å)/P(27Å)t]<sub>x15</sub>, FePtCu and [Fe(16Å)Cu(3)/Pt(24Å)Cu(3)]<sub>x15</sub> (referred as S1, S2 and S3 respectively) of nominal thickness 690Å deposited using DC magnetron sputtering method. X-ray diffraction has been done using Bruker D8 Discover x-ray diffractometer with Cu-K<sub>α</sub> rad (λ=0.154nm), MOKE microscopy (M/s Evico Germany).

### 3. RESULTS AND DISCUSSION

Fig.1(left) shows MOKE data taken in longitudinal geometry of three films taken after at RTA treatment at 400°C for 10 seconds and 70 seconds. One can clearly see that coercivity of films annealed for 10 sec lies below 20 Oe. But there is sudden jump in the coercivity values in S2 and S3 annealed for 70 sec and it reaches 4727 Oe and 4255 Oe respectively for multilayer and alloy film. This jump in coercivity is the marker of L<sub>10</sub> ordering. Thus, present results indicate that there is finite degree of L<sub>10</sub> ordering in S2 and S3 annealed for 70 Sec. Moreover coercivity is higher in S3 indicating larger degree of ordering in

S3. But there is no such rise found in S1 indicating no signature of ordering in S1.

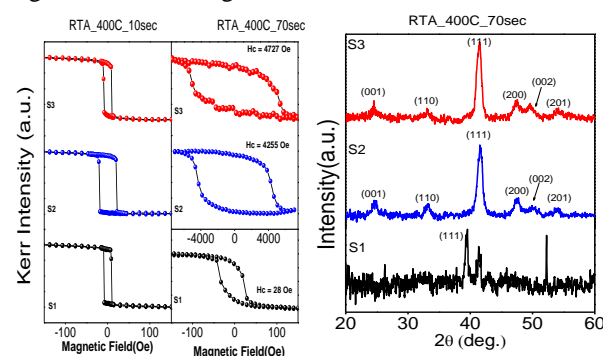


Fig.1. (left) MOKE data (right) XRD data of S1, S2 and S3 taken after indicated RTA treatment.

Fig.1(right) shows XRD data taken of three films taken after at RTA treatment at 400°C for 70 seconds. All the peaks in XRD could be indexed to L<sub>10</sub> ordered phase of FePt in S2 and S3 while in S1 there is no signature of L<sub>10</sub> ordering. These results are consistent with the MOKE data. Grain size calculated for S1, S2 and S3 from (111) peak of XRD which comes out to be 17nm, 9.0nm, 9.0nm for S1, S2 and S3 respectively. For S2 and S3 the observed grain size is very less in comparison to that of conventional heating[1].

### 4. CONCLUSIONS

These results indicate that enhancement in transformation kinetics and reduction in grain size is obtained by addition of Cu and RTA treatment. However addition of Cu in multilayer stack and RTA results in higher degree of ordering with reduced grain size.

### 5. ACKNOWLEDGEMENT

UGC-DA CSR (project No.-CSR-IC-ISUM-12/CRS - 295/2019-20/1347.)

BRNS (project no. 58/14/07/2019-BRNS/10381)

### REFERENCES

[1]. Berry, D. C. et al., (2006). Journal of applied physics, 99(8), 08G901.

## Stabilization of Magnetic Helix in Exchange-Coupled trilayer

Sadhana Singh, Dileep Kumar

UGC-DAE Consortium for Scientific Research, Indore, M. P., India 452001

Email: sadhanasingh240@gmail.com

**Abstract:** In the present work, an intuitive model is proposed to stabilize a helical structure using a combination of conventional antiferromagnetic (AFM)/ferromagnetic (FM) and unconventional Hard/Soft FM exchange bias (EB) in the form of Hard FM/Soft FM/AFM trilayer structure. An experimental attempt to achieve the same has been performed using FePt(L1<sub>0</sub>)/Co/CoO trilayer where soft FM Co layer is exchange coupled by FePt(L1<sub>0</sub>) hard FM layer at one interface and by AFM CoO layer at the other interface. It is observed that when trilayer is field cooled (FC) to 173 K in the direction opposite to the saturation of hard FM layer, a helical spin structure can be created in soft FM layer resulting in a net zero remanence in the trilayer.

### 1. INTRODUCTION

Nano size stable helices with only spin degree of freedom can play an important role in next generation purely spin based memory storage devices [1]. These devices require use of only internal interaction such as exchange, Ruderman–Kittel–Kasuya–Yosida (RKKY) and long range dipolar interaction instead of external current or magnetic field for data processing [1]. In thin films, stable helical structures can be developed using these internal interactions along with additional advantage of magnetic anisotropy. In contrast to skyrmions, helicity here does not arise from the symmetry breaking due to Dzyaloshinskii-Moriya (DM) interaction [2]. Creation and stabilization of these nano helices with stable magnetic property still remains an experimental challenge.

In the present work, formation of a stable helical structure in thin films using a combination of conventional antiferromagnetic (AFM)/FM [3] and unconventional Hard/Soft FM [4] EB system has been studied using intuitive model in form of Hard FM/Soft FM/AFM trilayer and experimentally via FePt(L1<sub>0</sub>)/Co/CoO trilayer.

### 2. INTUTIVE MODEL

It is proposed that when the Hard FM/Soft FM/AFM trilayer is FC below the Néel's temperature ( $T_N$ ) of AFM layer and opposite to saturation direction of hard magnetic layer, a helical spin structure can be achieved in the soft FM layer (as shown in fig 1a). This is attributed to the pinning of soft FM layer spins in opposite direction at the two interfaces resulting a magnetically frustrated state, which lowers its energy by forming a helical structure. The field used for FC should be less than that required field for reversal of hard layer.

### 2. EXPERIMENTAL

FePt(L1<sub>0</sub>)/Co/CoO trilayer was prepared by depositing FePt layer by DC magnetron sputtering and annealed at 823 K for 20 min in the presence of 1500 Oe in-plane magnetic field to obtain FePt(L1<sub>0</sub>) hard magnetic phase with its moments aligned in a particular direction. Co layer was then deposited in an UHV chamber using e-beam evaporation, which is thermally oxidised at 573 K in the presence of O<sub>2</sub> partial pressure to obtain CoO layer on surface. EB behaviour of the trilayer was studied using magneto-optical Kerr effect (MOKE) under following conditions (i) at RT, (ii) zero

field cooled (ZFC) to 173 K and (iii) FC to various temperatures ( from RT to 173 K) in 1500 Oe magnetic field applied in the direction opposite to saturation direction of hard FePt(L1<sub>0</sub>) layer. It is to be noted that MOKE loops were measured in the magnetic field that reverses only Co layer but remanence state of hard FePt(L1<sub>0</sub>) layer remains undisturbed.

### 2. RESULT AND DISCUSSION

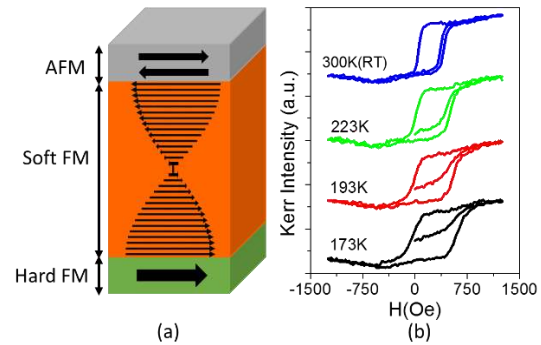


Fig.1. (a) Schematic representation of spin configuration of trilayer when FC to  $T < T_N$  in direction opposite to saturation of hard FM layer. and (b) Hysteresis loop of Co layer in FePt(L1<sub>0</sub>)/Co/CoO trilayer along  $\theta = 180^\circ$  as a function of FC temperature. Here  $\theta$  is azimuthal direction with respect to saturation of hard layer.

It is observed that when the trilayer was FC to 173 K in 1500 Oe field opposite to FePt(L1<sub>0</sub>) saturation, virgin curve starts from zero magnetization state. As the temperature increases, the virgin curve shifts downwards and reaches to saturation magnetization value of FePt(L1<sub>0</sub>) layer at RT. Zero remanence at 173 K may be due to pinning of Co layer in opposite direction at the two interfaces when trilayer was FC in direction opposite to FePt(L1<sub>0</sub>) saturation. This shows that at 173 K, 50 % of Co layer moments are coupled by FePt(L1<sub>0</sub>) layer and 50% by CoO layer. This indicates formation of helical structure in soft FM Co layer.

### REFERENCES

- [1]. L. Dzemiantsova, et al. Sci. Rep. 5 (2015) 16153.
- [2]. A. Fert, et al. Nat Rev Mater 2 (2017) 17031.
- [3]. W. H. Meiklejohn et al. Phys. Rev. 105 (1957) 904.
- [4]. A. Berger, et al. Appl. Phys. Lett. 85 (2004) 1571.

## Femtosecond laser-driven ultrafast demagnetization in ferromagnetic thin films: a comparative study using two theoretical models

S. Mukhopadhyay,<sup>1</sup> S. Majumder,<sup>1</sup> and A. Barman<sup>1\*</sup>

<sup>1</sup>Department of Condensed Matter Physics and Material Sciences, S. N. Bose National Centre for Basic Sciences, Block JD, Sector III, Salt Lake, Kolkata -700 106, India

\*Email: [abarman@bose.res.in](mailto:abarman@bose.res.in)

**Abstract:** The phenomenon of femtosecond laser-induced ultrafast demagnetization, first demonstrated in magnetic systems by Beaurepaire et al. in 1996, is one of the fastest known means for manipulation of magnetization. The phenomenon is of special interest in the field of spintronics as it implies that magnetization switching in spin-based memory devices could be achieved at these ultrashort timescales. In this work, we measure the ultrafast demagnetization in 20-nm thick cobalt (Co), nickel (Ni) and permalloy (Py) thin films and analyze our results using two distinct theoretical models.

### 1. INTRODUCTION

The pursuit of a thorough understanding of phenomena involved in subpicosecond magnetization manipulation in ferromagnetic systems is vital for the development of spin-based logic and memory devices promising ultrafast processing speeds and lower electric power consumption. To this end, we analyze using two distinct theoretical models the ultrafast demagnetization in 20 nm-thick Co, Ni and Py thin films measured all-optically and extract characteristic time constants associated with the observed magnetization quenching and values of microscopic parameters influencing it.

### 2. THEORY

#### 2.1. The 3-temperature model

The three-temperature model proposed by Beaurepaire et al. [1] describes the thermodynamics of the demagnetization phenomenon in terms of the energy exchange between three thermal reservoirs comprising the excited ferromagnet: the electrons at a temperature  $T_e$ , the lattice at temperature  $T_l$  and the electronic spin reservoir at temperature  $T_s$ . The model is phenomenological and does not follow from any microscopic considerations. Equilibration of the excited electrons with the spin and lattice reservoirs post-laser excitation must follow via energy transfer described by coupled rate equations in the following manner:

$$C_e(T_e) \frac{dT_e}{dt} = -G_{el}(T_e - T_l) - G_{es}(T_e - T_s) + P(t)$$

$$C_l(T_l) \frac{dT_l}{dt} = -G_{el}(T_l - T_e) - G_{ls}(T_l - T_s)$$

$$C_s(T_s) \frac{dT_s}{dt} = -G_{el}(T_s - T_e) - G_{ls}(T_s - T_l)$$

where  $G_{ab(a,b=e,l,s)}$  are the inter-reservoir coupling constants.

#### 2.2. The microscopic 3-temperature model

On the other hand, the microscopic three-temperature model proposed by Koopmans et al. [2] describes the ultrafast demagnetization as occurring due to spin-dependent scattering processes mediated by the intrinsic spin-orbit coupling of the material, occurring with a material-specific spin-flip probability  $a_{sf}$ .

By fitting experimental demagnetization traces (eg. Fig.1) to the above models, the values of the empirical coupling constants  $G_{el}$ ,  $G_{es}$  and  $G_{sl}$  and the spin-flip

probability  $a_{sf}$  were calculated as fit parameters. We extracted demagnetization times of 230-280 fs for Co, 160-210 fs for Ni, and 220-250 fs for Py, increasing with fluence, and an  $a_{sf} \sim 0.02$  for Co,  $\sim 0.05$ -0.06 for Ni, and  $\sim 0.03$ -0.06 for Py.

### 3. EXPERIMENT

#### 2.1. Sample fabrication

20 nm-thick Co, Ni and Py thin films were deposited by electron beam evaporation under an average pressure of  $10^{-7}$  Torr and using a deposition rate of  $0.2 \text{ \AA s}^{-1}$  on insulating  $8 \text{ mm} \times 8 \text{ mm}$  silicon wafers coated with 285 nm-thick  $\text{SiO}_2$ .

#### 2.2. All-optical measurement of ultrafast spin dynamics

All measurements are carried out using a two-color pump-probe time-resolved magneto-optical Kerr effect (TR-MOKE) setup with a 400 nm pump beam (repetition rate = 1 kHz, pulse width > 40 fs) and 800 nm probe beam (repetition rate = 1 kHz, pulse width ~ 40 fs) with a pump-probe cross-correlation width ~ 100 fs. Laser pump fluence dependence of ultrafast demagnetization is studied varying the pump fluence in the range  $0.87$ - $8.7 \text{ mJ/cm}^2$  keeping the probe fluence at  $0.4 \text{ mJ/cm}^2$ .

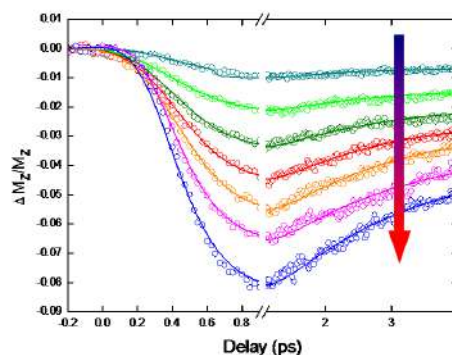


Fig.1. Pump fluence variation of demagnetization response in Co.

### REFERENCES

- [1] E. Beaurepaire et al., Phys. Rev. Lett. 76, 4250 (1995).
- [2] B. Koopmans et al., Nat. Mater. 9 (1995).



## Variation of Magnon–Magnon Coupling Strength with Microwave Power and Bias-Field Angle in Ni<sub>80</sub>Fe<sub>20</sub> Nanocross Array

Pratap Kumar Pal<sup>1</sup>, Sudip Majumder<sup>1</sup>, Anjan Barman<sup>1,\*</sup>

<sup>1</sup>Department of Condensed Matter Physics and Material Sciences, S. N. Bose National Centre for Basic Sciences, Block JD, Sector III, Salt Lake, Kolkata 700 106, India

\*Email: abarman@bose.res.in

**Abstract:** Microwave power-driven magnon-magnon coupling entangled with a stark variation of mode softening feature has been observed in ferromagnetic nanocross array. The dynamic dipolar interaction between the nanocross elements plays an important role in modulating the observed anti-crossing phenomenon. While the mode softening feature is appearing due to the phase transition, which is tunable with bias field angle.

### INTRODUCTION

Hybrid magnonic systems are becoming rising contenders for coherent information processing, owing to their capability of coherently connecting distinct physical platforms in quantum systems as well as the rich emerging physics for new functionalities [1,2]. Magnons have been demonstrated to efficiently couple to cavity quantum electrodynamics systems including superconducting resonators and qubits. Magnonic systems are therefore well-positioned for the next advances in quantum information. In addition, recent studies also revealed the potential of magnonic systems for microwave-optical transduction, which are promising for combining quantum information, sensing, and communication [3].

Here, we have been employed ferromagnetic nanocross array to investigate the role of spin-density in such kind of structures. We observe magnon-magnon coupling in permalloy (Py; hereafter) nanocross array with the virtue of broadband FMR technique and micromagnetic simulations. The number of spins in the nanocross structure is several orders of magnitude smaller than the smallest value ( $N \sim 10^{13}$ ) reported in the literature. We observe two anticrossing phenomena at two different bias fields entangled with a prominent mode-softening phenomena at very low bias magnetic field strength. The first anti-crossing gap shows strong dependence on microwave power, while the anti-crossing at higher field value does not appear to change much with external sources. The dynamic dipolar interactions between neighboring nanocross structures, driven by the microwave power tend to affect the strong magnon-magnon coupling. The mode-softening field varies systematically with microwave power leading towards control of phase transition in nanostructures system just by externally tuning microwave power.

### SAMPLE AND RESULTS

Py nanocross array with arm length ( $L$ ) of 350 nm, edge-to-edge separation ( $S$ ) of 150 nm, and thickness of 20 nm were fabricated on self-oxidized Si substrate (001) by a combination of e-beam lithography and e-beam evaporation and a coplanar waveguide (CPW) made by Au of 150 nm thickness, having 30- $\mu$ m central conductor width ( $w$ ), 300- $\mu$ m length, and 50  $\Omega$  nominal characteristic impedance ( $Z_0$ ), was integrated

on top of the nanocross array. Excitation power of the microwave input signal is varied in the range of  $-15$  dBm to  $+6$  dBm by a vector network analyzer (VNA). Additionally, an in-plane bias magnetic field  $H$ , is applied along the x-axis and the output scattering parameter  $S_{11}$  for reflection is measured by the VNA connected with the CPW. We have observed anti-crossing or avoided crossing phenomena at two bias field strengths entangled with a mode-softening phenomena at lower bias field value. The anti-crossing strength is tunable over a wide range with variation of microwave power. The simulated magneto-static field distribution plays a significant role in enhancing the magnon-magnon coupling strength. Whereas, the mode-softening phenomenon is appearing due to the phase transition from onion to S-magnetic state, which is widely tunable with bias field angle. Micromagnetic simulations have also reproduced the power-dependent FMR frequency shift. Overall, the observed tunability of magnon-magnon coupling over a wide range in ferromagnetic nanocross array is promising for applications in microwave-assisted fast magnetic storage, logic, and communication devices.

### REFERENCES

- [1] J. Chen, C. Liu, T. Liu, Y. Xiao, K. Xia, G. E. W. Bauer, M. Wu, and H. Yu, *Strong Interlayer Magnon-Magnon Coupling in Magnetic Metal-Insulator Hybrid Nanostructures*, Physical Review Letters **120**, 217202 (2018).
- [2] Y. Li, W. Cao, V. P. Amin, Z. Zhang, J. Gibbons, J. Sklenar, J. Pearson, P. M. Haney, M. D. Stiles, W. E. Bailey, V. Novosad, A. Hoffmann, and W. Zhang, *Coherent Spin Pumping in a Strongly Coupled Magnon-Magnon Hybrid System*, Physical Review Letters **124**, 1 (2020).
- [3] K. Adhikari, S. Sahoo, A. K. Mondal, Y. Otani, and A. Barman, *Large Nonlinear Ferromagnetic Resonance Shift and Strong Magnon-Magnon Coupling in N 180 F E20 Nanocross Array*, Physical Review B **101**, 54406 (2020).

## Magnetic field-induced magnetodielectric coupling and dielectric relaxation response in $\text{KBiFe}_2\text{O}_5$

K. Chandrakanta, Anil. Kumar. Singh\*

Department of Physics and Astronomy, National Institute of Technology, Rourkela-769008, Odisha, India,

\*Email: singhanil@nitrkl.ac.in

**Abstract:** Polycrystalline  $\text{KBiFe}_2\text{O}_5$  (KBFO), belonging to the brownmillerite class of monoclinic structure with space group  $P2/c$ , is synthesized using a solid-state reaction route. Magnetodielectric (MD) and magnetoimpedance (MI) characteristics of KBFO are studied over a wide temperature (10 K to 300 K), magnetic field (0 T to 1.3 T), and frequency (100 Hz to 1 MHz) range. At room temperature, MD and MI data as a function of the magnetic field shows maximum MD and MI coupling to be  $\sim -0.6\%$  and  $\sim 0.7\%$ , respectively, at 30 kHz. It is demonstrated that the magnetodielectric coupling is co-related to the observed magnetic field-induced dielectric relaxation mechanism in KBFO.

### 1. INTRODUCTION

Magnetoelectric (ME) materials are those in which magnetic and electric order parameters are strongly coupled. These ferro ordering, such as ferroelectric and ferromagnetic (antiferromagnetic) coupling, made ME materials more attractive [1]. For instance, magnetodielectric (MD) materials are characterized by the simultaneous existence of magnetic and dielectric order parameters with a certain degree of coupling between them [2]. MD coupling is a traditional approach to understanding the ME effect in multiferroic materials.

### 2. EXPERIMENTAL TECHNIQUE

$\text{KBiFe}_2\text{O}_5$  polycrystalline sample is synthesized using a solid-state reaction route. The detailed synthesis process is reported in our earlier report [2]. X-ray diffraction (XRD) measurement (RIGAKU JAPAN) having Cu-K $\alpha$  radiations ( $\lambda=1.5406 \text{ \AA}$ ) is carried out to confirm the phase of KBFO. The dielectric measurement is carried over a wide temperature (10 K to 300 K) and frequency (500 Hz to 1 MHz) range using high precision Wayne Kerr 6500B impedance analyzer following close cycle refrigerator (Cryo Industries, USA) to attain the low temperature.

### 3. RESULTS AND DISCUSSIONS

#### 3.1. X-ray diffraction studies

The room temperature (RT) Rietveld refined X-ray diffraction (XRD) patterns of  $\text{KBiFe}_2\text{O}_5$  (KBFO) polycrystalline shown in fig. 1. The absence of impurity peaks in the XRD data is confirmed through the refinement using FULLPROF software. It indicates that the prepared sample is in a pure phase. It is observed that the KBFO sample crystallizes in a monoclinic structure with a  $P2/c$  space group.

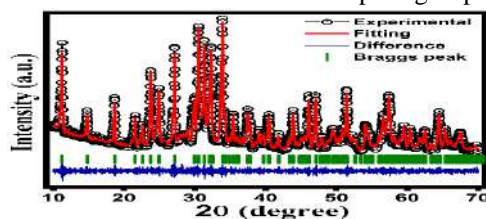


Fig.1. The RT Rietveld refined XRD patterns of KBFO.

The lattice parameters are found to be  $a = 7.8992 \text{ \AA}$ ,  $b = 5.9736 \text{ \AA}$ , and  $c = 5.7252 \text{ \AA}$ , and the goodness of fit parameter ( $\chi^2$ ) is found to be 3.37 respectively.

#### 3.2. Temperature and magnetic field dependent magnetodielectric studies

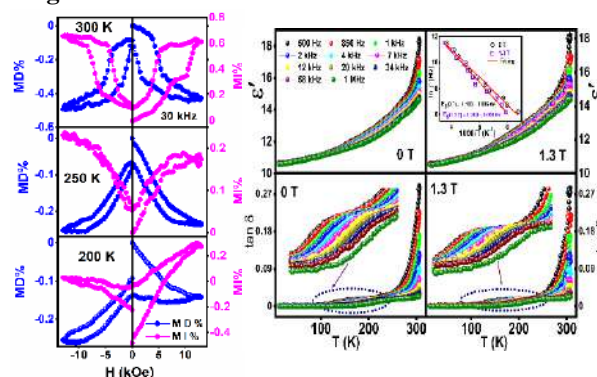


Fig.2. The temperature dependent MD and MI of KBFO

The dielectric constant ( $\epsilon'$ ) and dielectric loss ( $\tan \delta$ ) of KBFO is measured as a function of temperature (10 K to 300 K) at different fixed frequencies (100 Hz to 1 MHz) in zero-field and in the presence of 1.3 T magnetic field (figure 2). The applied magnetic field observed a slight shift in the relaxation peaks of dielectric loss data. It indicates the impact of the magnetic field on the relaxations of the electric dipoles in KBFO. Arrhenius fit yields the activation energy ( $E_g$ ) values to be  $0.204 \pm 0.0008 \text{ eV}$  for 1.3 T field and  $0.183 \pm 0.006 \text{ eV}$  for zero-field. To understand the origin of MD coupling, field-dependent magnetoimpedance (MI) measurement is done at a different fixed temperature. The combined MI% and MD% are shown in fig. 2.

### 4. CONCLUSIONS

The above results conclude that the field-dependent MD and MI loop is reflected from the capacitive origin.

### REFERENCES

- [1]. N. A. Spaldin et al., Nat. Mater. **18** (2019) 2003.
- [2]. K. Chandrakanta et al., J. Magn. Magn. Mater. **549** (2022) 169047.

**Probing magnetic anisotropy and spin-reorientation transition in 3D antiferromagnet,  
Ho<sub>0.5</sub>Dy<sub>0.5</sub>FeO<sub>3</sub>|Pt using spin Hall magnetoresistance**

**Priyanka Garg<sup>1,\*</sup>, Aditya A. Wagh<sup>1,\*</sup>, Arijit Haldar<sup>2</sup>, Kingshuk Mallick<sup>1</sup>, Tirthankar  
Chakraborty<sup>1</sup>, Suja Elizabeth<sup>1</sup> and P. S. Anil Kumar<sup>1</sup>**

<sup>1</sup>Department of Physics, Indian Institute of Science, Bangalore, India

<sup>2</sup>University of Toronto, Canada

**Email: priyankagarg@iisc.ac.in**

**Abstract:** Rare-earth orthoferrites (REFeO<sub>3</sub>), are 3D antiferromagnets (AFM) that exhibit a weak ferromagnetism originating from slight canting of the spin moments and display a variety of spin reorientation transitions in the magnetic field (H)-temperature (T) parameter space. We present spin Hall magnetoresistance (SMR) studies on a b-plate of single crystal Ho<sub>0.5</sub>Dy<sub>0.5</sub>FeO<sub>3</sub>|Pt hybrid, carried out by rotating H in the ac-plane ( $\alpha$ -scan) at various T down to 11 K. At 300 K ( $H \geq 800$  Oe) in  $\Gamma_4(G_x, A_y, F_z)$  phase, SMR vs.  $\alpha$  yielded a highly skewed curve with a sharp change, accompanied by a rotational hysteresis around a-axis. Notably,  $\alpha$ -scans ( $H < 800$  Oe) on the pre-pinned domain ( $\pm F_z$  domain) exhibited an anomalous sinusoidal signal of periodicity  $360^\circ$ . Low-T SMR ( $H \approx 2.4$  kOe) resulted in a weakening of the anisotropy possibly due to the T-evolution of Fe-RE exchange coupling. Besides, below 25 K the SMR modulation showed an abrupt change around c-axis, marking the presence of  $\Gamma_2(F_x, C_y, G_z)$  phase. We have employed a simple Hamiltonian and computed SMR, to examine the observed SMR modulations. Our SMR studies not only serve as an effective probe for magnetic anisotropy and spin reorientation but also, highlight the potential of Ho<sub>0.5</sub>Dy<sub>0.5</sub>FeO<sub>3</sub> for future AFM spintronic devices.

**Highly tunable spin Hall magnetoresistance in magnetoelectric Z-type hexaferrite,  
Sr<sub>3</sub>Co<sub>2</sub>Fe<sub>24</sub>O<sub>41</sub>|Pt hybrids**

**Aditya A. Wagh,\* Priyanka Garg,\* Kingshuk Mallick, Suja Elizabeth and P. S. Anil Kumar**

**Department of Physics, Indian Institute of Science, Bangalore, INDIA**

**Email: adityawagh@iisc.ac.in**

**Abstract:** We present spin transport studies on a low-field, room-temperature magnetoelectric multiferroic polycrystalline Sr<sub>3</sub>Co<sub>2</sub>Fe<sub>24</sub>O<sub>41</sub>|Pt heterostructure wherein, a transverse conical magnetic phase is responsible for static and dynamic magnetoelectric coupling. We measured angular dependence of spin Hall magnetoresistance (SMR) at various constant magnetic fields (H) in the range, 50 Oe to 100 kOe. Fields below a critical value of 2 kOe, yielded a negative SMR and SMR amplitude vs. H exhibited a negative gradient. Further, increase in the H resulted in the positive slope of SMR amplitude vs. H and near H ≈ 14 kOe, a crossover observed from negative to positive SMR. We employed a simple model to compute and understand SMR in Sr<sub>3</sub>Co<sub>2</sub>Fe<sub>24</sub>O<sub>41</sub>. We argue that the cone-tilting is dominant and in turn responsible for the observed nature of SMR below 2 kOe while, closing of the cone-angle is pronounced at higher H causing a reversal in sign of the SMR from negative to positive. Notably, SMR studies revealed that a change in the helicity with a reversal of H has no influence on the observed SMR. Our detailed spin transport studies on Sr<sub>3</sub>Co<sub>2</sub>Fe<sub>24</sub>O<sub>41</sub> demonstrate high tunability of the amplitude and the sign of the SMR highlighting its potential for magnetoresistance-based spintronic devices.



## Effect of Cr doping on the Structural, Surface Morphology, Magnetic and Antimicrobial Properties of Nickel ferrite

Sachin Kumar Godara<sup>1</sup>, Venuka Bhasin<sup>2</sup>

<sup>1,2</sup>Department of Chemistry, UGC Center for Advanced Studies-II, Guru Nanak Dev University, Amritsar, Punjab, India-143005  
Email: venuka12bhasin@gmail.com

**Abstract** : A well-known spinel magnetic material is nickel ferrite ( $\text{NiFe}_2\text{O}_4$ ). Cr-substituted Nickel ferrites with composition  $\text{Cr}_x\text{Ni}_{(1-x)}\text{Fe}_2\text{O}_4$  ( $x = 0.0, 0.025, 0.05, 0.1, 0.15, 0.2$ ) was prepared using sol-gel technique. Its preparation by traditional solid-state processes involves a high calcination temperature, which causes sintering and particle aggregation. The ferrite structures were validated using X-ray diffraction, Raman spectroscopy, and Fourier transform infrared (FTIR) spectroscopy. Antimicrobial susceptibility of the nanoparticles was tested against gram-negative (*Escherichia coli*) and gram-positive bacteria (*Staphylococcus aureus*). Ferrites in powder form were produced and calcined at  $900^\circ\text{C}$ .

### 1. INTRODUCTION

Nickel ferrite is such a well known soft magnet possessing an inverse spinel structure, with  $\text{Fe}^{3+}$  evenly distributed at the tetrahedral and octahedral sites and  $\text{Ni}^{2+}$  at the octahedral site.  $\text{NiFe}_2\text{O}_4$  nanoparticles are commonly employed as core materials in transformers, inductors, and biomedical applications. For MRI applications,  $\text{NiFe}_2\text{O}_4$  NPs are particularly essential because of their low cost, great electromagnetic performance, modest Ms, and good chemical stability. Hyperthermia can be utilised to treat cell differentiable cancers with  $\text{NiFe}_2\text{O}_4$  NPs. Coating with suitable biological organic molecules, as with other spinel ferrite Nanoparticles, is essential to lower degradation rates and promote biocompatibility[1].

### 2. EXPERIMENTS AND RESULTS

Antimicrobial susceptibility of the nanoparticles was tested against gram-negative and gram-positive bacteria. Antimicrobial activity was assessed using a modified agar well diffusion method. Antimicrobial activity was tested against pathogenic bacteria using 100  $\mu\text{l}$  nanoparticles solution (100mg/ml) and 10  $\mu\text{l}$  antibiotic solutions (100mg/ml)[2]. Ampicillin was employed as a positive control, while triple distilled water was used as a negative control. For bacteria growth, the Petri plates were incubated at  $37^\circ\text{C}$  for 16-18 hours. All of the tests were performed three times. The sizes of the inhibition zones formed around the wells were measured in millimetres (mm) using the HiMedia antibiotic zone scale[3].

#### 2.2. Effect of Cr doping on the antimicrobial properties of cobalt ferrite

The inhibition zones (in mm) of varying sizes were obtained as mentioned in **Figure 1**. The inhibition zones were measured by taking the amount of 100 $\mu\text{l}$  of nanoparticles solution and ampicillin in different wells. In gram-positive bacteria *i.e.*, *S.aureus*,  $\text{Ni}_{0.8}\text{Cr}_{0.2}$  nanoparticles

showed highest zone of inhibition ( $12.3 \pm 0.538$ ) whereas,  $\text{Ni}_{0.95}\text{Cr}_{0.05}$  nanoparticles showed minimum zone of inhibition ( $11.5 \pm 0.521$ ).  $\text{Ni}_{0.975}\text{Cr}_{0.025}$ ,  $\text{Ni}_{0.85}\text{Cr}_{0.15}$  and  $\text{Ni}_{0.9}\text{Cr}_{0.1}$  nanoparticles showed no zone of inhibition. In gram-negative *i.e.*, *E. coli*,  $\text{Ni}_{0.85}\text{Cr}_{0.15}$ ,  $\text{Ni}_{0.8}\text{Cr}_{0.2}$ ,  $\text{Ni}_{0.95}\text{Cr}_{0.05}$  nanoparticles showed good zone of inhibition ( $15 \pm 0.534$ ), ( $14.5 \pm 0.568$ ), ( $13.7 \pm 0.545$ ), respectively, whereas,  $\text{Ni}_{0.975}\text{Cr}_{0.025}$ ,  $\text{Ni}_{0.9}\text{Cr}_{0.1}$  nanoparticles showed no zone of inhibition.

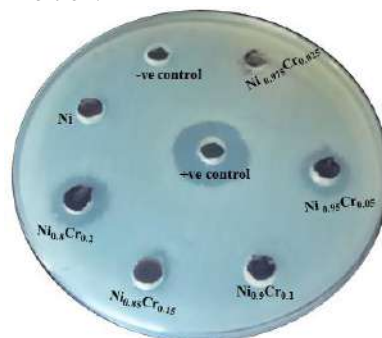


Fig.1. antimicrobial activity shown by Cr-substituted Nickel ferrites with composition  $[\text{Cr}_x\text{Ni}_{(1-x)}\text{Fe}_2\text{O}_4$  ( $x = 0.0, 0.025, 0.05, 0.1, 0.15, 0.2$ )]

### REFERENCES

1. Mmesi et al., Mater Sci Semicond Process. 123, (2020) 105523.
2. Swati et al., J Environ Chem Eng. 8 (2020) 103730.
3. Morones et al., Nanotechnol. 16 (2005) 2346.

## Spin pumping and inverse spin Hall effect study in CoFeB/ IrMn bilayers

Koustuv Roy<sup>1</sup>, Abhisek Mishra<sup>1</sup>, Pushpendra Gupta<sup>1</sup>, Shaktiranjana Mohanty<sup>1</sup>, Braj Bhusan Singh<sup>1</sup>,  
Subhankar Bedanta<sup>1,2,\*</sup>

<sup>1</sup>Laboratory for Nanomagnetism and Magnetic Materials (LNMM), School of Physical Sciences, National Institute of Science Education and Research (NISER), HBNI, Jatni-752050, Odisha, India

<sup>2</sup>Center for Interdisciplinary Sciences (CIS), National Institute of Science Education and Research (NISER), HBNI, Jatni 752050, India

Email: koustuv.roy@niser.ac.in

**Abstract:** Spin current propagation efficiency through the ferromagnet (FM)/ Heavy metal (HM) interface is one of current interest in modern research. Generation of spin current and its dissipation through a HM efficiently depends on the low damping FM layer and high spin orbit coupling (SOC) of HM layer. Recently, antiferromagnetic materials (AFM) has been shown potentials to replace HM due to high resistivity, and high SOC. AFM may work as an efficient spin source also. Here, we report spin pumping via measuring inverse spin Hall effect on CoFeB/ IrMn (AFM) bilayers.

### 1. INTRODUCTION

Efficient generation of spin current and its manipulation in different materials is one of the emergent research topics in modern days due to applications in the development of power efficient and faster spintronics devices. Spin pumping [2] and inverse spin Hall effect (ISHE) [3] are the tools to study the spin current efficiency in the materials. In last one decade, ISHE and spin pumping are heavily investigated in ferromagnet (FM)/ heavy metal (HM) heterostructures. Recently the antiferromagnetic (AFM) materials are found to be a good replacement of heavy metals (HM) due to presence of high spin orbit coupling [4]. Understanding the role of different AFM layers in ISHE or spin pumping study is still limited. In this context, we have performed the ISHE in CoFeB/ IrMn bilayers, where IrMn is an AFM layer.

### 2. EXPERIMENTAL DETAILS

A series of samples of the structure CoFeB(20 nm)/ Cu(3 nm)/ IrMn( $t$  nm)/ AlOx(3 nm) have been prepared on top of Si(100) substrate using dc magnetron sputtering where the ' $t$ ' value varies from 0 to 20 nm. The deposition is performed at the base pressure of  $1 \times 10^{-9}$  mbar. All the samples are prepared using 20 rpm rotation to avoid the growth induced uniaxial anisotropy and better uniformity. The sample layers are prepared with the Ar flow of 10 sccm. The Cu layer is used to improve the growth of IrMn as a buffer layer and also avoid any induced magnetism in IrMn layer. AlOx layer is prepared to protect the sample from environmental contamination. The ISHE measurements are performed on home modified broadband FMR based set-up [5].

### 3. RESULTS AND DISCUSSION

The FMR measurement is carried out at +15 dBm rf excitation power. Fig. 1 shows the measured ISHE voltage for the sample with IrMn(10 nm) at  $\phi$  value of  $30^\circ$ . The angle  $\phi$  denotes the angle between contacts to measure voltage and direction of applied dc magnetic field ( $H$ ). Angle dependent ISHE study is carried out in order to disentangle the different spin rectification effect components.

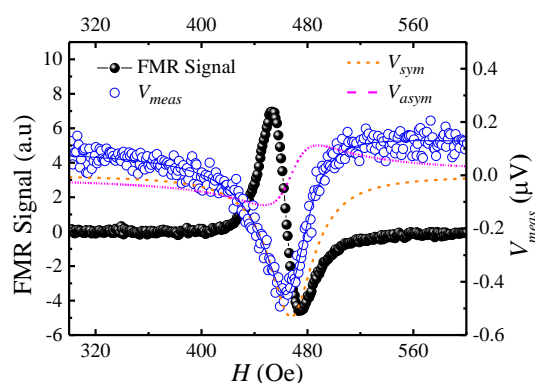


Fig.1. Voltage ( $V_{meas}$ ) measured across the sample with applied magnetic field along with FMR signal for sample with IrMn(10 nm) at the  $\phi$  value of  $30^\circ$ .

The angle dependent ISHE study reveals the spin pumping component in the measured voltage in the sample with IrMn(10) is  $-1.08 \mu\text{V}$ , which found to be higher than other rectification effects. The systematic damping and ISHE measurement analysis are carried out for all the samples to understand the spin current efficiency on the bilayers [6].

### ACKNOWLEDGEMENT

The authors acknowledge DAE and DST, Govt. of India, for the financial support for the experimental facilities. KR thanks CSIR for JRF fellowship. BBS acknowledges DST for INSPIRE Faculty fellowship.

### REFERENCES

1. S.D. Bader *et al.*, Annual Review of Condensed Matter Physics **1**, 71-88 (2010).
2. Y. Tserkovnyak *et al.*, Rev. Mod. Phys. **77**, 1375 (2005).
3. E. Saitoh *et al.*, Appl. Phys. Lett. **88**, 182509 (2006).
4. Wei Zhang *et al.*, Phys. Rev. B **92**, 144405 (2014).
5. Singh *et al.*, Physica Status Solidi (RRL) **13**, 1800492 (2019).
6. Roy *et al.*, J. Phys. D: Appl. Phys. **54**, 425001 (6pp) (2021).

## On the Room Temperature Weak Localization and Anomalous Temperature Dependence of Phase Coherence Length in $L2_1$ ordered Heusler Alloy CoFeMnSi Thin Films

Vireshwar Mishra, Lalit Pandey, Vineet Barwal, Soumyarup Hait, Nanhe Kumar Gupta, Nikita Sharma, Nakul Kumar, Amar Kumar and Sujeet Chaudhary\*

<sup>1</sup>*Thin Film Laboratory, Department of Physics, Indian Institute of Technology Delhi, 110016 (INDIA)*

\**Corresponding author:sujeetc@iitd.ac.in*

The spin gapless semiconducting (SGS) compounds have been reported to possess excellent properties in order to be utilized in various spintronics based devices. Here, we report the room temperature weak localization in  $L2_1$  ordered CoFeMnSi (CFMS) Heusler alloy thin films grown over Si(100) substrates using pulsed-DC magnetron sputtering technique. We have observed the (111) reflection in the grazing incidence X-ray diffraction curve which confirms its crystallinity of  $L2_1$  order. Longitudinal resistivity trend shows similar non-metallic behaviour akin to other reported SGS materials. The temperature-dependent longitudinal conductivity curve fitted with two carrier model revealed that one channel of the system is gapped while the other channel has some band overlap. Further analysis of longitudinal resistivity curve confirmed that weak localization factor dominates over other scattering factors and is larger in higher temperature regime compared to lower temperature regime. Detailed analysis of the magnetoresistance behaviour confirmed the existence of weak localization (sharp negative cusp at low field) even up to room temperature with an *anomalous* increase of phase coherence length with temperature. Further analysis of magnetoresistance behaviour showed that the CFMS system lies in quantum diffusive regime. The anomalous Hall effect study revealed nearly temperature-independent carrier concentration and mobility, which is a characteristic signature of the SGS materials, with room temperature values of  $2.77 \pm 0.36 \times 10^{22}$  and  $1.13 \pm 0.14$   $\text{cm}^2/\text{V} \cdot \text{s}$ , respectively. The anomalous Hall conductivity values obtained at 5K and 300K are 37.75 S/cm and 56.58 S/cm, respectively.

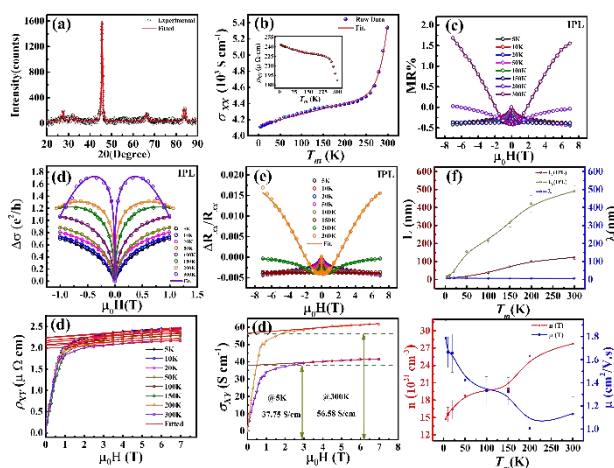


Figure 1: (a) GIXRD plot for optimized CFMS thin film, (b) Temperature dependence of longitudinal conductivity (fitted curve shown by solid red line) and the inset showing temperature dependence of electrical resistivity, (c) MR curves traced at different  $T_m$ , (d) conductivity correction ( $\Delta\sigma$ ), fitted in small field range (-1T to 1T) using eq. (2), (e) resistivity correction fitted in full field range (-7T to 7T) using eq. (3), (f) plot of  $L_\phi$ ,  $L_e$ , and  $\lambda$ , (g) Hall resistivity vs. magnetic field curves recorded at 5K, 10K, 20K, 50K, 100K, 150K, 200K and 300K for CFMS film in five-point contact geometry, (h) Hall conductivity plot as a function of magnetic field for CFMS film at 5K and 300K and (i) Temperature dependence of carrier concentration and mobility (Lines connecting the data symbols guide to the eye).

- [1] J. Hu and T. F. Rosenbaum, *Classical and Quantum Routes to Linear Magnetoresistance*, Nature Materials **7**, 697 (2008).

## Correlating magnetic and synchrotron x-ray diffraction studies of chiral magnet MnSi

S. Shanmukharao Samatham<sup>1</sup>, Akhilesh Kumar Patel<sup>2</sup>, A. K. Sinha<sup>3,4</sup>, M. N. Singh<sup>3</sup> and K. G. Suresh<sup>2</sup>

<sup>1</sup>Department of Physics, Chaitanya Bharathi Institute of Technology, Gandipet, Hyderabad 500075,

<sup>2</sup>Department of Physics, Indian Institute of Technology Bombay, Powai, Mumbai 400076, India

<sup>3</sup>Synchrotrons Utilization Section, Raja Ramanna Center for Advanced Technology, Indore 452013, India

<sup>4</sup>Homi Bhabha National Institute, Training School Complex, Anushakti Nagar, Mumbai 400094, India

Email: [shanmukharao\\_physics@cbit.ac.in](mailto:shanmukharao_physics@cbit.ac.in)

**Abstract:** We report on the structural sensitivities of non-centrosymmetric B20 cubic chiral magnet MnSi corresponding to the magnetic transition using the combined results of temperature-dependent synchrotron x-ray diffraction, dc-magnetization and ac-susceptibility measurements. The lattice constant exhibits an anomaly at the long-range magnetic ordering temperature. Altogether, we confirm the first order nature of the zero-field magnetic phase transition of MnSi.

### 1. INTRODUCTION

Among the 3d-metal based alloys, transition metal monosilicides with formula TSi (T = Mn, Fe, Co etc.) have been studied. FeSi was reported to be a strongly correlated Kondo-type narrow band gap ( $\sim 60$  meV) semiconductor akin to some of the Ce based rare-earth compounds. CoSi is a diamagnetic pseudo gap semi-metal with hidden metal-to-insulator transition. MnSi is fascinating for its exemplary itinerant magnetic behavior with chiral magnetic order below 30 K [1]. The helical wavelength of MnSi ( $\lambda_{\text{helix}}$ ) is about 180 Å [2, 3] while the lattice constant is about 4.553 Å (at room temperature). In the recent times, the renewed interest in MnSi is due to the existence of skyrmion lattice just below the ordering temperature under the perturbation of small magnetic fields.

With an interest to investigate the role of structural transformation/modifications of MnSi, we have performed temperature dependent synchrotron x-ray diffraction measurements. The considerable changes in the lattice constant in the vicinity of  $T_C$  reveal the involvement of latent heat, in favor of the first order phase transition.

### 2. EXPERIMENTAL METHODS

MnSi was prepared by arc-melting the high pure constituent elements under the continuous flow of argon gas. X-ray diffraction pattern was recorded on a powder specimen at room temperature. Synchrotron x-ray diffraction (SXR) measurements were performed using synchrotron x-ray radiation at Angle Dispersive X-ray Diffraction beamline (BL-12), INDUS-2, RRCAT, India.

### 3. RESULTS AND DISCUSSION

To investigate the possible structural modifications near  $T_C$ ,  $T$ -dependent synchrotron x-ray diffraction analysis is carried out. However, the shift in the peak positions with  $T$  is noticed. The peak at 300 K (not shown here) shifts to higher angles at 100 K indicating the decrease in the lattice constant. However, 30 K peak shows the highest shift in  $2\theta$ , indicating large decrease in lattice constant at 30 K ( $= T_C$ ).

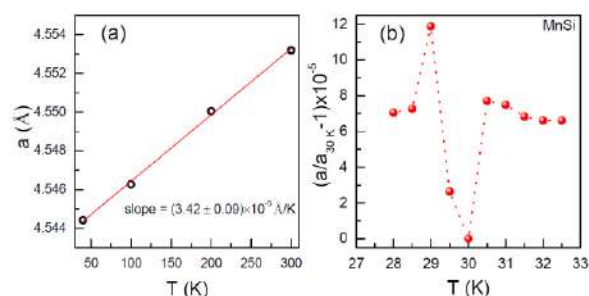


Fig.1. Temperature variation of the relative change in lattice constant, defined as  $\delta a = (a/a_{30K}) - 1$ . It (a) varies linearly from 300 to 40 K and (b) exhibits an anomaly at the magnetic ordering temperature along with a shoulder slightly above  $T_C$ .

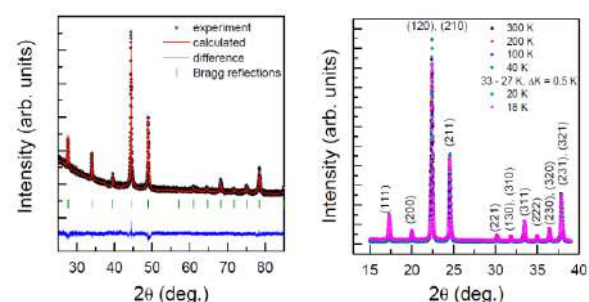


Fig.2. Room temperature laboratory x-ray diffraction. (b) Synchrotron x-ray diffraction patterns collected using the wavelength of  $\lambda = 0.7889$  Å.

### 4. SUMMARY

The lattice parameter exhibits an anomaly at the ordering temperature while it linearly decreases down to 40 K from room temperature. Altogether, our observations confirms the first order nature of the zero-field magnetic phase transition of MnSi as evident from the involved latent heat inferred from the behavior of lattice constant in the vicinity of the long-range ordering temperature.

### REFERENCES

- [1]. Wernick et al., Mat. Res. Bull. 7, 1431 (1972).
- [2]. Shirane et al., Phys. Rev. B 28, 6251 (1983).
- [3]. Ishida et al., J. Phys. Soc. Jpn. 54, 2975 (1985).



## Dominant mechanism behind Ultrafast demagnetization correlating with Gilbert damping in $\beta$ -Ta/CoFeB bilayers

Soma Dutta, Surya Narayan Panda, Anjan Barman

Department of Condensed Matter Physics and Material Sciences, S N Bose National Centre for Basic Sciences, Block JD, Sector III, Salt Lake, Kolkata-700106, India

Email: abarman@bose.res.in

**Abstract:** Using all optical TR-MOKE technic we have established a linear relationship between the change of demagnetization rate and Gilbert damping induced by spin chemical potential at the interface which states about the dominant contribution of spin pumping. We have also extracted the spin accumulation coefficient at the interface. Our work will give further insights into ultrafast spin dynamics.

### 1. INTRODUCTION

Detection, understanding and manipulation of ultrafast spin dynamics of Ferromagnet(FM)/Nonmagnet(NM) thin film heterostructure is an important topic for emerging field of spintronics. Among different mechanism, ultrafast demagnetization [1] is one of the fastest spin manipulation mechanism. When a laser pulse is incident on a magnetic material, it partially or fully lost it's magnetization within hundreds of femtosecond, this is called ultrafast demagnetization. In this work we have explored the actual mechanism behind ultrafast demagnetization in  $\beta$ -Ta/CoFeB heterostructure (where Ta act as a nonmagnet and CoFeB is an important ferromagnetic amorphous alloy) by all optical time resolved magneto optical kerr effect magnetometry from femtosecond to nanosecond time scales.

### 2. CORRELATION

The relationship between demagnetization time and Gilbert damping provides the idea of dominant contribution behind ultrafast demagnetization i.e., linear relationship indicates the spin-flip scattering contribution while inverse proportional relationship indicates spin current contribution. Although there are various mechanism to generate spin current, spin pumping is an efficient method. In our case the nature of damping over Ta and CoFeB thickness variation indicate the transfer of spin angular momentum via spin pumping from CoFeB to Ta [2].

1)The correlation between  $\tau_m$  and  $\alpha$  clarifies the above assumption i.e. we have established an inverse proportional relationship which clearly indicates that the nonlocal spin current contribution is the dominating factor behind demagnetization [3].

2)We have also shown experimentally that the thicknesses of the NM play an important role to generate spin current. The NM with thickness below spin diffusion length creates large spin backflow current (from NM to FM) due to the accumulation of spin at the interface which decreases the net amount of spin current from FM to NM and above the spin diffusion length, NM act as a good spin sink material with less spin chemical potential at the interface which enhances the damping mechanism and increases the demagnetization rate.

### 2.1. Equations

Damping and demagnetization is correlated with spin chemical potential by

$$\Delta \frac{1}{\tau_m} = \frac{\mu_s}{\hbar} \Delta \alpha \quad (1)$$

Where  $\mu_s$  is the spin chemical potential.

$$\mu_s(x=0) = 4\pi \frac{\tau_{SF} \delta_{SD} / \hbar}{\tanh(t/\lambda_{SD})} I_s \quad (2)$$

### 3. FIGURES AND IMAGES

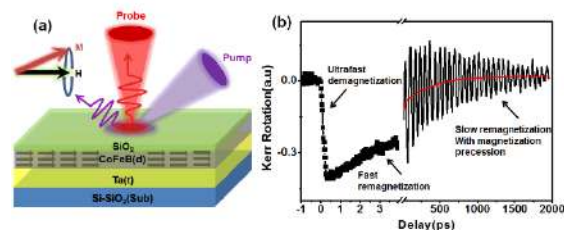


Fig.1. (a) Schematic of experimental geometry and (b) typical TR-MOKE data from Sub/CoFeB(3nm)/SiO<sub>2</sub>(2nm) heterostructure at an applied bias in-plane magnetic field of 1.73 kOe

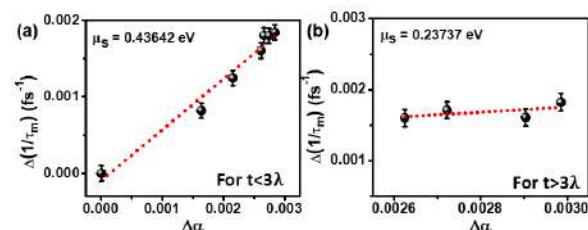


Fig.2. Correlation for Ta thickness variation for (a) less than and (b) greater than spin diffusion length.

### ACKNOWLEDGEMENT

We acknowledge financial support from S. N. Bose National Centre for Basic Sciences (grant no.: SNB/AB/18-19/211). SD acknowledge UGC and SNP acknowledges S. N. Bose National Centre for Basic Sciences for respective research fellowships.

### REFERENCES

- [1]. E. Beaurepaire et al, Phys. Rev. Lett. **76**, 4250 (1996).
- [2]. S. N. Panda et al, Sci. Adv. **5**, eaav7200 (2019).
- [3]. W. Zhang et al, Phys. Rev. B **100**, 104412 (2019)..

## **A scheme to determine the carrier density distribution, potential profile, and subband quantization of a conducting interface $\text{LaVO}_3/\text{SrTiO}_3$**

Anamika Kumari<sup>1</sup>, S. Chakraverty<sup>1\*</sup>

1. Quantum Material and Device Unit, Institute of Nano Science and Technology, Sector 81, Punjab, 140306, India.

### **Abstract**

The carrier-density distribution near a conducting interface and related band structure is an important topic of condensed matter physics. We propose a scheme combining Photoluminescence (PL) spectroscopy, time-correlated photon counting (TCSPC) with electrical measurements to reveal the distribution of the carriers, the shape of the quantum well, energy subbands, and Fermi surfaces of the conducting interface of  $\text{LaVO}_3$  and  $\text{SrTiO}_3$  (LVO/STO). Electronic properties such as Carrier density, mobility estimated from the electrical measurements are in excellent agreement with that estimated from optical spectroscopy-based methods through theoretical modeling. The proper knowledge of band structure can help us to understand the fascinating physics of “Rashba band splitting” due to high spin orbit coupling which give rise to planar hall effect, non-trivial berry phase, etc.

## Controlling Interfacial Magnetism of Transition Metal Oxides in Proximity of Ferroelectrics

Abhishek Ranna<sup>1</sup>, Debakanta Samal<sup>2,3</sup>, Samir Kumar Biswas<sup>1</sup>

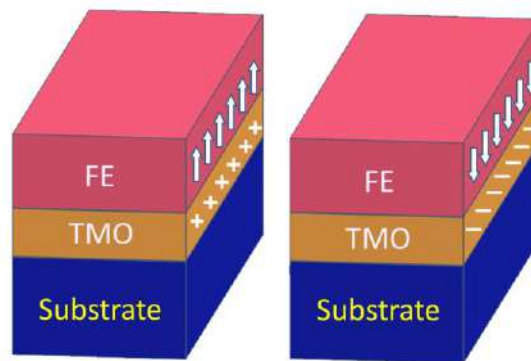
<sup>1</sup>Department of Physical sciences, Indian Institute of Science Education and Research Mohali, 140306, India.

<sup>2</sup>Institute of Physics, Sachivalaya Marg, Bhubaneswar 751005, India.

<sup>3</sup>Homi Bhabha National Institute, Anushakti Nagar, Mumbai 400085, India

Email: [abhishekranna@iisermohali.ac.in](mailto:abhishekranna@iisermohali.ac.in)

**Abstract:** Electric field control of magnetism has gained a lot of recent interest, the idea to couple magnetic thin films with a ferroelectric to observe electronic structure modification in the interface can be exploited to a large extent. In this study, we try to explore the possibilities of electrostatic doping in ferromagnetic interfaces to observe changes in the magnetisation of the heterostructure. From the synthesis of the strained ferroelectric material via solid-state synthesis to stabilise the thin-film phase and optimisation of the heterostructures grown via pulsed laser deposition method, this work looks into interfacial magnetic control in candidate transition metal oxides via external perturbations induced by the intrinsic polarization of a strained ferroelectric oxide.



**Frequency dependent inverse spin Hall effect in  $\text{La}_{0.67}\text{Sr}_{0.33}\text{MnO}_3/\text{Pt}$  bilayer system****Pushpendra Gupta<sup>1\*</sup>, Braj Bhusan Singh<sup>1</sup>, Anirban Sarkar<sup>2</sup>, Markus Waschk<sup>2</sup>, Thomas Brueckel<sup>2</sup>, and Subhankar Bedanta<sup>1,3</sup>**<sup>1</sup>Laboratory for Nanomagnetism and Magnetic Materials (LNMM), School of Physical Sciences, National Institute of Science Education and Research (NISER), HBNI, P.O.- Bhipur Padanpur, Via Jatni, 752050, India<sup>2</sup>Forschungszentrum Jülich GmbH, Jülich Centre for Neutron Science (JCNS-2) and Peter Grünberg Institut (PGI-4), JARA-FIT, 52425 Jülich, Germany<sup>3</sup> Center for Interdisciplinary Sciences (CIS), National Institute of Science Education and Research (NISER), HBNI, Jatni-752050, India

**Abstract:** In this work we have shown the relation between FMR absorption intensity to inverse spin Hall effect voltage. We have performed angle dependent spin pumping measurement for  $\text{La}_{0.67}\text{Sr}_{0.33}\text{MnO}_3/\text{Pt}$  bilayer system at different frequencies. It has been observed that spin Hall angle has a clear dependency on frequency. We have shown that at higher frequency spin Hall angle is higher than that of at lower frequencies. The maximum value of spin pumping voltage at 14 GHz is 128  $\mu\text{V}$  and its corresponding spin Hall angle is calculated to 0.08.

**1. INTRODUCTION**

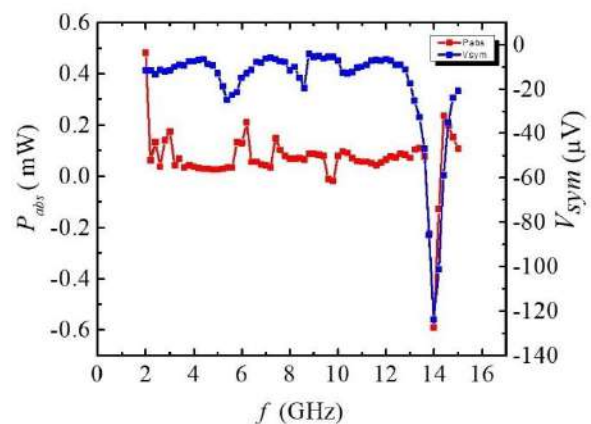
Manganite are materials with rich physics in terms of magnetic properties and have drawn attention due to their rich electronic and magnetic phase diagram.  $\text{La}_{0.67}\text{Sr}_{0.33}\text{MnO}_3$  (LSMO) films prepared by oxide based molecular beam epitaxy (OMBE) have shown very interesting properties. In our previous work we have observed that, due to domination of anti-damping like torque in LSMO/Pt bilayer system Gilbert damping constant decreases in comparison to LSMO single layer [1]. During the damping measurement where ferromagnetic resonance (FMR) spectra for the different frequencies has been taken, the intensity of FMR spectra is not linearly dependent on frequency, rather it is much larger at certain frequencies. Further to explore the relation of FMR absorption intensity with spin pumping voltage a detailed study has been performed at certain frequencies. Observed results depicts that spin pumping voltage is directly related with FMR absorption intensity. We have also calculated the spin Hall angle ( $\theta_{SHA}$ ) for this sample at different frequencies.

**2. EXPERIMENTAL DETAILS**

LSMO (20 nm)/Pt ( $t_{Pt} = 0, 3\text{nm}$ ) bilayer samples have been prepared on  $\text{SrTiO}_3(001)$  substrate using an oxygen plasma assisted molecular beam epitaxy system. ISHE measurements are performed using home modified coplanar wave-guide (CPW) based ferromagnetic resonance (FMR) spectroscopy [6] and microwave absorption spectra has been measured using Vector Network Analyzer (VNA).

**3. RESULTS**

Relation between spin pumping voltage and microwave absorption intensity has been shown in Fig.1. It is clear from the plot that when absorption intensity increases spin pumping voltage also increases. The maximum spin pumping voltage has been observed at 14 GHz. Further we have calculated  $\theta_{SHA}$  at different frequencies and highest value 0.08 has been calculated at 14 GHz.

Fig.1. microwave absorption ( $P_{abs}$ ) and  $V_{sym}$  vs  $f$  plot.**ACKNOWLEDGEMENT**

The authors acknowledge DAE and DST, Govt. of India, for the financial support for the experimental facilities. Mr. Pushpendra Gupta acknowledge UGC for JRF fellowship grant. Dr. B. B. Singh thanks DST for INSPIRE faculty fellowship. Dr. S. Bedanta acknowledges German Academic Exchange Services (DAAD) for the fellowship to visit Forschungszentrum Jülich for this collaborative work

**REFERENCES**

- [1]. P. Gupta et al., Nanoscale, 13, 2714, (2021).
- [2]. B. B. Singh, S. K. Jena, M. Samanta, Phys. Status Solidi Rapid Res. Lett. 13, 1800492 (2019)



Surinder Singh\*, Anumeet Kaur, Parwinder Kaur, Lakhwant Singh

Department of Physics, Guru Nanak Dev University, Amritsar 143005, Punjab, India

Email: [surinderphy.rsh@gndu.ac.in](mailto:surinderphy.rsh@gndu.ac.in)

**Abstract:** LaFeO<sub>3</sub> modified Sodium Bismuth Titanate (NBT) with composition (LaFeO<sub>3</sub>)<sub>x</sub>-(Na<sub>0.5</sub>Bi<sub>0.5</sub>TiO<sub>3</sub>)<sub>1-x</sub> where  $x = 0, 0.01, 0.03$  and  $0.05$  (abbreviated as LFNBT0, LFNBT1, LFNBT3 and LFNBT5) have been synthesized via sol-gel method. The Rietveld refinement of room temperature XRD data certified the phase purity and the coexistence of a cubic ( $Pm\bar{3}m$ ) and a monoclinic phase (Cc). LFNBT1 sample is found to be paramagnetic where as weak ferromagnetic character is observed in LFNBT3 and LFNBT5. The overlapped ZFC and FC magnetization curves in both LFNBT3 and LFNBT5 assured the absence of any kind of magnetic ordering.

## 1. INTRODUCTION

Na<sub>0.5</sub>Bi<sub>0.5</sub>TiO<sub>3</sub> (NBT), originally discovered by Smolenskii et al. is considered as one of the most promising material to replace the lead-based materials [1] because of its high Curie temperature ( $\sim 325^\circ\text{C}$ ), relatively high remnant polarization ( $38 \mu\text{C cm}^{-2}$ ) and coercive field ( $73 \text{ kV.cm}^{-1}$ ). The Bi<sup>3+</sup> ions with electronic configuration ( $4f^{14}5d^{10}6s^2$ ) have lone pair of active 6s electrons which are responsible for high polarization [2]. The replacement of a rare earth element at A-site in NBT enhances its electrical as well as magnetic properties. So, with this aim, we have investigated  $x\text{LaFeO}_3-(1-x)\text{Na}_{0.5}\text{Bi}_{0.5}\text{TiO}_3$ ,  $x = 0, 0.01, 0.03, 0.05$  system and the present plan of work is to focus on the synthesis of LaFeO<sub>3</sub> doped NBT system and to investigate their structural and magnetic properties.

## 2. X-RAY DIFFRACTION

The Rietveld refined room-temperature (RT) X-Ray diffractograms in the  $2\theta$  range from  $20^\circ$ – $80^\circ$  for the samples LFNBT0, LFNBT1, LFNBT3 and LFNBT5 are shown in Fig. 1. The proper phase formation of polycrystalline perovskite was confirmed by the sharp peaks of the XRD diffractograms of sintered powder.

We have refined LFNBT system using Cc +  $Pm\bar{3}m$  structural model. There is a good match of experimental data and theoretically fitted data indicating the exactness of the phase coexistence model.

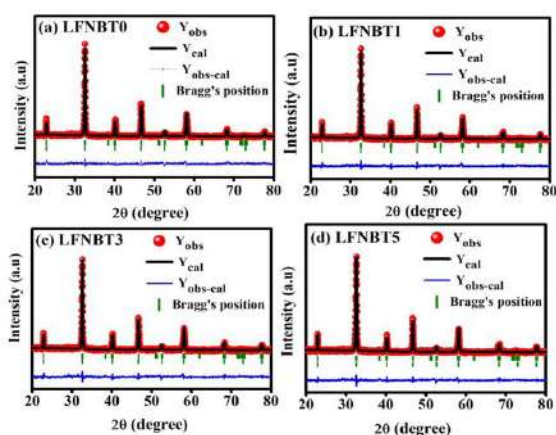


Fig.1: Rietveld refined XRD diffractograms for (a) LFNBT0 (b) LFNBT1 (c) LFNBT3 and (d) LFNBT5 samples fitted by using Cc+  $Pm\bar{3}m$  space group.

## 3. MAGNETIC PROPERTIES

(M–H) hysteresis loops evaluated at two different temperatures 10 K and 300 K (RT) under an applied magnetic field of up to  $\pm 20$  kOe and M–T ZFC and FC curves quantification under a magnetic field of 500 Oe of LFNBT1, LFNBT3, and LFNBT5 are represented in Fig. 2. LFNBT1 is paramagnetic, however weak ferromagnetic character is observed in LFNBT3 and LFNBT5 samples. In LFNBT1, there is divergence in ZFC and FC curves suggesting that there is no true long-range magnetic order. However, in the case of LFNBT3 and LFNBT5 both ZFC and FC magnetization curves overlaps thus confirming the absence of any magnetic ordering. Curie-Weiss law shows that samples are not ideal paramagnets but there is some magnetic interaction between but this interaction is weak enough to give a finite hysteresis.

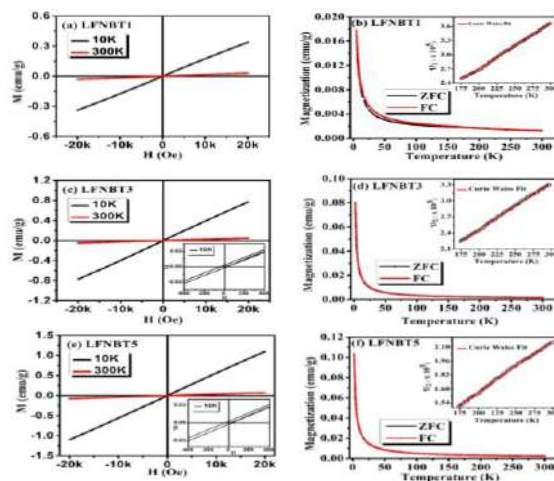


Fig.2. M-H measurements at 10K and 300K and M-T measurements in the temperature range from 10–300 K for (a)-(b) LFNBT1 (c)-(d) LFNBT3 and (e)-(f) LFNBT5 respectively.

## ACKNOWLEDGEMENT

Surinder Singh would like to thank the DST-INSPIRE for fellowship. Authors are also thankful to UGC-DAE-CSR, India for providing research facilities.

## REFERENCES

- [1]. Shvartsman et al, J. Am. Ceram. Soc. 95 (2012)
- [2]. He et al, Phys. Rev. B. 94 (2016)

## Electron-Phonon interaction on the Surface of the Three-Dimensional Topological Insulators

Amit Kumar<sup>a</sup>, Shiv Kumar<sup>a,b</sup>, Kenya Shimada<sup>a,b</sup>

<sup>a</sup> Graduate School of Science, Hiroshima University, Kagamiyama 1-3-1, Higashi-Hiroshima 739-8526, Japan

<sup>b</sup> Hiroshima Synchrotron Radiation Center, Hiroshima University, Kagamiyama 2-313, Higashi-Hiroshima 739-0046, Japan

Email: amik-physics19@hiroshima-u.ac.jp

**Abstract:** We investigate the interaction of 2D electron states belonging to the Dirac cone at the surface of a three-dimensional (3D) topological insulator (TIs) using a laser-based high-resolution angle-resolved photoemission spectroscopy (ARPES). From the ARPES line shape analysis, the average electron-phonon interaction is found to be too small,  $\lambda_{ep} \sim 0.05$  at Fermi level. Our research contributes to a better understanding of many-body interactions in TIs, which are tied to transport properties, and will aid in the development of future spintronic applications.

### 1. INTRODUCTION

Three-dimensional (3D) topological insulators (TIs) have attracted great attention in condensed matter physics for the past decade because of their fascinating fundamental physical properties and promising applications in the “*spintronics*”[1]. The 3D TIs are remarkable because there exist topological surface states (TSSs) with linear Dirac-cone-like dispersion. The TSSs are metallic, and the backscattering is reduced due to the helical spin texture, which is robust against weak non-magnetic disorder or crystal defects as far as the topological property is conserved. These unusual physical properties of the TIs would have potential applications in high-speed dissipationless electronic devices such as quantum computers in the future[2]. Based on the Fermi liquid theory, the transport properties are directly related to the quasiparticles (electrons or holes under the influence of the many-body interactions, such as the electron-phonon and electron-electron interactions) near the Fermi level ( $E_F$ ). Therefore, quantifying these many-body interactions in the TIs is essentially important for *spintronic* applications.

### 2. RESULTS AND DISCUSSION

In this study, we have examined detailed many-body interactions in the prototypical TIs such as  $\text{Bi}_2\text{Se}_3$  and  $\text{Bi}_2\text{Te}_3$  using a laser-based high-resolution ARPES [3]. We have done temperature-dependent ARPES measurements with the *s*-polarization geometry. We cleaved the single crystals below 20 K in the ultrahigh vacuum to get clean surfaces. Figures 1(a1) and 1(b1) show the ARPES results of  $\text{Bi}_2\text{Se}_3$  and  $\text{Bi}_2\text{Te}_3$ . One can see that they are both n-type semiconductors (the conduction band is closer to the Fermi level) and linearly dispersive Dirac-cone-like spectral feature at the  $\bar{\Gamma}$  point ( $k_{\parallel} = 0 \text{ \AA}^{-1}$ ). The high symmetry directions in the surface Brillouin zone can be determined by measuring the Fermi surface (FS) shapes [see Figs. 1(a2) and (b2)]. Figures 1(a3) and (b3) show the enlarged view of selected regions

[rectangle box in Figs. 1(a1) and (b1)] near the  $E_F$ . The peak positions were obtained by fitting the peak in the momentum distribution curves (MDCs) to a Lorentzian, as illustrated in Figs. 1(a3) and 1(b3) by the solid black line. One can see clearly in Figs. 1(a3) and 1(b3), no band renormalization (so-called kink, which is the whole mark of electron-phonon interaction), indicating weak electron-phonon interaction in the TSS. In this poster, I will discuss the magnitudes of the electron-phonon interaction in more detail based on the quantitative ARPES lineshape analyses.

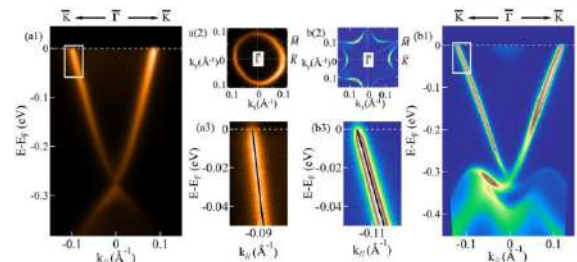


Figure 1. ARPES spectrum measured at 17 K. (a1)-(a3) from  $\text{Bi}_2\text{Se}_3$  (BS) and (b1)-(b3) from  $\text{Bi}_2\text{Te}_3$  (BT) respectively. (a1) and (b1) band dispersion along  $\bar{\Gamma}$ - $\bar{K}$  direction in the surface Brillouin zone. (a2) and (b2) Fermi surface (FS) at  $E_F$ . (a3) and (b3) Enlarged view of ARPES spectrum near  $E_F$  corresponding to the rectangles in (a1) and (b1), respectively. Solid lines (black) represent peak positions obtained from the MDC lineshape analyses.

### REFERENCES

- [1] M. Z. Hasan and C. L. Kane, Reviews of Modern Physics **82**, 3045 (2010).
- [2] D. Pesin and A. H. MacDonald, Nat. Mater. **11**, 409 (2012).
- [3] H. Iwasawa, E. F. Schwier, M. Arita, A. Ino, H. Namatame, M. Taniguchi, Y. Aiura, and K. Shimada, Ultramicroscopy **182**, 85 (2017).

## Reconfigurable Magnonics Driven by Spin Texture in Diatomic Nanodot Array

Sreya Pal<sup>‡</sup>, Amrit Kumar Mondal and Anjan Barman\*

Department of Condensed Matter Physics and Material Sciences, S. N. Bose National Centre for Basic Sciences, Block JD, Sector- III, Salt Lake, Kolkata 700106, India

\*Corresponding author: [abarman@bose.res.in](mailto:abarman@bose.res.in)

<sup>‡</sup>Presenting author: [sreya.pal@bose.res.in](mailto:sreya.pal@bose.res.in)

**Abstract:** Fully reconfigurable magnonic band structure has been observed with the variation of two distinct spin textures in diatomic nanodot array.

### 1. INTRODUCTION

Research in spin-textures and spin-texture-based magnonics has gained ample momentum owing to its potential application in energy-efficient on-chip communication and processing devices [1]. Understanding and control over spin-wave (SW) dynamics in a myriad of patterned nanostructures have unraveled a wealth of information during the last couple of decades. Magnonic crystals (MCs) are ferromagnetic structures with periodically modulated magnetic properties with SWs acting as information carriers through them and they act as building blocks of the magnonic devices. Manipulation of SW properties by tuning geometric properties of MCs have been useful but spin-textures provide a novel route to define on-demand MCs only by subtle variation of external magnetic or electric field or current leading towards far more energy efficiency and flexibility in MCs.

### 2. DISCUSSION

Here, we present the development of reconfigurable magnonic band structure (MBS) and band gap by a bias-field ( $H_b$ ) controlled spin texture in a two-dimensional (2D) di-atomic nanodot lattice with a complex double-dot unit cell made of  $\text{Ni}_{80}\text{Fe}_{20}$  nanodots with diameters of 470 nm and 260 nm separated by 200 nm, forming a binary basis. We have investigated the SW frequency vs. wave-vector dispersion experimentally by Brillouin light scattering (BLS) technique by choosing an anisotropic SW propagation direction [2] in the Damon-Eshbach (DE) geometry (Fig. 1) and verified the results theoretically. As the internal spin texture attuned the SW propagation significantly [3], we have studied the MBS at two different spin configurations, namely, a leaf state ( $H_b = 1$  kOe) and an S-state ( $H_b = 330$  Oe) attained on specific regions of the magnetic hysteresis loop of the sample. Our results reveal a fully reconfigurable

MBS with the variation of two distinct spin textures. A significant variation in the nature of the spin-wave modes is observed from an isotropic to an anisotropic nature due to the contrast in coupling of the two different spin textures. Reconfigurability of MBS is originated from an additional magnetic periodicity present in the S-state which can be explained from the magnetic phase diagram of the sample.

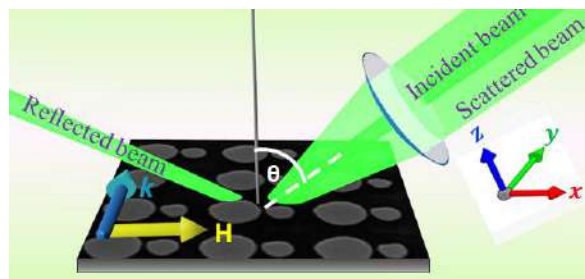


Fig.1. Schematic of the BLS measurement with the sample in the Damon-Eshbach geometry.

### ACKNOWLEDGEMENT

We gratefully acknowledge the financial support from S. N. Bose National Centre for Basic Sciences (grant no.: SNB/AB/18-19/211). SP acknowledges CSIR, Govt. of India, for the senior research fellowship.

### REFERENCES

- [1] A. Barman et al., J. Phys.: Condens. Matter **33**, 413001 (2021).
- [2] A. De et al., J. Magn. Magn. Mater. **491**, 165557 (2019).
- [3] F. Garcia-Sanchez et al., Phys. Rev. Lett. **114**, 247206 (2015).



Topic:

**Itinerant Magnetism in  $\text{CaMn}_2\text{Al}_{10}$ : Self-Consistent Renormalisation (SCR) Theory study**Bharathiganesh Devanarayanan<sup>a,b,\*</sup>, Akariti Sharma<sup>a</sup>, Pratik D.Patel<sup>a</sup>, Navinder Singh<sup>a</sup><sup>a</sup>Theoretical Physics Division, Physical Research Laboratory, Navrangpura, Ahmedabad, India – 380009<sup>b</sup>Indian Institute of Technology, Gandhinagar, Palaj, Gujarat, India – 382355

\*Email: dbharathiganesh@gmail.com

**Abstract:** We have applied the powerful self-consistent renormalization theory of spin fluctuations for the system  $\text{CaMn}_2\text{Al}_{10}$  discovered in 2015 and was conjectured to be an itinerant magnet. We have calculated the inverse static i.e., (paramagnetic) susceptibility and have compared it with the experimental data (Phys. Rev. B 92, 020413, 2015). The agreement is very good. We have calculated spin fluctuations at various temperatures and have also estimated the strength of the electronic correlation i.e., ( $I = 0.3136$  eV) in the Hubbard Hamiltonian. Based on our quantitative explanation of the inverse static i.e., (paramagnetic) susceptibility data within the framework of SCR theory, we can decisively conclude  $\text{CaMn}_2\text{Al}_{10}$  exhibits the phenomena of itinerant magnetism. Further, our DFT and DFT+U calculations corroborate the strong Mn-Al hybridization which is the key behind the itinerant magnetism in this system. Our estimated correlations strength will provide a foundation for further studies of itinerant magnetism in this system.

**1. INTRODUCTION**

Itinerant magnetism in Mn compounds is a rare phenomenon due to the presence of strong Hund's coupling. By conventional wisdom if Mn-Mn distance in a Mn system is more than  $2.7\text{\AA}$  then the system should exhibit local magnetism. However  $\text{CaMn}_2\text{Al}_{10}$  has been experimentally observed to be an itinerant magnet [1]. This motivates us to apply the Self Consistent Renormalisation (SCR) Theory to this system. We also find through our DFT studies that the strong Mn-Al hybridization is the reason for the moments to be itinerant [2].

**2. SCR THEORY STUDY**

We apply the Self consistent Renormalisation (SCR) Theory given by T.Moriya and A.Kawabata to the  $\text{CaMn}_2\text{Al}_{10}$  system [3]. We start with a single band Hubbard Hamiltonian and employ a modified Random Phase Approximation (RPA) which has to be solved self consistently to obtain the inverse paramagnetic susceptibility as a function of temperature. We obtain the value of the interaction parameter in the Hubbard Hamiltonian ( $I = 0.3136$  eV) by fitting the plot of inverse susceptibility with temperature [2].

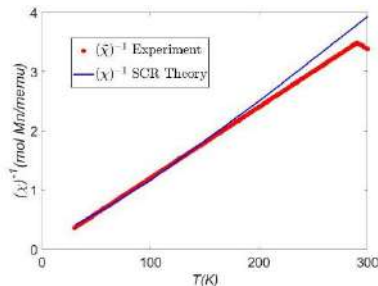


Fig.1. Plot of  $(\chi)^{-1}$  vs T for  $\alpha = 6.205$  and  $q_c = 2.5$  along with experimental data

**3. DFT and DFT+U STUDY**

We have studied  $\text{CaMn}_2\text{Al}_{10}$  in Density Functional Theory (DFT) and DFT+U where U is the Hubbard interaction. Here, we use the value of U obtained from the SCR Theory study. We see various signatures of hybridisation between Mn and Al such as pseudogap and overlapping of Mn and Al orbitals near the Fermi

surface. This confirms that there is strong hybridisation between Mn and Al orbitals leading to itinerant moments in  $\text{CaMn}_2\text{Al}_{10}$  [2].

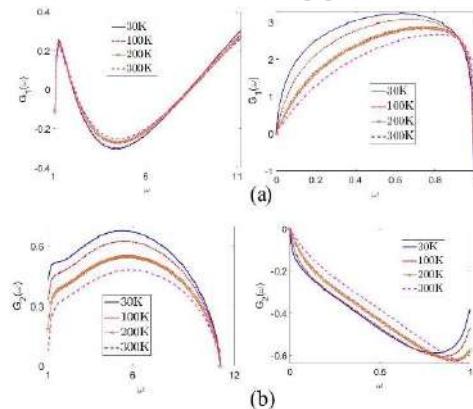


Fig.2. Spin fluctuations  $G(\omega)$  as a function of frequency ( $\omega$ ) for various values of temperature

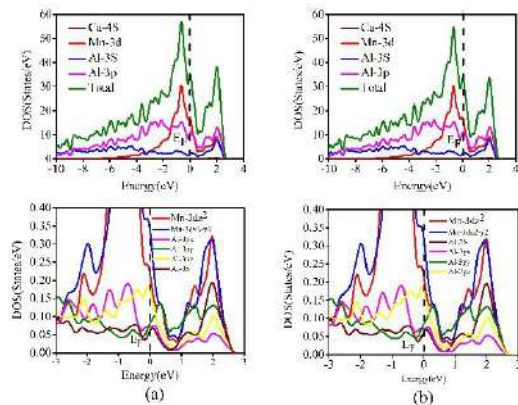


Fig.3. Total DOS, PDOS and orbital resolved DOS from (a) DFT and (b) DFT+U calculations

**ACKNOWLEDGEMENT**

We thank (Vikram-100 HPC) in PRL in which DFT calculations were performed.

**REFERENCES**

- [1]. L.Stienke et al, *Phys. Rev. B*, 92:020413, 2015.
- [2]. B.Devanarayanan et al, arXiv:2202.07619.
- [3]. T.Moriya et al, *J. Phys. Soc. Jpn.* 34 (1973).

## Study of skyrmion and antiskyrmion Hall Effect in a synthetic ferrimagnet

Susree Sucharita Mohapatra, Shaktiranjana Mohanty, Brindaban Ojha, Subhankar Bedanta  
 Laboratory for Nanomagnetism and Magnetic Materials (LNMM), School of Physical Sciences,  
 National Institute of Science Education and Research (NISER), HBNI,  
 P.O. Bhipur-Padanpur, Via –Jatni, Odisha-752050, India  
 \*Email: sbedanta @niser.ac.in

**Abstract:** In this work, we have studied skyrmion hall effect in synthetic ferrimagnet using micromagnetic simulations. We modelled a synthetic ferrimagnetic system where only the bottom NM/FM interface has isotropic/anisotropic DMI. We have applied spin polarised current to bottom layer to nucleate skyrmions/antiskyrmions and due to RKKY type interlayer exchange coupling, another skyrmions/antiskyrmion will be generated at top layer with different chirality. The interlayer exchange coupling  $J$  is varied to observe the effect of the coupling strength on skyrmion hall effect in both layers. We have also varied the thickness of the non-magnetic spacer to examine the effect of dipolar coupling on the stabilization of skyrmions. We have shown the skyrmion hall effect is suppressed to zero while using synthetic antiferromagnet(SAF) with strong interlayer exchange coupling.

### 1. INTRODUCTION

The ever-increasing need for massive storage capabilities and processing speeds demands more energy consumption which hugely impacts our environment. Magnetic skyrmions are nanoscale sized, topologically-protected solitons and can be driven by very low current density. Room-temperature magnetic skyrmion has been also observed in heavy metal/ferromagnet heterostructures with broken inversion symmetry, owing to an interfacial Dzyaloshinskii-Moriya interaction (DMI) induced by strong spin-orbit interaction.[1] However skyrmion hall effect is one of the problems for systems using skyrmions as information carriers.

The skyrmions in case of synthetic ferrimagnet move towards the edge diagonally with respect to the current flow because of topological magnus force producing a sizable skyrmion hall effect. However, for SAF, the motion of skyrmions along the transverse direction is insignificant when the strength of interlayer exchange coupling is high.[2] For current-induced motion of skyrmion, skyrmion hall angle is given by  $\theta_{sk} = \tan^{-1}(l_y/l_x)$  where  $l_x$  and  $l_y$  are displacement in the x and y directions (x-direction is parallel to the direction of current).[1]

### 2. SIMULATION DETAILS

The 3D solver of the object oriented micromagnetic framework (OOMMF) i.e. Oxsii was used for the simulations. Isotropic DMI is used for the stabilization of skyrmions and anisotropic DMI is used for antiskyrmions. We have considered 3 systems where the ratios of saturation magnetization of top and bottom FM layers are 0.75, 1, and 1.25. The value of  $M_s$  for the bottom layer is fixed to be  $700 \times 10^3 \frac{A}{m}$ . The interlayer exchange coupling  $J$  is varied to observe the effect of coupling strength. We have also varied the thickness of the NM spacer from 1nm to 10nm to check the effect of dipolar coupling on skyrmions stabilization in the top layer.

### 3. RESULTS AND DISCUSSION

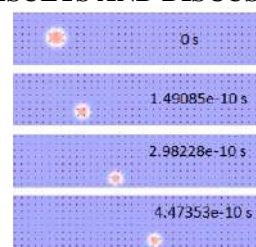


Fig.1:Skyrmion Hall Effect

Spin polarized current is applied to the bottom layer of the system to generate skyrmion/antiskyrmion and because of RKKY coupling, we can observe another skyrmion/antiskyrmion in the top layer. On increasing the thickness of the spacer, we observe that skyrmions cannot be stabilized in the top layer of the system. Skyrmion hall angle is calculated for different  $J$  values for the 3 systems. For SAF, the skyrmions hall angle is found to be negligible.

### 4. TABLE

Table 1. Calculation of Skyrmion Hall Angle

$M_{s_{top}}/M_{s_{bottom}}$	$J \text{ J/m}^2$	$\theta_{sk}^\circ$
0.75	$2 \times 10^{-3}$	$36.61^\circ$
1.25	$2 \times 10^{-5}$	$5.92^\circ$

### ACKNOWLEDGEMENT

We thank Department of Atomic Energy (DAE), Govt. of India for providing the funding to carry out the research work.

### REFERENCES

- [1]. Dohi, Takaaki, et al. "Formation and current-induced motion of synthetic antiferromagnetic skyrmion bubbles." *Nature communications* 10.1 (2019): 1-6.
- [2]. Zhang, Xichao, Motohiko Ezawa, and Yan Zhou. "Thermally stable magnetic skyrmions in multilayer synthetic antiferromagnetic racetracks." *Physical Review B* 94.6 (2016): 064406.

## Domain wall and Skyrmion dynamics on synthetic antiferromagnet for variable tensile stress - a micromagnetic study

Gaurav Kanu\*, Brindaban Ojha, Shaktiranjana Mohanty, Ashish K Moharana, Adyashakti Dash, Subhankar Bedanta

Laboratory for Nanomagnetism and Magnetic Materials (LNMM), School of Physical Sciences,

National Institute of Science Education and Research (NISER), HBNI, Jatni-752050, Odisha, India

Email: [gaurav.kanu@niser.ac.in](mailto:gaurav.kanu@niser.ac.in)

**Abstract:** Synthetic antiferromagnets (SAFs) have a wide range of applications in current data storage technology. It comprises of three stacked layers i.e. two ferromagnetic layers on top and bottom with intermediate spacer layer. The ferromagnetic films interact through RKKY interaction where, the spin polarized electrons in metals play an important role. Currently magnetic domains are used for storing data and transferring and new studies reveal that topologically stable magnetic skyrmions can be more efficient for this purpose. Having this skyrmions on the track for real time data storage, anisotropy of the thin film has a very important role. If we consider the case of flexible spintronics, then the anisotropy changes remarkably upon applying compressive or tensile stress. In this study through micromagnetic simulations the effect of tensile stress on DW velocity and skyrmion velocity is measured, where the applied tensile stress changes the anisotropy of the material.

### Introduction

In modern data storage technology, higher data storage, faster data transfer rate, read and write speed has become very important part. The interruption due to the stray field from consecutive bits are undesired due to which SAFs are preferred. Also, in SAF, the skyrmion Hall effect is minimized due to the antiferromagnetic coupling which is advantageous for us. SAFs are basically with Ferromagnetic (FM) layers periodically interleaved with metallic or insulating spacers, where the magnetization of adjacent FM layers alternates owing to the antiferromagnetic (AF) interlayer exchange coupling (IEC). For metallic spacers, IEC is achieved via Ruderman-Kittel-Kasuya-Yosida (RKKY) type exchange interaction mediated by spin polarized charge carriers in the spacer [1]. In general, the direction of magnetization is used for storing information and the DW speed gives the transfer rate. A magnetic skyrmion is a local whirl of the spin configuration in a magnetic material. The spins inside a skyrmion rotate progressively with a fixed chirality from the up direction at one edge to the down direction at the center, and then to the up direction again at the other edge [2].

Here we are using spin polarized current in plane (CIP) to induce spin transfer torque (STT) to manipulate local magnetization, which is responsible for moving of the DW and magnetic skyrmion.

### Simulation Details

The micro-magnetic simulations were performed on OOMMF software developed by NIST. The dimensions of the SAF layer are 1000nm x 20nm x 3nm (FM), 1000nm x 20nm x 3nm (Spacer), 1000nm x 20nm x 3nm (FM). The other maintained parameters are as follows: interlayer RKKY interaction strength  $\sigma = -3 \times 10^{-4}$ , Heisenberg exchange  $A = 20 \text{ pJ/m}$ , saturation magnetization  $M_s = 580 \text{ kA/m}^3$ , DMI exchange  $D = 1.25 \text{ mJ/m}^2$ , current density  $J = 1.17778 \times 10^{13} \text{ A/m}^2$ . For nucleation of skyrmion the above parameters needed to be tuned. Keeping the dimensions of the SAF same, the interlayer RKKY interaction strength

is  $\sigma = -2 \times 10^{-3}$ , Heisenberg exchange  $A = 15 \times 10^{-12} \text{ J/m}$ , saturation magnetization  $M_s = 580 \text{ kA/m}^3$ , DMI exchange  $D = 3.4 \text{ mJ/m}^2$ , current density  $J = 2.277 \times 10^{12} \text{ A/m}^2$ .

### Result and Discussion

The maximum velocity of DW was found to be  $v = 0.2126 \text{ m/s}$  and for  $K_u = 0.3 \times 10^6 \text{ J/m}^3$  (Fig.1(a)). For skyrmions the maximum velocity was found to be  $v = 0.0616 \text{ m/s}$  and for  $K_u = 0.7 \times 10^6 \text{ J/m}^3$  (Fig.1(b)).

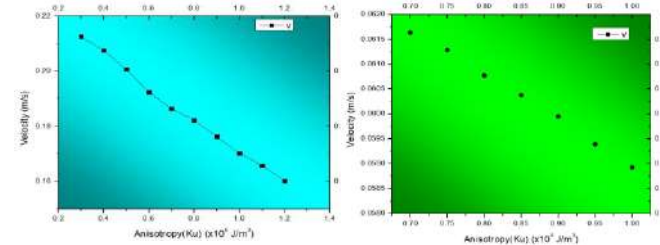


Fig. 1: (a) Domain wall velocity vs Anisotropy. (b) Skyrmion velocity vs Anisotropy.

### Conclusion

It is found that velocity of the DW is nearly 3.5 times higher than skyrmion in a SAF system.

### Acknowledgement

Authors would like to thank DAE, Govt. of India for the financial support to carry out the experiments.

### Reference

1. Kay Yakushiji *et al* 2015 *Appl. Phys. Express* 8 083003
2. Fert, A., Reyren, N. & Cros, V. Magnetic skyrmions: advances in physics and potential applications. *Nat Rev Mater* 2, 17031 (2017).
3. Donahue, M. (1999), OOMMF User's Guide, Version 1.0, - 6376, National Institute of Standards and Technology, Gaithersburg, MD



**Effects of Swift heavy ion-irradiation on Magnetic properties of Co-codoped TiO<sub>2</sub>****Shashi Ranjan Kumar<sup>1</sup>, Ratnesh Gupta<sup>2</sup>****<sup>1,2</sup>School of Instrumentation, Devi Ahilya University, Khandwa Road, Indore 452001 India****Email: gratnesh\_ioi@yahoo.com**

**Abstract:** Co codoped TiO<sub>2</sub> thin film has been prepared on Si (100) substrate using RF sputtering method at room temperature and irradiated with 100 MeV Au ions. X-ray reflectivity measurement shows increment in the surface roughness and decrease of film thickness as we go from the as-deposited to irradiated film. XAS spectra collected at Co L<sub>3,2</sub> –edge infers that the Co is in the metallic state. Further, The XMCD and Kerr microscopy measurement were used to understand the origin of the ferromagnetism. From Kerr microscopy measurement at room temperature a clear change occurs from isotropic hysteresis loop for the as-deposited sample to magnetic anisotropy with varying different ion fluences. Using sum rule calculation from the XMCD spectra we obtain total magnetic moment for the Co atoms which reduces from  $1.77 \pm 0.016 \mu_B$  (for as-deposited) to  $0.382 \pm 0.014 \mu_B$  (in the case of Au irradiated film with the fluence  $5 \times 10^{12}$  ions/cm<sup>2</sup>).